

Master Thesis

Cyclopolymerizable Monomers for Radical Photopolymerization based on Difunctional (Meth)acrylamides

performed at

Institute of Applied Synthetic Chemistry
Technische Universität Wien



under the supervision of

Univ. Prof. Dipl.-Ing. Dr.techn. Robert Liska

and

Dipl.-Ing. Dr.techn. Gernot Peer

by

Larissa Alena Ruppitsch, BSc

01425730

Robatschgasse 17, 9020 Klagenfurt

Vienna, 08.10.2020



Die approbierte gedruckte Originalversion dieser Masterarbeit ist an der TU Wien Bibliothek verfügbar.
The approved original version of this thesis is available in print at TU Wien Bibliothek.

Danksagung

In erster Linie möchte ich mich bei Prof. Dr. Robert Liska für die Möglichkeit bedanken, meine Diplomarbeit in seiner Arbeitsgruppe in einem so spannenden Fachgebiet verfassen zu dürfen. Danke, nicht nur für deine tolle fachliche Unterstützung und dein Vertrauen, sondern auch für deine herzliche Art der Betreuung, wodurch du einen einzigartigen Teamgeist in deiner Gruppe geschaffen hast.

Einen großen Dank möchte ich auch meinem Mitbetreuer Dr. Gernot Peer aussprechen. Danke, dass du mich mit deinem umfangreichen Wissen, deinem immerwährenden offenen Ohr und deiner stetigen Motivation auf meinem Weg begleitet und bestmöglich gefördert hast.

Vielen Dank auch an meine Praktikantin Kristina Durstberger, die mich mit ihrem großen Engagement bei den zahlreichen Synthesen tatkräftig unterstützt hat. Außerdem möchte ich mich herzlich bei Thomas Koch für die Durchführung der Zugversuche bedanken.

Einen besonderen Dank möchte ich meiner FB-MC Mädelsrunde Anna, Babsi und Lisa, sowie meinem „partner in crime“ Alex aussprechen. Vielen Dank, dass ihr mir nicht nur während der Arbeit mit euren Ratschlägen bestens zur Seite gestanden seid, sondern auch für die lustige und schöne Zeit, die wir abseits des Laboralltags miteinander verbringen konnten. Ich freue mich auf weitere unvergessliche Stunden mit euch!

Vielen Dank auch an alle „jungen & alten“ Mitgliedern der MC-Arbeitsgruppe für das tolle Arbeitsklima und die großartigen Momente abseits des Laboralltags. Besonders möchte ich mich hiermit auch bei Patzi, Sebi und Ralle für den tollen fachlichen Support sowie eure helfenden Hände herzlich bedanken. Ebenso gilt ein großes Danke meinen H35 Laborkollegen (Elise, Markus, Philip und Yazgan) für die guten Ratschläge und die freundliche Arbeitsatmosphäre.

Un ringraziamento speciale va a te, Luca, per il tuo amorevole sostegno e per la forza e la motivazione che mi hai dato. Non vedo l'ora di vivere molti altri momenti e soprattutto di viaggiare insieme a te.

Zuletzt gilt mein größter *DANK* meinen Eltern Lydia und Peter sowie meiner Schwester Carina (inklusive Daniel). *DANKE*, dass ihr immer an mich geglaubt und mich in jeder Lebenslage, sowie bei jedem meiner Vorhaben bedingungslos unterstützt habt. Ohne EUCH wäre all dies nicht möglich gewesen.

DANKE!

Abstract

Free radical photopolymerization is one of the most used curing methods in industry and its photocurable polymers offer an enormous number of applications, such as coatings, additive manufacturing, dental and medical industry. Furthermore, this method offers various advantages, especially compared to thermal polymerization approaches, like low energy consumption, solvent-free usage and fast reaction times. Unfortunately, one of the major drawbacks of free radical photopolymerization is the appearance of volumetric shrinkage during polymerization, and, consequently, the development of shrinkage stress in the cured material. This behavior triggers major problems in several application sectors, especially in the sector of bulky curing, *e.g.* dental and medical applications.

Therefore, it is not surprising that, at an industrial level, there is a significant desire to develop monomers showing reduced or ideally zero shrinkage. Many different strategies are pursued in the research and development industry to achieve this goal, whereas one promising approach is the use of so-called cyclopolymerizable monomers, which yield linear polymers with cyclic structure in the polymer backbone upon polymerization. Recent studies were focusing on the development and investigation of difunctional cyclopolymerizable monomers, leading to crosslinked polymers with reduced shrinkage stress. Furthermore, it was shown that the material properties could be tuned by modifying the spacer unit of the difunctional species.

The aim of this work was to create new difunctional cyclopolymerizable monomers with reduced volumetric shrinkage based on (meth)acrylamides. Furthermore, their reactivity was investigated *via* photo-DSC, RT-NIR photorheology as well as their thermomechanical behavior by DMTA and tensile testing.



Die approbierte gedruckte Originalversion dieser Masterarbeit ist an der TU Wien Bibliothek verfügbar.
The approved original version of this thesis is available in print at TU Wien Bibliothek.

Kurzfassung

Radikalische Photopolymerisation ist eine der am häufigsten verwendeten industriellen Aushärtungsmethoden. Ihre Polymere bieten attraktive Eigenschaften und finden in verschiedensten Bereichen Anwendung, wie etwa in Beschichtungen, Additiven Fertigungstechnologien, sowie in der Dental- und Medizinindustrie. Darüber hinaus weist diese Methode – besonders im Vergleich zur thermischen Polymerisationsstrategie – diverse Vorteile auf, wie z.B. einen geringen Energieverbrauch, lösungsmittelfreie Verwendung und schnelle Reaktionszeiten. Einer der größten Nachteile der radikalischen Photopolymerisation ist das Auftreten volumetrischer Schrumpfung während des Polymerisationsprozesses, und folglich die Entwicklung von Schrumpfspannungen im ausgehärteten Material. Dieses Verhalten ist für viele Anwendungsgebiete hoch problematisch, insbesondere im dentalen und medizinischen Bereich.

Somit ist es nicht verwunderlich, dass großer industrieller Aufwand betrieben wird, um Monomere zu entwickeln, bei denen die Aushärtung mit reduziertem bzw. keinem Schrumpf möglich ist. In der Forschung und Entwicklung werden viele verschiedene Strategien verfolgt, um dieses Ziel zu erreichen. Ein sehr vielversprechender Ansatz ist die Verwendung so-genannter zyklopolymerisierbarer Monomere, die nach der Polymerisation Ringstrukturen in der ansonsten linearen Polymerhauptkette aufweisen. Neuere Studien konzentrierten sich auf die Entwicklung und Untersuchung von difunktionellen zyklopolymerisierbaren Monomeren, die zu vernetzten Polymeren mit reduzierter Schrumpfspannung führen. Darüber hinaus wurde gezeigt, dass die Materialeigenschaften durch Modifizierung des Gliedteiles der difunktionellen Spezies beeinflusst werden können.

Das Ziel dieser Arbeit bestand darin, basierend auf (Meth)acrylamid Einheiten, neuartige difunktionelle zyklopolymerisierbare Monomere herzustellen, die auch ein verringertes Schrumpfverhalten aufweisen sollten. Diese Monomere wurden hinsichtlich ihrer Reaktivität mittels Photo-DSC und RT-NIR-Photorheologie, sowie hinsichtlich ihres thermomechanischen Verhaltens mittels DMTA und Zugversuchen analysiert.



Die approbierte gedruckte Originalversion dieser Masterarbeit ist an der TU Wien Bibliothek verfügbar.
The approved original version of this thesis is available in print at TU Wien Bibliothek.

Table of Contents

Introduction		1
Objective		16
General Part		17
Summary		62
Experimental Part		67
	Gen.	Exp.
1. State of the Art	17	-
2. Diacrylamides	26	67
2.1. Synthesis of CPM 1 and REF 1	26	67
2.1.1. Synthesis of N,N'-(hexane-1,6-diyl)bis(N,N'-bisacrylamide) - CPM 1	26	67
2.1.2. Synthesis of N,N'-(hexane-1,6-diyl)bis(N-methyl-N'-acrylamide) – REF 1	27	69
2.2. Reactivity studies of CPM 1 and REF 1	28	71
2.2.1. RT-NIR-photorheology of CPM 1 and REF 1	28	71
3. Dimethacrylamides	32	73
3.1. Synthesis of CPM 2, CPM 3 and CPM 4	33	73
3.1.1. Synthesis of N,N'-(hexane-1,6-diyl)bis(N,N'-bismethylacrylamide) - CPM 2	33	73
3.1.2. Synthesis of N,N'-(dodecan-1,12-diyl)bis(N,N'-bismethacrylamide) - CPM 3	34	75
3.1.3. Synthesis of N,N'-(2,2,4(2,4,4)-trimethylhexane-1,6-diyl) bis(N,N'-bismethylacrylamide) - CPM 4	35	77
4. CPMs and REFs based on (2,2,4)/(2,4,4)-trimethylhexane-1,6-diamine	36	79
4.1. Synthesis of the REF 2 and REF 3	37	79

4.1.1.	Synthesis of N,N'-(2,2,4(2,4,4)-trimethylhexane-1,6-diyl) bis(N-methylacrylamide) – REF 2	37	79
4.1.2.	Synthesis of N,N'-(2,2,4(2,4,4)-trimethylhexane-1,6-diyl) bis(N-methyl-N'-methylacrylamide) - REF 3	38	81
4.2.	Synthesis of CPM 5, CPM 6, CPM 7, and CPM 8	39	83
4.2.1.	Synthesis of 1,6-bis(diallylamino)-2,2,4(2,4,4)-trimethylhexane – CPM 5	39	83
4.2.2.	Synthesis of tetraethyl-2,2',2'',2'''-(((2,2,4-trimethylhexane-1,6 diyl)bis(azanetriyl))tetrakis(methylene))tetraacrylate - CPM 6	40	85
4.2.3.	Synthesis of N,N'-(2,2,4(2,4,4)-trimethylhexane-1,6-diyl) bis(N-allyl-N'-methylacrylamide) - CPM 7	41	87
4.2.4.	Synthesis of N,N'-(2,2,4(2,4,4)-trimethylhexane-1,6-diyl) bis(N-(ethyl-2- (chloromethyl)acryloyl)-N'-methylacrylamide) - CPM 8	41	-
4.3.	Reactivity studies of REF 2, REF 3, CPM 4, CPM 5, CPM 6, and CPM 7	44	89
4.3.1.	Photo-DSC measurement of REF 2, REF 3, CPM 4, CPM 5, CPM 6, and CPM 7	45	89
4.3.2.	RT-NIR photorheology of REF 2, REF 3, CPM 4, CPM 5, CPM 6, and CPM 7	49	89
4.3.3.	ATR-IR spectroscopy of polymerized CPM 4 and CPM 6	55	89
4.4	Mechanical studies of REF 2, CPM 4, CPM 6, and CPM 7	57	90
4.4.1.	DMTA of REF 2, CPM 4, CPM 6, and CPM 7	57	90
4.4.2.	Tensile Tests of REF 2, CPM 4, CPM 6, and CPM 7	59	90
	Materials & Methods		91
	Abbreviations		94
	References		96

Introduction

Photopolymerization

Light-induced polymerization, which is commonly known as photopolymerization, describes the process of initiating a chemical reaction *via* electromagnetic radiation to create polymers and polymeric materials out of organic materials. The induction of the polymerization is triggered *via* the absorption of light in the ultra-violet (UV), visible (VIS) or infrared (IR) part of the electromagnetic spectrum. Also, absorption of higher energy sources with shorter wavelengths (*e.g.* electron beam) is possible.¹

The initiating species can be radicals, cations, anions, and bases, whereby the subsequent polymerization follows then the same scheme (Figure 1).

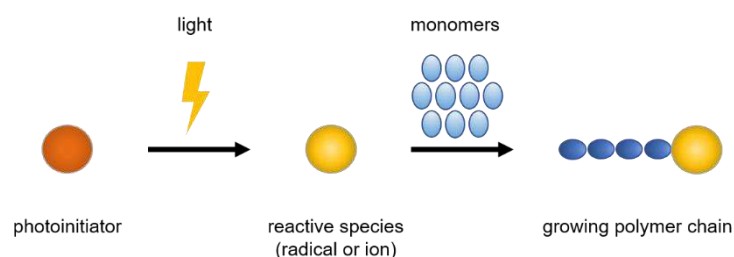


Figure 1: General schematic representation of photoinitiated polymerization.²

During initiation, a photoinitiator (PI) is activated *via* the absorption of light and converted to a reactive species (radical, cation, anion, or base). This reactive species can then be added to several monomeric species, with the active center always being passed to the new end of the growing polymer chain. Hence, this type of reaction is called a chain-growth polymerization.²

Photopolymerization offers various advantages compared to thermal operating technologies, leading to its association with the term “green chemistry”. The main benefits of this method are outlined below:^{3, 4}

- Fast reaction time (rapid curing)
- Reduction of side reactions and branching
- Operation at room temperature and atmospheric pressure
- Non-pollutive and cost effective
- Solvent-free formulations
- Higher energy efficiency

Consequently, photocurable polymers show a vast range of applications, which can also be interconnected with each other. Therefore, only the most commonly known examples are explained in more detail (Figure 2).³⁻⁵

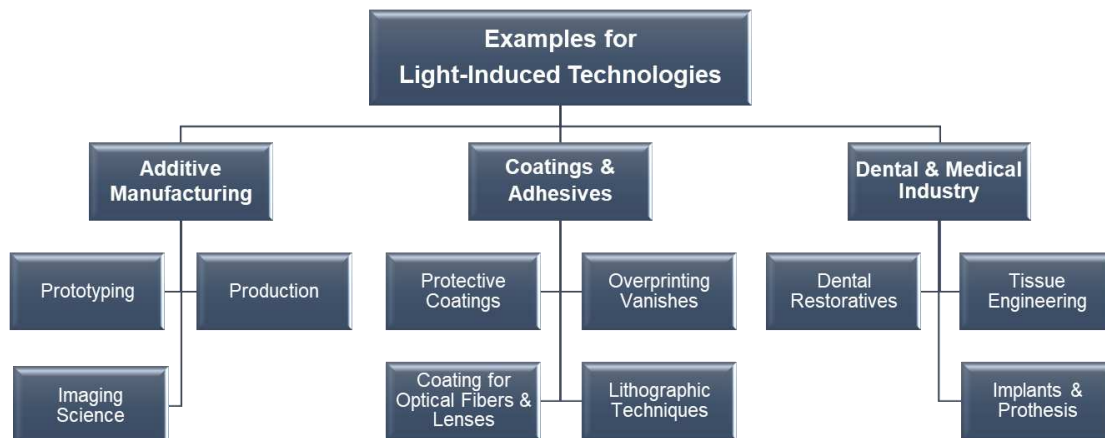


Figure 2: Examples of industrial applications for photopolymers.³⁻⁵

Additive Manufacturing (AM) is a technique that usually works layer by layer to create a three-dimensional structure out of a broad range of materials, like polymers, ceramics, metals or composites.⁶ Photo-based AM offers not only different commercially developed processes like, for example, stereolithography (SLA), fusion deposition modeling (FDM), or three-dimensional printing (3DP), but also various commercially available resins to tune the mechanical properties of the material.⁷ The focus of the AM-process lies nowadays on direct production technologies of customized products. Many different application sectors are using AM-techniques, like, for example, aerospace⁸ or personalized medicine.⁹ Consequently, a large number of different AM-processes are available depending on the application, e.g. visual prototyping, functional prototyping, rapid tooling, and rapid manufacturing.¹⁰ The major advantages of light-based AM compared to traditional manufacturing techniques are the design of complex parts with high precision in a cost- and time-efficient due to the fast curing process, without wasting unmanufactured materials.⁶ Unfortunately, this method still shows some major challenges mainly caused by insufficient material properties, like high brittleness and shrinkage stress in the cured material.¹⁰

The sector of UV-curing coatings and adhesives has been continuously growing for the last two decades due to their significant advantages compared to other methods like thermal curing of coatings. It offers not only high energy efficiency and fast curing but also enhances the material properties, like scratch resistance, life-time, and tearing strength. The coating process itself can also be performed in several different ways, like roll coating, dipping, or spraying. Consequently, there is a wide field of applications for this sector, for example protective or decorative coating for wood, metals, papers or plastics as well as coatings for improving the mechanical properties, like flexural strength for optical fibers.^{5, 11}

Photocurable polymers have also been used in the dental and medical industry for decades, due to their biocompatibility.⁵ In dentistry, one main focus is set on dental restoratives to replace dental amalgams, since their negative influence on the human body is still controversial.¹²

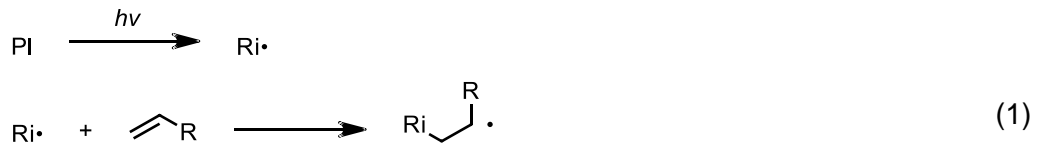
The medical industry offers many different applications for photopolymers, like the previously mentioned photo-based AM,¹³ where patient-specific models and functional parts (implants or prostheses) can be produced, or tissue engineering⁹ to replace and restore damaged human tissue. As already mentioned, the light-based AM techniques show some major advantages (*e.g.* fast curing and high precision), but also a few disadvantages (*e.g.* brittle materials and high shrinkage stress), which are the main challenges of this technique and therefore already in the focus of the research.

Free radical photopolymerization

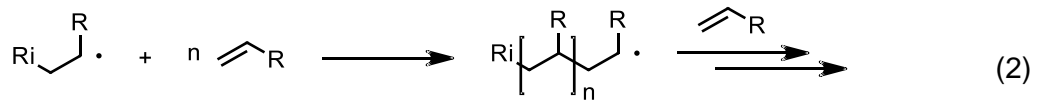
Free radical photopolymerization (FRP) is one of the most used chain growth reactions in industry, and it occurs *via* a three-step mechanism. The first step is the initiation (1), where an initiating molecule, the so-called photoinitiator (PI), decomposes under the absorption of light to form free radicals (Ri). These radicals start the polymerization by adding to the double bond (DB) of a monomer species, thereby converting it into a propagating species. During the second step, propagation (2), several monomers are added to the growing molecule, with the radical always being passed to the chain end until termination occurs.

There are two termination possibilities, which depend on temperature: recombination (3) and disproportion (4). Recombination is preferred at low temperatures leading to an increase in the molecular weight due to the combination of two active chain ends. Higher temperatures favor disproportion, where the molecular weight remains unchanged.³

Initiation



Propagation



Termination

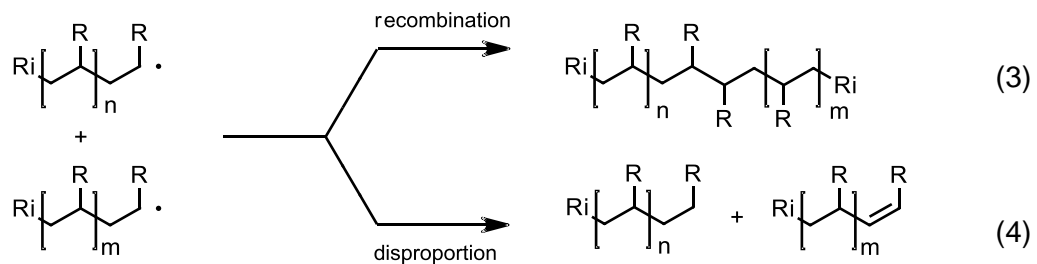


Figure 3: Mechanism of FRP (initiation, propagation, and termination).

Chain transfer reactions (CTR) are side reactions, which can occur during the propagation step, and they cause branching *via* H-abstraction at the polymer chain. There are two different types of CTR: intermolecular (5) and intramolecular CTR (6). Intermolecular CTRs transfer the radical to another molecule, which leads to long-chain branching. During intramolecular CTRs, the radicals are transferred to another position in the same molecule causing short-chain branching.¹⁴

Chain transfer

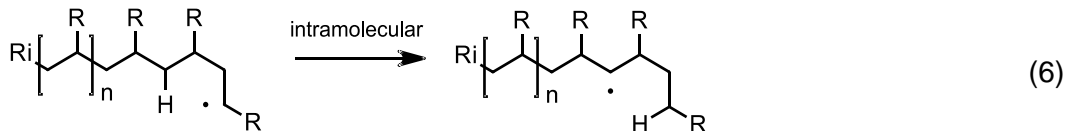
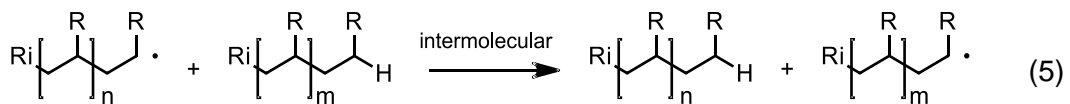


Figure 4: Schematic representation of inter- and intramolecular CTRs.

Oxygen inhibition

FRP is still the most dominant industrial technology in the field of photopolymerization, even though it has many disadvantages, especially in comparison with the growing sector of cationic polymerization. The most significant drawbacks are the rather costly monomers, due to the necessity of olefinic DB, and the occurrence of oxygen inhibition.³

Oxygen inhibition is a deactivation process because the reactive radical of a growing polymer chain (Pn) can be trapped by an oxygen diradical to form a non-reactive radical species. This inhibition occurs extremely fast due to the triplet state biradical nature of oxygen and the diffusion of oxygen in the polymerization media.¹⁵



Figure 5: Mechanism of oxygen inhibition.

Oxygen inhibition can lead not only to a lower polymerization rate, but also to a more extended induction period, low conversion, shorter polymer chains, and reduced surface properties. Therefore, the reduction of oxygen inhibition is needed in industry, for example during the curing process of thin films for electronic application and coatings. There are several ways to obtain this reduction. Some industrial implementation possibilities could be the use of inert atmosphere during the radical polymerization process or a high concentration of PI, which consumes dissolved oxygen during the formation of initiating radicals.^{3, 15} Other methods include the use of certain additives, which suppress the inhibition of oxygen. These additives get incorporated into the polymeric network without influencing the material properties. The most promising examples try to reinitiate the polymerization (e.g. hydrogen donors like thiols) and consequently eliminate the detrimental effect of oxygen.¹⁶

Photoinitiators

A photoinitiator (PI) or a photoinitiating system is an important component of the photopolymeric system. It absorbs the energy of the light, converts it into chemical energy, and, therefore, the PI initiates polymerization.¹⁷ The choice of the PI is of high importance as it mainly affects curing speed, yellowing, and cost. The PI should also show high commercial availability, good solubility in several monomeric systems, high storage stability, low migration, and low odor.

Furthermore, the emitted wavelengths of the light source need to be absorbed by the PI to generate the active species effectively.² The Jablonski diagram (Figure 6) describes this energy absorption process in detail.

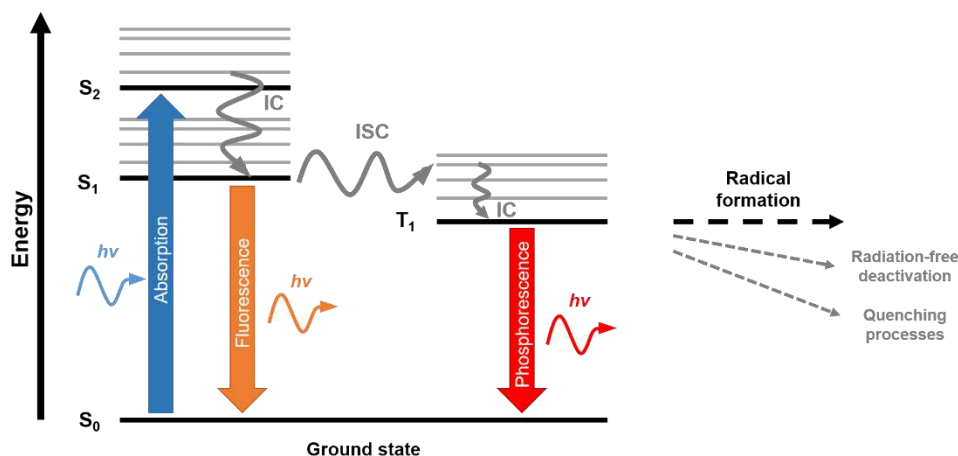


Figure 6: Jablonski Diagram.^{18, 19}

The absorption of light ($h\nu$) leads to the excitation of a photoinitiating molecule, which means that an electron leaves the ground state (S_0) and goes to a higher energy state (S_1 or S_2). In the ground state, the electrons are paired with an antiparallel spin. After excitation to a singlet state (S_1 or S_2), the spin remains antiparallel. The excited electron can then either release the absorbed energy *via* fluorescence, where the electron drops back to S_0 and a photon is emitted, or it undergoes one of the two possible non-radiative processes: Internal Conversion (IC) or Intersystem Crossing (ISC). IC leads to a conversion of the excessive energy into vibrational heat, while the electron goes to a lower, but still excited, singlet state. ISC leads to a transfer of the electron to the excited triplet state (T_1), in which the spins of the electrons are located in a parallel direction. Due to the shift of the spins from an antiparallel to a parallel direction, the triplet state shows a longer lifetime than the excited singlet state.

Hence, the formation of radicals is possible. However, it is in concurrence with some deactivating pathways, such as fluorescence from the singlet state or phosphorescence from the triplet state (electron drops back to S_0 and a photon gets emitted), and bimolecular quenching processes (*e.g.* due to oxygen or monomers). Radicals can be created in two possible ways, and therefore, the PIs can be classified into two different categories:²⁰

- Type I (Norrish Type I reaction)
- Type II (Norrish Type II reaction)

Type I PIs are characterized by a unimolecular mechanism. Two radicals are generated *via* a homolytic α -cleavage of the initiator since the dissociation energy of the bond is lower than the energy of the excited states. Consequently, this type of PI shows a higher reactivity towards the initiation of polymerization, and a smaller quantity of PI is needed. However, it is also more sensitive to deactivation processes like quenching reactions with oxygen or monomers.^{3, 20, 21}

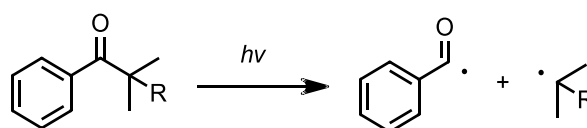


Figure 7: Schematic representation of the α -cleavage mechanism of Type I PIs.

Most Type I PIs are aromatic carbonyl compounds with different substituents. There are many different commercially available Type I PIs on the market (see Figure 8), of which benzoin derivatives, hydroxyl alkyl acetophenones (*e.g.* Darocur 1173), and acylphosphine oxides (*e.g.* BAPO) are just a few representatives.² Another very efficient and recently developed Type I PI is germanium-based Ivocerin[®], applied in dental fillings.²²

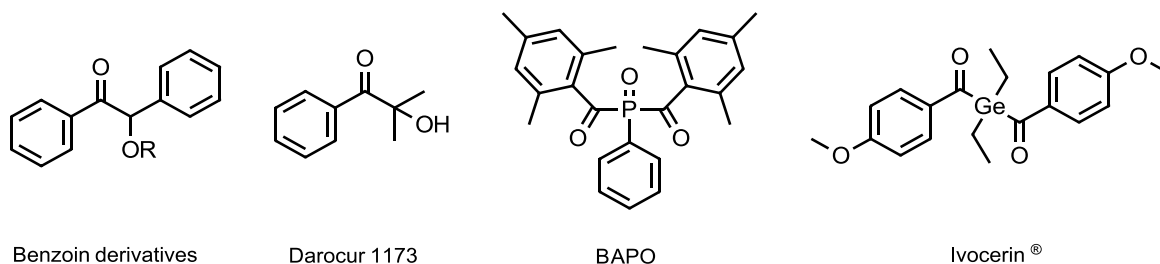


Figure 8: Industrial used Type I PIs: Benzoin derivatives, Darocur 1173, BAPO and Ivocerin[®].

Type II PIs are characterized by a bimolecular mechanism. After excitation, the PI does not cleave, but it reacts with a co-initiator (CI) to create radicals. The formation of radicals can happen *via* H-abstraction (*e.g.* from ethers) or electron and subsequently proton transfer (*e.g.* tertiary amines), with only the created CI-radical showing high reactivity. Type II PIs show lower efficiencies as well as slower decomposition rates compared to Type I PIs due to the probability of back-electron transfer. Furthermore, Type II PIs also exhibit the possibility of chain branching due to H-abstraction.

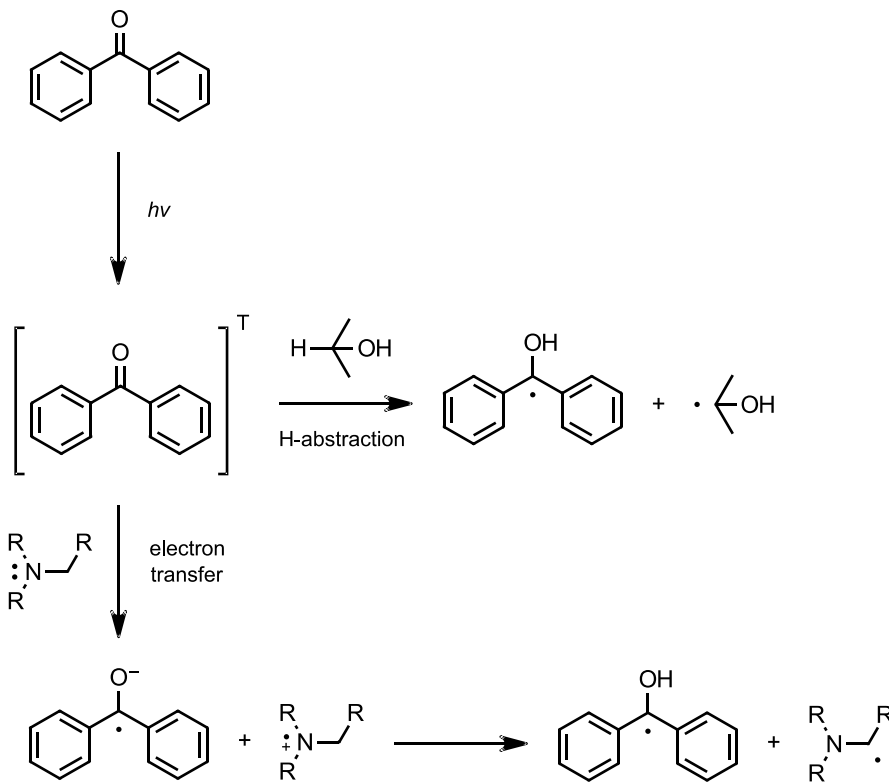


Figure 9: Schematic representation of the bimolecular mechanism of Type II PIs.

The major advantage of Type II PIs is the possibility for application at higher wavelengths and the reduction of quenching reactions through monomers and oxygen. Typical examples for Type II PIs (Figure 10) are benzophenone, thioxanthone, and camphorquinone, while typical examples for CIs are tertiary amines, but also to the fewer extent alcohols, ethers and thiols.^{2, 16}



Figure 10: Industrial used Type II PIs: Benzophenone, thioxanthone and camphorquinone.

Monomers

The final properties of photopolymers depend on the structure and functionality of the monomer. The monomer can influence the following parameters of the photopolymer and its curing process:

- Reactivity (high curing speed, conversion rate, scratch resistance, *etc.*)
- Tuning of chemical and mechanical properties (viscosity, toxicity, odor, polymerization shrinkage, *etc.*)
- Reduction of oxygen inhibition
- Photostability, water absorption, and moisture expansion of the cured photopolymer

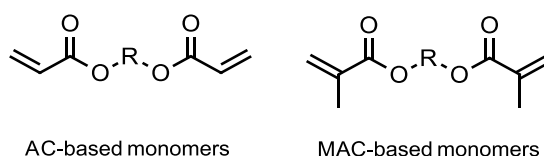


Figure 11: Schematic representation of acrylate (AC)- and methacrylate (MAC)-based monomers.

In FRP, mainly di- and multifunctional acrylate (AC) and methacrylate (MAC) based monomers with long spacers (R) are used. Generally, AC-based monomers create secondary radicals, which are less stable, and therefore more reactive, than the tertiary radicals of the MAC-based monomers. Despite their lower reactivity, MACs can be used, for example, in biocompatible materials like dental fillings especially because of their much lower toxicity range and their compatible heat deflection temperature.

Many different spacer units are used in industry, where its choice mainly depends on the application sector. The chemical and mechanical properties (*e.g.* flexibility, hardness, thermal, or chemical resistance) of the final product can be influenced by the bridging unit leading to further interactions between the macromolecule. Some commonly used spacers are alkyl chains, polyesters, polyethers, polyurethanes, and epoxy oligomers. Alkyl spacers (*e.g.* polyethylene and polypropylene) usually show thermoplastic properties, whereas polyester (*e.g.* polyethylene terephthalate) exhibits a thermoplastic or thermosetting nature. Polyurethanes and polyethers (*e.g.* polyethylene glycol) can offer elastomeric, thermosetting, as well as thermoplastic behaviors. Figure 12 shows some industrially used methacrylate-based monomers with different spacer units, which are particularly used in the dental field.²³

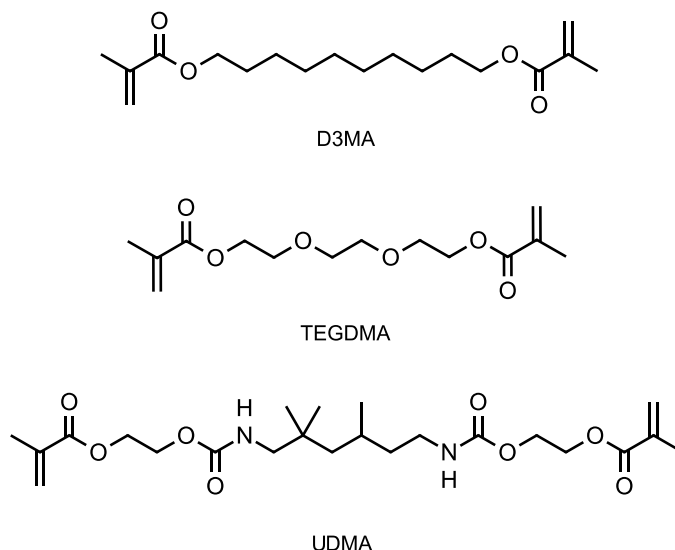


Figure 12: Typical methacrylate-based monomers used in industry: 1,10-decanediol dimethacrylate (D3MA), triethyleneglycol dimethacrylate (TEGDMA) and urethane dimethacrylate (UDMA).

Some monomers are difficult to process due to their high viscosity. One very prominent example is bisphenol-A-glycidyl-dimethacrylate (Bis-GMA), commonly used in industry as a feedstock in dental restorative composite formulations due to its low polymerization shrinkage. Unfortunately, it shows extremely high viscosity, and hence, dilution is necessary for easier handling and higher conversion.²⁴ Therefore, so-called reactive diluents are used to reduce the viscosity of the polymerizable system. Since they are getting incorporated into the cured polymeric system, they can be monofunctional but also act as crosslinkers to achieve higher crosslinking density. These reactive diluents are usually low molecular weight compounds and based again on AC- or MAC-compounds, whereas the previously mentioned compounds D3MA and TEGDMA (Figure 12) can also be used as such reactive diluents. Isobutylmethacrylate (iBMA) dipropylenglycol di(meth)acrylate (DPGD(M)A), trimethylolpropane tri(meth)acrylate (TMPT(M)A) and pentaerythritol tetra(meth)acrylate (PET(M)A) are further industrial examples for reactive diluents (Figure 13).^{5, 25}

R = -H (acrylate) or -CH₃ (methacrylate)

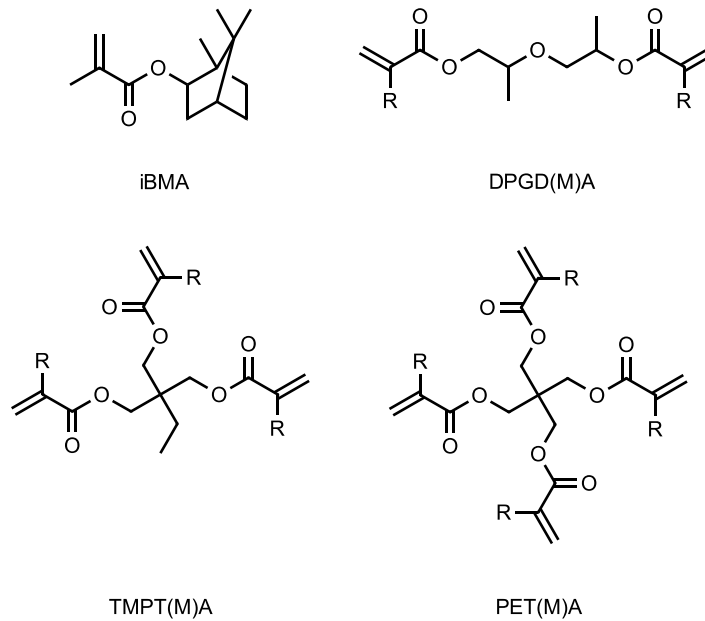


Figure 13: Commonly used reactive diluents in industry: isobutylmethacrylate (iBMA), dipropylglycol di(meth)acrylate (DPGD(M)A), trimethylolpropane tri(meth)acrylate (TMPT(M)A) and pentaerythritol tetra(meth)acrylate (PET(M)A).⁵

Most monomers (M) show relatively high reactivities, and hence, polymerization during storage can occur. The addition of so-called inhibitors prevents unwanted polymerization for some time, up until they are consumed. Two types of inhibitors can be differentiated:

- Addition type (e.g., oxygen or quinone)

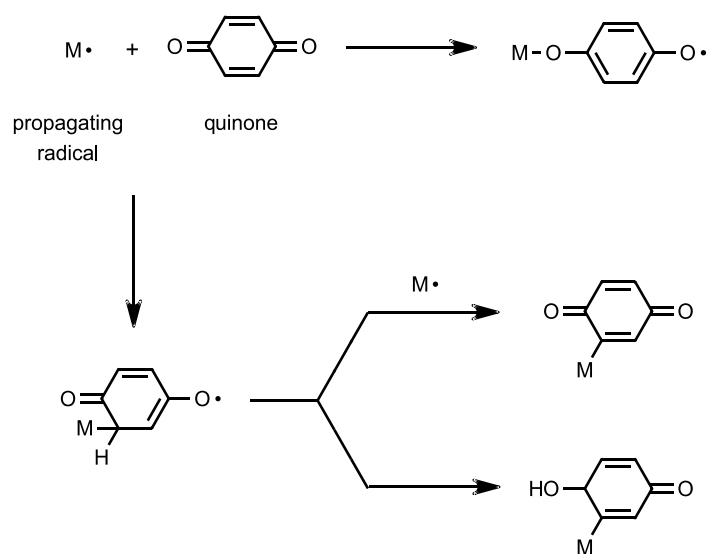


Figure 14: Mechanism of the radical inhibition with quinone as inhibitor.

- Chain transfer type (e.g., *p*-Methoxyphenol (MEHQ))

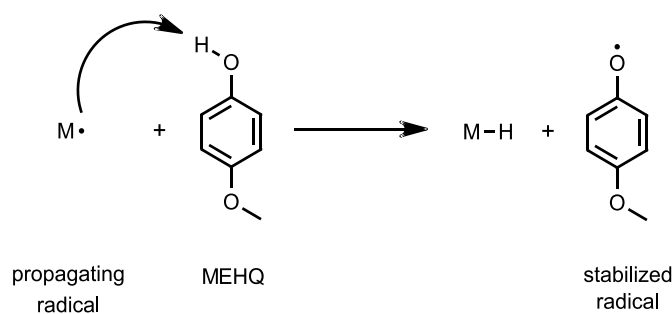


Figure 15: Mechanism of the radical inhibition with MEHQ as inhibitor.

Addition-type inhibitors lead to deactivation of the radical species because the active radical adds onto the inhibitor and forms a deactivated, more stabilized radical. Chain-transfer-type inhibitors terminate the radical species *via* H- or halogen transfer. The inhibitor transforms into a stabilized radical, which gets deactivated, and consequently polymerization reaction cannot occur anymore.²⁶

p-Methoxyphenol (MEHQ) is one of the most commonly used inhibitors in the polymeric industry. It acts as an inhibitor in the presence of dissolved oxygen since the peroxy radicals initiate the quenching of alkyl radicals effectively. A more effective inhibitor, but rather rarely used in industry is phenothiazine, due to its dark color. However, the inhibition with phenothiazine is possible in the absence of oxygen since phenothiazine inhibits the alkyl radicals directly *via* an electron transfer mechanism. The higher effectivity is based on the regeneration of phenothiazine during the inhibition process, and hence lower amounts of the inhibitor are necessary.^{27, 28}

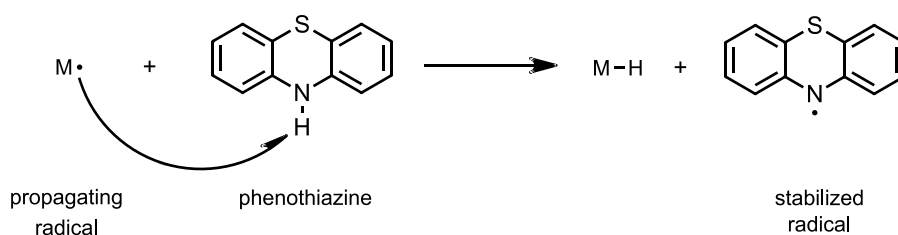


Figure 16: Mechanism of the radical inhibition with phenothiazine as inhibitor.

Shrinkage Stress

One of the significant disadvantages of FRP is the occurrence of volumetric shrinkage and consequently shrinkage stress in cured materials. This disadvantage leads to drastic problems in several application sectors like dental composites and additive manufacturing technologies. Therefore, monomers, which show zero or positive volume change during polymerization, are desired in industry. Volumetric shrinkage can be traced back to changes in distance between the monomers during the polymerization process. In bulk, the distance between the monomers is equal to the Van-der-Waals distance of around 3.4 Å. During polymerization, a covalent bond is formed, and hence, the distance is reduced to about 1.5 Å. Even though a small volume expansion of around 0.2 Å, which is contributed to the conversion of a carbon-carbon DB to a carbon-carbon single bond, is working against this reduction, the negative net change of around 1.9 Å causes significant volumetric shrinkage.²⁹

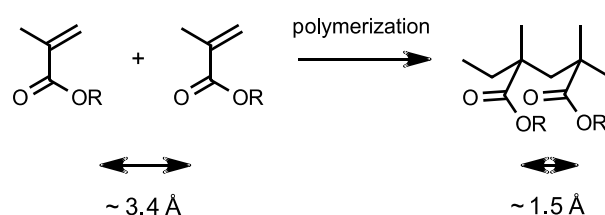


Figure 17: Schematic representation of the distance reduction between monomers during polymerization.³⁰

Volumetric shrinkage can appear until the so-called gelation point (t_g) is reached. The t_g is defined as the time point when the formulation converts from the liquid to the solid, gel-like state due to crosslinking. Before polymerization occurs, the bulk formulation is in the liquid state with mobile monomers. Due to crosslinking of these mobile monomers, volumetric shrinkage appears. Since crosslinking happens extremely fast due to high functional group density, the t_g is reached at low conversion of about 20%. This gelation then leads to a lack of mobility for the growing chains, and volumetric shrinkage is limited. Therefore, the ongoing conversion leads to an inhomogeneous network with inner tension causing shrinkage stress (Figure 18, left).

If the t_g is shifted to higher conversion, the whole network stays flexible for a longer time. Less crosslinking happens after gelation because a reduced volume of monomers is available at this time, and this leads to reduced shrinkage stress (Figure 18, right).^{31, 32}

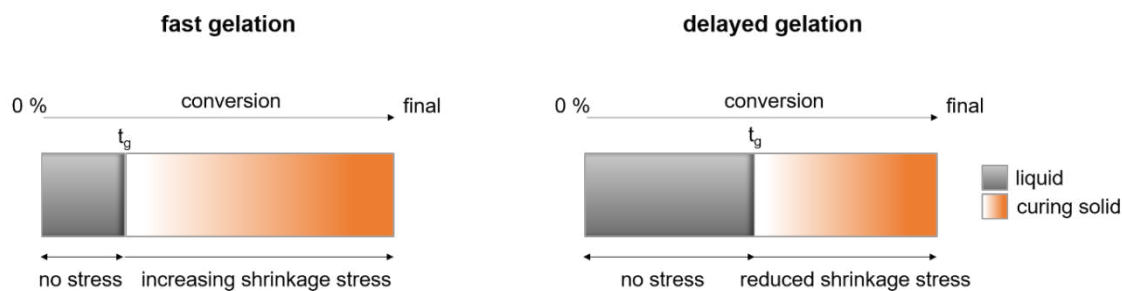


Figure 18: Schematic representation of the relationship between the t_g and the shrinkage stress.^{31, 32}

The shift of t_g is one possible strategy to obtain cured polymeric materials with reduced shrinkage stress. One promising example of this strategy is the use of so-called chain transfer agents (CTA).³³ These CTAs terminate growing polymer chains and initiate new ones at the same time, which leads to a homogeneous chain length distribution and a shift of t_g to higher conversion. Different substances, like nitroxides,³⁴ transition metal compounds,³⁵ or thiols,³⁶ can be used as CTAs. Another promising class of CTA are vinyl sulfone esters, which showed a significant improvement of the mechanical properties (e.g. high toughness) as well as a fast curing time in methacrylate-based formulations for 3D structuring. Therefore, these compounds are of high interest.³⁷ Due to the wide range of monomers, this method is already in the focus point of the industrial sector.

Since there is a high demand in industry for monomers with reduced volumetric shrinkage and shrinkage stress in the cured polymeric material, several other strategies can be found in literature to achieve this reduction. Some examples are presented in the following section.

In the beginning, the use of ring-containing monomers, which were polymerized *via* a ring-opening polymerization (ROP) process and should expand their volume after polymerization, were investigated. Unfortunately, the required monomers showed extremely poor reactivity, and consequently, they found no use in industrial applications.²⁹

Another strategy is the use of high molecular weight monomers like the previously mentioned Bis-GMA and UDMA. These compounds show preorganization, high mechanical strength as well as low polymerization shrinkage. Hence, they are used in industry as a matrix phase for several compositions. The main drawback of these compounds is the usually high viscosity and the limited final conversion. Consequently, the interest in this research field is increasing to improve the processability of this class of monomers without losing the mechanical properties and low shrinkage behavior.^{24, 38}

Surprisingly, one very promising strategy is the so-called cyclopolymerization, which was first discovered and introduced by Butler in the 1950s. Here, two DBs are taking part in a radical reaction to form cyclic units during polymerization *via* altering intermolecular and intramolecular steps. These ring structures lead to linear, non-crosslinked and soluble polymers, which are supposed to show reduced volumetric shrinkage and shrinkage stress compared to their (meth)acrylate analogs.³⁹ Stansbury *et al.* could prove this concept by revealing the low shrinkage behavior of difunctional, oligomeric ether derivatives, which exhibit high cyclization tendency showing a preference for 6-membered ring formation.⁴⁰

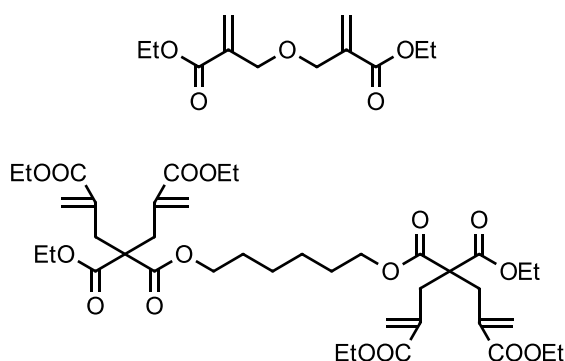


Figure 19: Schematic representation of the difunctional, oligomeric ethyl-ether derivative⁴⁰ and bis-malonate compound.^{30, 41}

Another recent research focused on difunctional cyclopolymerizable monomers (CPM) based on bis-malonates, which also caused low volumetric shrinkage.^{30, 41} Therefore, the topic of difunctional CPMs used as low shrinkage monomers are of high industrial interest.

Objective

Photopolymerization is a major industrial technology since it offers a broad spectrum of advantages, like high energy efficiency, time- and cost-effectiveness, as well as solvent-free usage. Curable photopolymers are widely used in many different application sectors, where coating, additive manufacturing, and the use in the dental and medical industry are only a few representatives. Nevertheless, this method also causes some major problems in several application sectors, like the occurrence of volumetric shrinkage during polymerization. This volumetric shrinkage triggers the development of shrinkage stress in the cured material, which compromises the thermomechanical properties of the final product. Consequently, there is a significant demand in industry for monomers showing reduced volumetric shrinkage, and cyclopolymerization is one possible strategy to overcome this problem.

The aim of this thesis is the creation and investigation of new difunctional 1,6-diene-based cyclopolymerizable monomers based on (meth)acrylamides. These difunctional compounds should show cyclic structures in the polymer backbone upon cyclopolymerization (Figure 20), which is believed to improve the thermomechanical properties (*e.g.* high rigidity), as well as the shrinkage behavior.

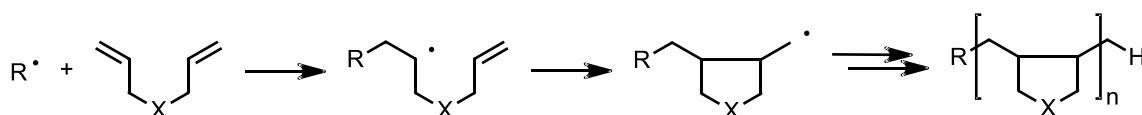


Figure 20: General mechanism of cyclopolymerization.

Several CPMs based on different spacers and their symmetric and asymmetric modifications (*e.g.* with (meth)acrylamide-, allyl-, and allyl-esters-functionalities) should be examined towards their reactivity *via* photo-DSC and RT-NIR photorheology. The most reactive CPMs should then be analyzed regarding their cyclization efficiency, as well as their thermomechanical properties, which should be performed with DMTA and tensile tests.

General Part

1. State of the Art

In the 1950s, Butler *et al.* discovered a completely new mechanism for the polymerization of several polymers, which were based on diallylic quaternary ammonium salts. Hereby, both allylic double bonds (DB) were taking part in a radical reaction to form linear, non-crosslinked, saturated, and soluble polymers *via* an alternating intra-inter-molecular chain growth mechanism (Figure 21).⁴²

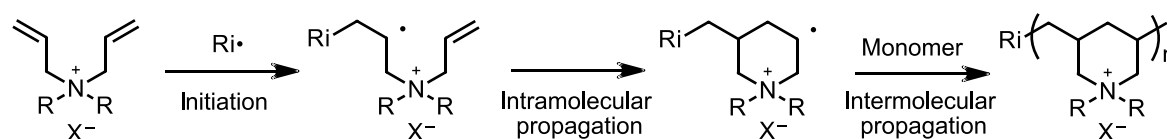


Figure 21: Cyclopolymerization of a diallylic quaternary ammonium salt – proposed mechanism by Butler *et al.*⁴²

The unique characteristic of this so-called cyclopolymerization is the formation of cyclic units in the polymer backbone during the polymerization process without any crosslinking or network formation. This result caused a significant change of view in the chemical society since, until then, it was assumed that polymerization of two or more monomeric DBs would only lead to crosslinked and non-soluble polymers. However, the concept of cyclopolymerization could be proven *via* several analysis methods like NMR and IR studies, potentiometric titration, as well as polymer degradation and fragmentation.⁴²

Mechanism of Cyclopolymerization

In 2004, Hall *et al.* could give a full description of the cyclopolymerization mechanism for the first time, which can be described as an intra-inter-molecular polymerization mechanism. All possibly formed structures, which can appear after a cyclopolymerization of an unspecified substituted diene with a seven-atom center, could be exhibited and are illustrated in Figure 22. However, the formation of different polymer products depends on the initiation as well as on the stability of the free radical.⁴³

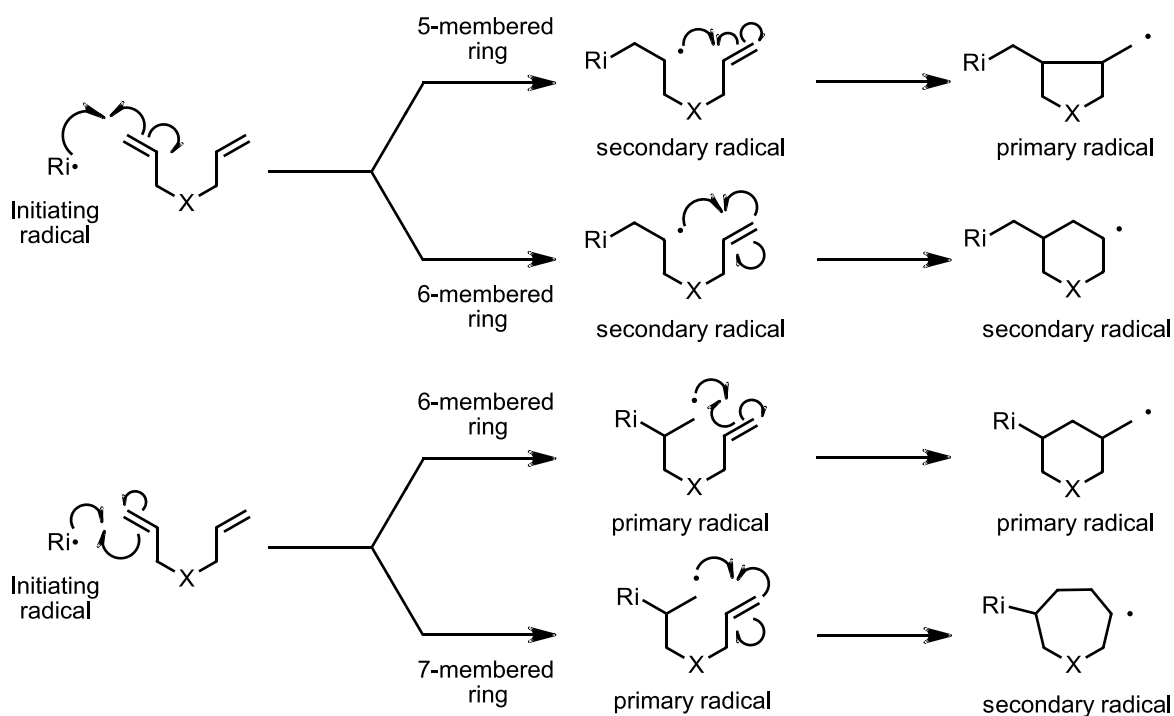


Figure 22: Full description of the cyclopolymerization mechanism by Hall *et al.* yielding 5-membered, 6-membered and 7-membered rings.⁴³

Interestingly, many cyclopolymerizable monomers (CPMs) show a predominance for the formation of 5-membered rings despite the more extensive ring strain and the creation of a less stabilized radical. The 5-membered ring formation is a head-to-head-connection creating a primary radical, which has lower stability and higher reactivity than a secondary one. Consequently, 5-membered rings are seen as kinetically favored, while 6-membered rings, which create the more stabilized secondary radical, are thermodynamically favored.^{42, 43} Hence, the propagation mechanism can be influenced by temperature, chemical environment (*e.g.* solvent), as well as by steric and electronic factors.⁴⁴

Hall *et al.* further suggested that cyclopolymerization is a kinetically favored reaction, and that it should lead to a mixed polymeric system with mainly 5- and 6-membered rings. 7-membered rings are not favored because of the direct rigid backbone linkage without any methylene bridges.⁴³

Kodaira *et al.* stated that specific molecules show a higher tendency to perform an intramolecular propagation than an intermolecular homopolymerization. This consideration is based on the change of the Gibbs Free Energy (ΔG) during polymerization, which can be illustrated *via* the Gibbs-Helmholtz-Equation (Equation 1).

$$\Delta G = \Delta H - T\Delta S$$

Equation 1: Gibbs-Helmholtz-Equation.

If polymerization occurs, ΔG has to be below zero. In general, polymerization usually leads to a loss of entropy, but it is exothermic with a negative change of enthalpy (ΔH). Therefore, most molecules can undergo polymerization until a specific temperature, the so-called ceiling temperature (T_c).

For some molecules, ΔH cannot compensate the significant loss of entropy (ΔS), and therefore, homopolymerization cannot occur. However, the intramolecular step during cyclopolymerization shows a smaller ΔS , even though it is also not favored due to the loss of rotational and translational freedom. This smaller loss of ΔS can be compensated by the more significant change of enthalpy (ΔH), which is driven by the conversion of both π -bonds into σ -bonds with less DBs left after the reaction. Hence, cyclopolymerization can occur, even though homopolymerization is not favored. The intermolecular propagation step during cyclopolymerization can be seen as co-polymerization, and it can occur since some molecules can undergo co- but no homopolymerization. Consequently, cyclopolymerization is energetically favored.

Due to these considerations, it can be stated that bifunctional monomers, where the monofunctional counterpart show low or no homopolymerization tendency, can undergo cyclopolymerization, if these monomers can perform a polymerization reaction at all.⁴⁵

Cyclopolymerizable Monomers

A high degree of cyclization can be achieved by suppressing the intermolecular reactions of the monomer and promoting of intramolecular ones. Therefore, the tendency for cyclization can be influenced by the choice and the position of substituents (R) of the monomer.

Several studies showed that introducing different substituents at the center atom (*e.g.* nitrogen) influences not only the cyclization tendency but also the mechanical and material properties of the cured polymeric material.⁴⁵

Bulky and sterically hindered substituents, like alkyl or aromatic moieties, are known to increase cyclization tendency due to increased rigidity of the polymer backbone. One proof of this concept, which was based on the investigation of literature-known monomers⁴⁶ for photopolymerization reactions, analyzed different photopolymerized allyl-ester compounds (Figure 23) regarding their reactivity and mechanical properties.⁴⁷

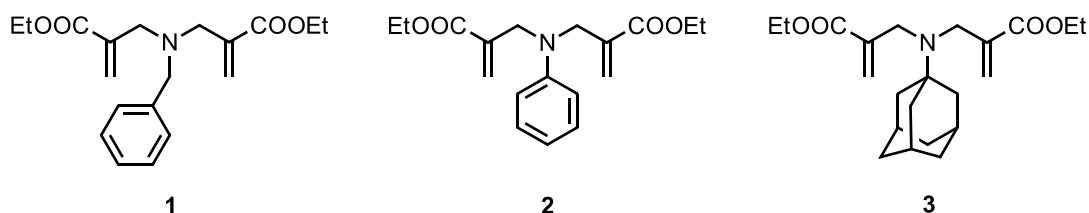


Figure 23: Schematic representation of allyl-ester compounds with different substituents on the nitrogen: benzyl-compound (1), phenyl-compound (2) and adamantyl-compound (3).⁴⁷

Hereby, the more rigid phenyl derivative (2) showed an increased reactivity compared to the benzyl derivative (1). The bulky and most sterically hindered adamantyl carbocycle derivative (3) showed not only the highest reactivity of all compounds, which was in the same range as its comparable methacrylate counterpart but also fast gelation and high molecular weight (MW). Furthermore, it could be proven for the example of the adamantyl-based compound (3) that bulky side groups and rigid backbones also increase the glass transition temperature (T_g), which indicates the transition of a material from a hard, brittle, and glass-like state to a viscous and rubber-like state.⁴⁷

Overall, several studies confirmed that bulky substituents are preferable for cyclopolymerization, and they are also able to tune the material properties, even though they generally reduce the polymerization tendency. Furthermore, these substituents also influence the final structure by varying the ratio of 5- and 6-membered ring formation.⁴⁸

High reactivity and high degree of cyclization can be achieved by the variation of the functional groups (FG) of the bifunctional monomer. A very prominent example is the N-substituted dimethacrylamide (4), which generates completely cyclized polymerizes with various substituents (Figure 24). The high cyclization tendency could be explained by the polymerization inertia of the monoene-counterpart (5), as well as by the activation of the monomer *via* the electron-withdrawing group, the carbonyl group.⁴⁵

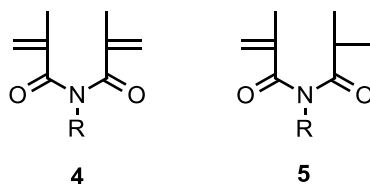


Figure 24: Schematic representation of a dimethacrylamide (4) and its monofunctional counterpart (5).

Asymmetric unconjugated dienes usually show lower cyclization tendency but higher polymerization tendency than symmetrical ones because there is a preference for one DB over the other, which leads to pendant unsaturation.

To achieve asymmetrical unconjugated dienes with a high degree of cyclization, the monoene-part of both side chains should show low or no homopolymerization. Kodaira *et al.* could prove this concept by showing that N-allylmethacrylamide (6) (Figure 25) exhibits high degree of cyclization, while the monomethacryl- and monoallyl-counterpart (7 and 8) have no homopolymerization tendency at all.⁴⁵

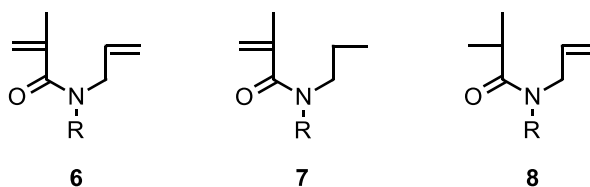


Figure 25: Schematic representation of an N-allylmethacrylamide (6) and its monoene counterparts (7 and 8).

Diacrylamides are also known to have high polymerization tendency as well as self-initiating properties, which means that these monomers can start a photopolymerization reaction without photoinitiator (PI). Therefore, PI-traces cannot influence material properties.⁴⁹

Another study focused on the characterization of diacrylamides (9) with several substituents (R) and the influence of asymmetrically substituted acrylamide-based dienes (e.g. methacryloyl-modification (10)) on their polymerization behavior (Figure 26).⁵⁰

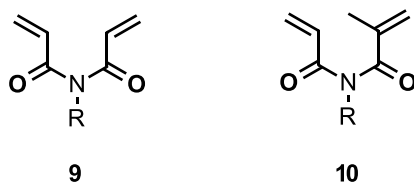


Figure 26: Schematic representation of diacrylamide (9) and asymmetric acrylamide-based compound modified with methacryloyl (10).⁵⁰

The asymmetric methacryloyl-based compound (**10**) exhibit lower reactivity during photopolymerization than the symmetric diacrylamide (**9**) due to steric hindrance caused by the methyl-group. In general, all asymmetric compounds of this study did not show any self-initiating properties and relatively low polymerization behavior.⁵⁰

Overall, increased polymerization tendency and cyclization tendency can be achieved by introducing α -substituents on the allylic DB. Hereby, the α -substituents are usually electron-withdrawing groups like esters (**11**)^{51, 52} or aromatic moieties (**12**)⁵³ and exhibit high conjugative nature (Figure 27).

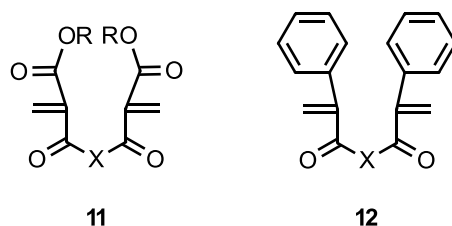


Figure 27: Schematic representation of an α -substituted cyclopolymerizable monomer; ester-activation (11) and phenyl-activation (12).

These substituents increase the reactivity of the formed radical, which prefers intramolecular cyclization reactions due to steric effects. Furthermore, the reactivity of the whole polymeric system could be improved. The monoene-counterparts of these α -substituted compounds are also known to have no or low polymerization tendency, which is also caused by steric factors.^{52, 54, 55}

Kodaira *et al.* stated that monomers, such as unconjugated dienes, show increased reactivity and cyclization tendency by introducing functional groups, like bulky esters with high conjugative nature and low homopolymerization tendency, at the allylic moiety.^{48, 55}

One of many examples for his proposal is the N-substituted N-2-(methoxycarbonyl)-allyl(meth)acrylamide (**13a**, **13b**) and its monofunctional counterparts (**14a**, **14b** and **15a**, **15b**) (Figure 28). Both acryl-functionalities (**14a**, **14b**) show a high conjugative nature and no homopolymerization tendency. In the case of the (meth)allyl-group (**15b**), also no homopolymerization could be observed, whereas the (H)allyl-functionality (**15a**) does have such a tendency.

Consequently, N-2-(methoxycarbonyl)allyl-(meth)acrylamide (**13a**, R = CH₃) reaches a high conversion of up to 60% with a cyclization tendency of around 100%, whereas N-2-(methoxycarbonyl)allylacrylamide (**13b**, R = H) shows just half of this conversion of approximately 30% with a cyclization tendency of maximum 60%.⁵⁶

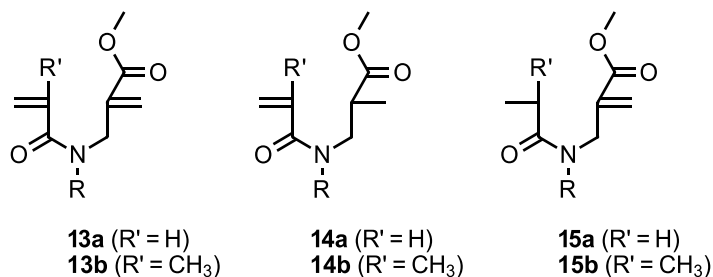


Figure 28: Schematic representation of a *N*-2-(methoxycarbonyl)allyl(meth)acrylamide (13) and its monofunctional counterparts (14 and 15).

However, diallyl compounds (Figure 29), like diallyl ether or diallyl amines, are also able to perform cyclopolymerization, even though they show low reaction rates.⁵⁷

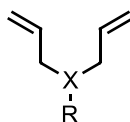


Figure 29: Schematic representation of a diallyl compound.

Despite the lower reactivity compared to acrylate as well as methacrylate compounds, diallylamines and their derivatives are of high industrial interest because the cured polymer shows improved mechanical properties such as low shrinkage, good adhesion and no odor. Furthermore, diallylamines are stable monomers with reduced autopolymerization and can be used without solvent.

The low degree of polymerization (DP) can be traced back to chain transfer reactions (Figure 30). Hereby, the growing polymer chain abstracts an allylic hydrogen and gets terminated. The created radical is more resonance-stabilized. Hence, polymerization efficiency and the molecular weight (MW) decrease.^{58, 59}

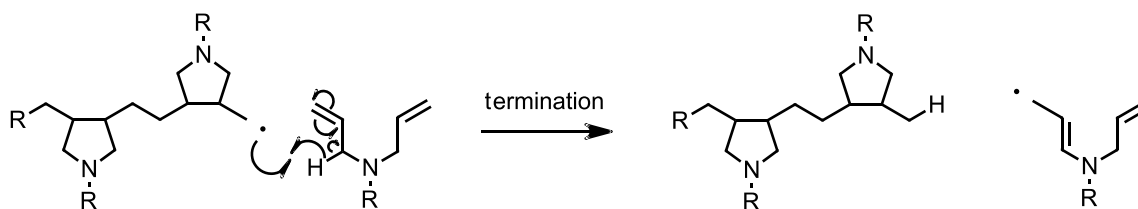


Figure 30: Termination of cyclopolymerization via chain transfer degradation.⁵⁹

Hall *et al.* showed one possibility to improve the low DP by using difunctional compounds with diallylamide or diallylammonium salt groups (Figure 31), which create a three-dimensional polymer network after polymerization.⁵⁹ Hereby, the so-called spacer or bridging unit can also influence the material properties, and a great variety of spacers are commercially available like oligomeric polyamides, polyurethanes, or polyethers.



Figure 31: Schematic representation of a difunctional diallylamine.⁵⁹

Furthermore, diallylamines are easily able to perform copolymerization with various commercially available photoinitiators and other monomers, which also leads to tuned material properties. Therefore, diallylamines and their derivatives are suitable for several application sectors like coatings and adhesives.⁵⁹

However, the topic of light-induced cyclopolymerization of difunctional compounds is rather untouched, even though difunctional CPMs can be used as crosslinking monomers and also show tunable material properties.

Noteworthy research was already done by Kopeinig and co-workers, who focused on the investigation of difunctional diacrylamides (Figure 32) with different spacers, like alkyl, ether or siloxane chain units.^{50, 60}



Figure 32: Schematic representation of a difunctional diacrylamide with different spacer units.⁵⁰

These difunctional diacrylamides showed high polymerization tendency as well as self-initiating properties. Furthermore, it could be demonstrated that the material and mechanical properties of these compounds could be tuned through the variation of the spacer unit.⁵⁰

Another recent research project investigated difunctional CPMs based on bis-malonate compounds as low shrinkage crosslinkers for dental materials. This study evaluated the reactivity, the shrinkage, and the mechanical properties of several difunctional malonate-based CPMs (Figure 33) with different alkyl spacers and compared the results with commercially available compounds.³⁰



Figure 33: Schematic representation of a difunctional malonate-based CPM.³⁰

It could be shown that these difunctional CPMs have a similar reactivity as well as reduced shrinkage stress compared to chosen commercially available reference compounds and that copolymerization of these CPMs with different dimethacrylate compounds, which are widely used in the dental industry, is a reachable possibility.³⁰

2. Diacrylamides

As a starting point of this thesis, a literature-known cyclopolymerizable monomer (CPM) was chosen for investigation to get a better understanding of this topic. It is already known that diacrylamides like CPM 1 show not only fast polymerization behavior but also a high tendency for cyclopolymerization as well as self-initiating properties.⁵⁰

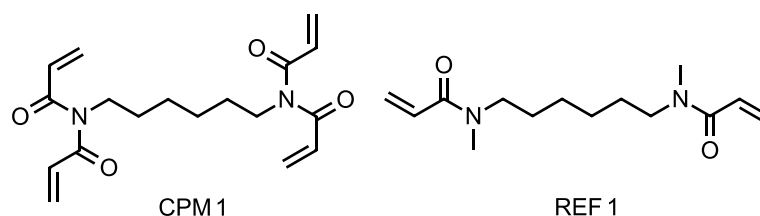


Figure 34: Schematic representation of CPM 1 and REF 1.

Hexamethylenediamine is a commercially available starting material, and its amine groups present an easy opportunity for further functionalization. Therefore, N,N'-(hexane-1,6-diyl)bis(N,N'-bisacrylamide) (CPM 1) was selected for synthesis and investigation of its reactivity. As a reference, the difunctional acrylamide based substance N,N'-(hexane-1,6-diyl)bis(N-methyl-N'-acrylamide) (REF 1), which is supposed to perform homopolymerization, was also synthesized and investigated concerning its polymerization behavior. All reactivity tests should be performed *via* real time near infrared (RT-NIR) photorheology, where not only the reactivity but also the shrinkage behavior of the monomer could be analyzed.

2.1. Synthesis of CPM 1 and REF 1

2.1.1. Synthesis of N,N'-(hexane-1,6-diyl)bis(N,N'-bisacrylamide) - CPM 1

The synthesis of CPM 1 was carried out in one-step reaction in accordance with a procedure published by Kopeinig *et al.*⁶⁰

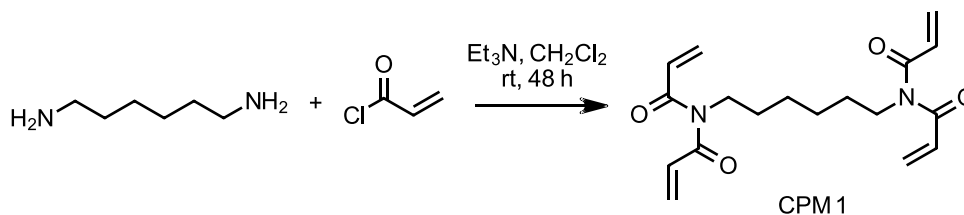


Figure 35: Schematic representation of the synthesis of CPM 1.⁶⁰

For the synthesis of CPM 1, hexamethylenediamine and 6 equivalents (equ) of triethylamine (Et_3N) was converted with 6 equ of freshly distilled acryloyl chloride in dry dichloromethane (CH_2Cl_2) under argon atmosphere. The reaction progress was monitored *via* NMR and TLC. After the work-up procedure (extraction), the crude product was purified *via* column chromatography to obtain CPM 1 as a slightly yellow liquid with a yield of around 15%.

Several synthetic attempts, as well as different work-up procedures, were carried out to aim for an increased yield of CPM 1. The first approach focused on conversion. To obtain higher conversion and consequently a higher final yield of CPM 1, the synthetic procedure was modified using increased temperature (80 °C), a higher amount of inhibitor (1000 ppm MEHQ and 1000 ppm phenothiazine) or greater excess of acryloyl chloride (9 equ). None of these trials increased the conversion of CPM 1. Therefore, the second approach focused on the modification of the work-up procedure, especially the extraction, using either distilled water or 1 N HCl, followed by NaHCO_3 and brine. The work-up was also tried to be performed without any extraction step giving no product at all. Unfortunately, none of those approaches led to a successful strategy for the synthesis of CPM 1. The high reactivity of CPM 1 and consequently the challenging stabilization of this monomer were assumed to be the primary source for the relatively low yield.

2.1.2. Synthesis of N,N'-(hexane-1,6-diy)bis(N-methyl-N'-acrylamide) – REF 1

The monofunctional reference substance REF 1 is synthesized according to a procedure of Moszner *et al.*⁶¹

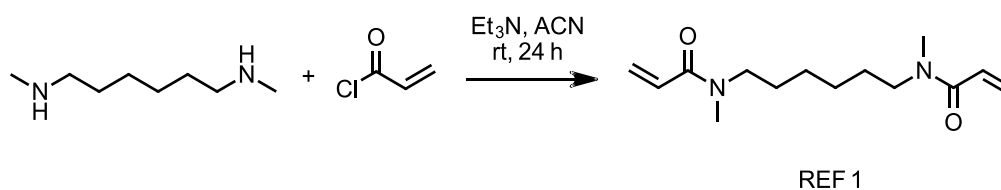


Figure 36: Schematic representation of the synthesis of REF 1.⁶¹

For the synthesis of REF 1, N,N'-dimethyl-1,6-hexanediamine and 3 equ of Et_3N was reacted with 3 equ of freshly distilled acryloyl chloride in anhydrous acetonitrile (ACN) under argon atmosphere. The reaction progress was monitored *via* NMR and TLC. After the work-up procedure (extraction), the crude product was purified *via* column chromatography to obtain REF 1 as a slightly yellow liquid with a yield of 44%.

2.2. Reactivity studies of CPM 1 and REF 1

After the partially successful synthesis of CPM 1 and its acrylamide reference substance REF 1, the reactivity of both compounds could be investigated *via* RT-NIR-photorheology measurements and compared to each other. Furthermore, the rheological behavior (shrinkage force) of these diacrylamide compounds could be analyzed as well.

2.2.1. RT-NIR-photorheology of CPM 1 and REF 1

The kinetic and rheological behavior of a monomer can be examined *via* RT-NIR photorheology measurements. Therefore, the photorheological measurements of CPM 1 were conducted and compared to the reference substance REF 1 as well as to the commercially available acrylate-based compound 1,6-hexanedioldiacrylate (HDDA). It is expected that CPM 1 shows a reactivity higher than REF 1 and HDDA due to its higher functionalization and the possibility to perform cyclopolymerization.

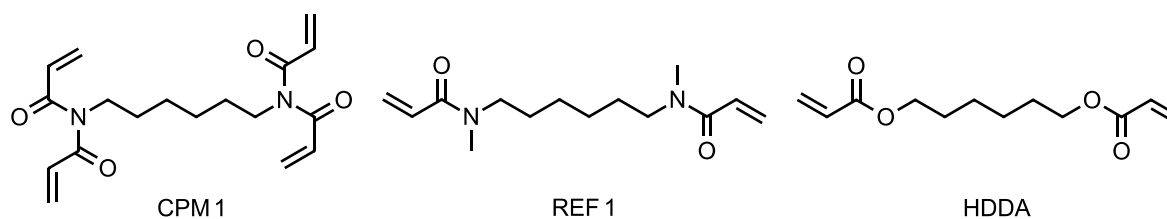


Figure 37: Schematic representation of CPM 1, REF 1 and HDDA.

The measurements were performed in triplicates with 0.5 mol% photoinitiator (PI) Ivocerin® at 25 °C. The irradiation of the samples was performed with a broadband Hg-lamp using a 400-500 nm filter and a light intensity of 1 W cm⁻² at the end of the light guide. For each measurement, 150 µL of the sample was applied with an Eppendorf pipette on the glass disk protected with a PE-tape. The gap between the glass disk and the measuring system (PP25) was kept at a constant size of 200 µm. The double bond conversion (DBC in %) could be calculated by integrating the DB-IR-signal around 6170 cm⁻¹, and comparing it over time to the integrated DB-signal at t₀.

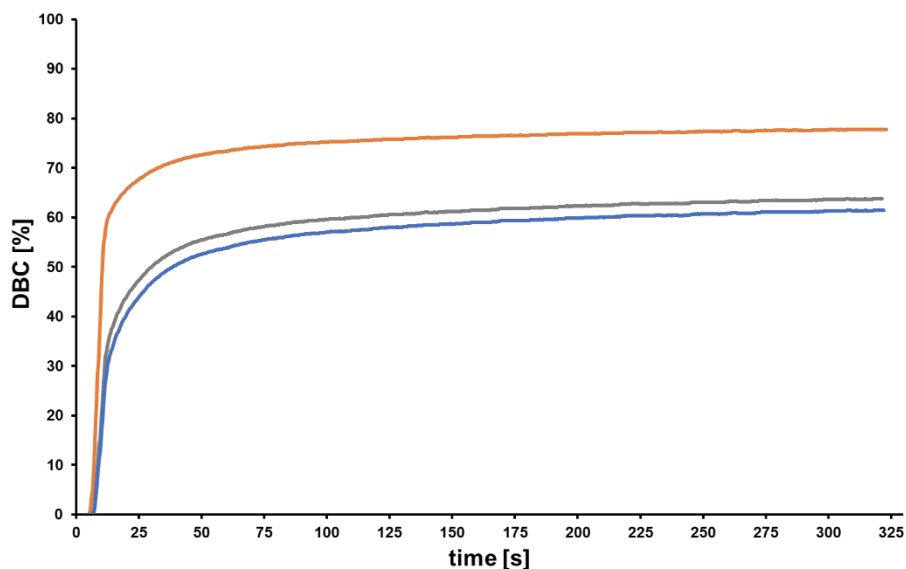


Figure 38: Conversion over time of CPM 1 (-), REF 1 (-), and HDDA (-) (25 °C, 0,5 mol% PI), light starts after 5 s.

Figure 38 shows the conversion of CPM 1, REF 1 and HDDA over time at 25 °C and 0.5 mol% PI. As expected, CPM 1 shows not only the highest conversion of around 78% but also the fastest reaction speed (12.1 \% s^{-1}), which can be evaluated *via* the slope of the curve (DBC per s) (Table 1).

Table 1: DBC per s of CPM 1, REF 1 and HDDA.

	DBC per s [% s ⁻¹]
CPM 1	12.1
REF 1	5.7
HDDA	7.1

The reference substances REF 1 and HDDA just reach a conversion of around 64% and 61% respectively. Additionally, the reaction speed of both compounds is slower than that of CPM 1. It can be stated that CPM 1 shows not only the highest conversion but also the fastest reaction speed compared to its reference compound REF 1 and the conventional acrylate-based substance HDDA. The exact values for the final DBC (DBC_{final}), as well as the time at 95% conversion (t_{95}), are summarized in Table 2.

The gel point of a photocurable formulation is the transition point from the liquid to the gel-like state, and it can be determined with RT-NIR photorheology measurements. The polymerization time until gelation (t_g) corresponds with the intersection point of the storage modulus G' and the loss modulus G'' ($G'/G'' = 1$). The obtained t_g was then used to calculate the conversion at the gel point (DBC_g) summarized in Table 2.

Table 2: Summarized results of the RT-NIR-photorheology measurements of CPM 1, REF 1, and HDDA.

	t_g [s]	DBC_g [%]	t_{95} [s]	DBC_{final} [%]	G' [MPa]
CPM 1	1.4 ± 0.1	30.1 ± 1.0	60.1 ± 7.3	78.0 ± 1.0	566 ± 8
REF 1	12.2 ± 0.0	39.8 ± 0.3	118.5 ± 1.5	61.1 ± 0.3	538 ± 60
HDDA	2.6	23.4	125.3	63.7	585

As expected, CPM 1 shows the fastest t_g of 1.4 s, followed by the commercially available HDDA of 2.6 s. The reference substance REF 1 shows a relatively late t_g of around 12.2 s. This can be explained by the higher reaction speed of the other compounds as well as the more rigid conformation of REF 1.

The comparison of the DBC at t_g (DBC_g) exhibit the high reactivity of CPM 1, since it reaches the t_g fastest, showing higher DBC_g as HDDA. Therefore, it is expected that CPM 1 shows a reduced shrinkage compared to HDDA since volumetric shrinkage can appear after the gelation point. However, REF 1 reaches its t_g relatively late and therefore, the DBC_g -value is also at a higher level.

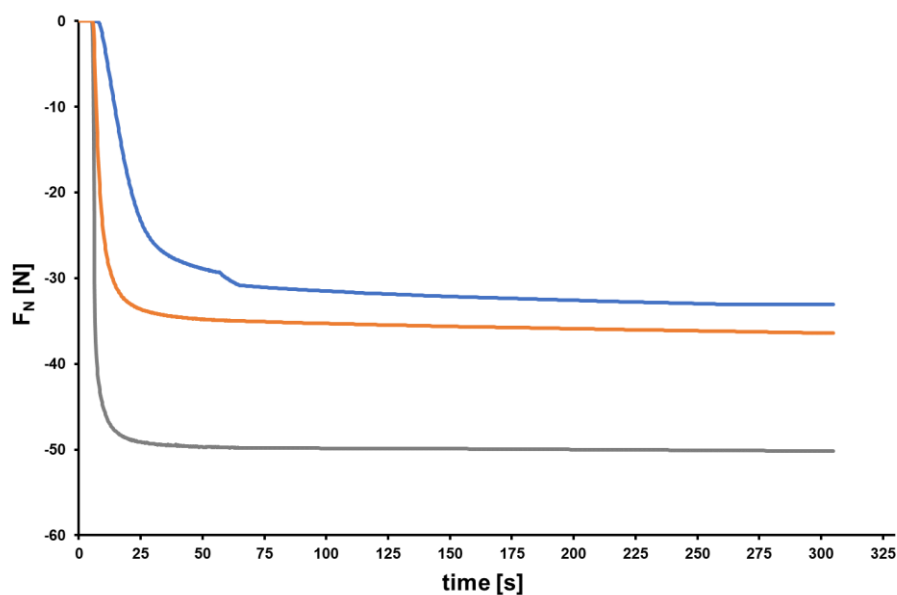


Figure 39: Shrinkage force over time of CPM 1 (●), REF 1 (●), and HDDA (●), (25 °C, 0,5 mol% PI), light starts after 5 s.

The shrinkage force (F_N) can be obtained from the rheological measurement, and it was recorded over time. Hereby, it is important to mention that F_N depends directly on the conversion. Since there is a relatively large variation in the DBC_{final} values, the final F_N values cannot directly be compared with each other. To solve this issue, F_N was determined at a DBC-value of 60%, and this F_N (60% $_{\text{DBC}}$) was used for comparison.

Table 3: Shrinkage forces of CPM 1, REF 1 and HDDA.

	F_N (final) [N]	F_N (60% $_{\text{DBC}}$) [N]
CPM 1	-35.7 ± 0.7	-28.9 ± 1.3
REF 1	-32.0 ± 0.8	-31.8 ± 0.3
HDDA	-44.6	-49.7

The comparison of F_N at 60% DBC reveals that CPM 1 clearly shows the lowest shrinkage force ($F_N = -28.9$ N) of all three compounds. The commercially available HDDA has almost the double amount of shrinkage ($F_N = -49.7$ N), while the shrinkage force of the monofunctional reference REF 1 ($F_N = -31.8$ N) is similar to that of CPM 1 due to the more rigid structure of the homopolymerized monomer.

In summary, it was proven that CPM 1 shows not only a fast reaction speed and a high conversion compared to the chosen reference substances (REF 1 and HDDA), but also a reduced shrinkage force. The high reactivity of the acryloyl-group prevented an economically successful synthesis of CPM 1. Therefore, the focus of this work was changed to the less-reactive, but more stable methacrylamide compounds.

3. Dimethacrylamides

Dimethacrylamides are known to be less-reactive, but more stable than diacrylamides, due to the steric hindrance of the methyl-group. This steric hindrance contributes to the high degree of cyclization. The monofunctional counterparts additionally show comparably low homopolymerization tendency to improve the cyclization tendency further.⁴⁵ Consequently, difunctional dimethacrylamides seem to be suitable compounds for different modifications and further investigations regarding their kinetic and mechanical behavior.



Figure 40: Schematic representation of a difunctional dimethacrylamide with exchangeable spacer unit.

Different alkyl-based spacers were investigated in order to find the most suitable bridging unit for reactivity-enhancing modifications. As a starting point, the previously investigated 1,6-hexamethyldiamine spacer, which already generated liquid CPMs with the acryloyl-functionalizations, was modified with methacryloyl-groups to obtain CPM 2. Unfortunately, CPM 2 was obtained as white crystals with a melting point (mp.) of around 95 °C.

The melting point of a monomer can be lowered by extending the chain length of the spacer unit. Therefore, 1,12-diaminododecan was also modified with methacryloyl-groups to obtain CPM 3, which shows a reduced melting point (mp. = ~ 50 °C), but was still obtained as white crystals.

Another promising strategy is the use of branched spacer units. Hence, the established UDMA-spacer, which is a steric mixture of (2,2,4) and (2,4,4) trimethylhexane-1,6-diamine, was used for modification (CPM 4) and further investigated regarding its kinetic and mechanical behavior.

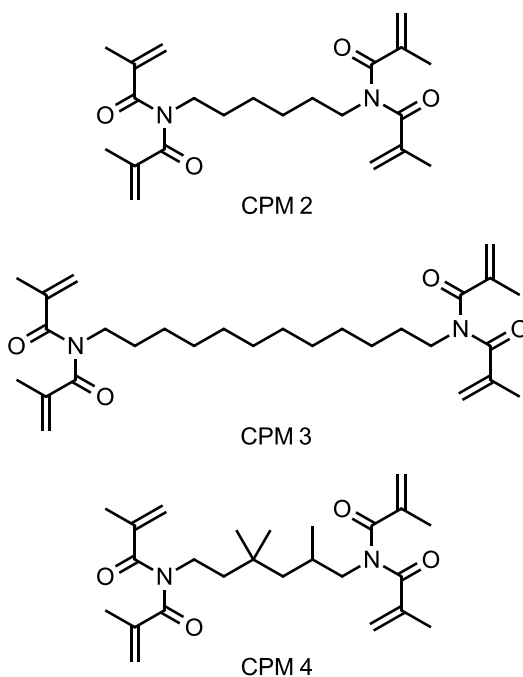


Figure 41: Schematically representation of CPM 2, CPM 3 and CPM 4.

3.1. Synthesis of CPM 2, CPM 3, and CPM 4

3.1.1. Synthesis of N,N'-(hexane-1,6-diyl)bis(N,N'-bismethylacrylamide) - CPM 2

The synthesis of CPM 2 was carried out in a one-step reaction in accordance with a procedure published by Kopeinig *et al.*⁶⁰

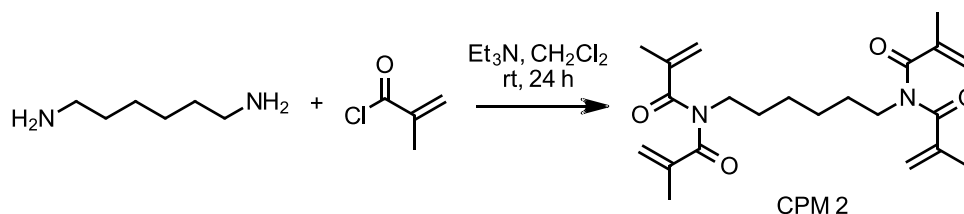


Figure 42: Schematic representation of the synthesis of CPM 2.⁶⁰

For the synthesis of CPM 2, hexamethylenediamine and 6 equ of Et_3N was converted with 6 equ of freshly distilled methacryloyl chloride in dry CH_2Cl_2 under argon atmosphere. The reaction progress was monitored *via* NMR and TLC. After the work-up procedure (extraction), the crude product was purified *via* column chromatography and recrystallization in methanol (MeOH) to obtain CPM 2 as white crystals with a yield of around 38% and a melting point of 95.4-96.6 °C.

Unfortunately, CPM 2 could not be dissolved in the reactive diluent 1,10-decandiol dimethacrylate (D3MA) and dimethylacrylamide (DMAA), and hence the kinetic and mechanical properties could not be investigated.

Liquid CPMs can be obtained by exchanging the spacer unit of the difunctional dimethacrylamide compound. One strategy for spacer modification would be to extend the alkyl chain and consequently lower the melting point of the final CPM.

3.1.2. Synthesis of N,N'-(dodecan-1,12-diyl)bis(N,N'-bismethacrylamide) - CPM 3

A chain-length extension of the spacer unit can lead to a lowering of the melting point, and consequently to a liquid CPM. Therefore, 1,12-diaminododecan was chosen as one possible spacer unit and modified with methacryloyl-groups. The synthesis of CPM 3 was again carried out in a one-step reaction in accordance with a procedure published by Kopeinig *et al.*⁶⁰

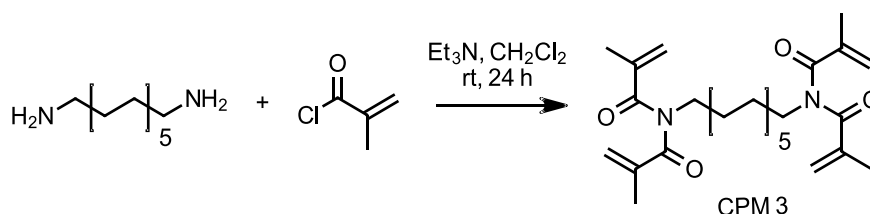


Figure 43: Schematic representation of the synthesis of CPM 3.

For the synthesis of CPM 3, 1,12-diaminododecane and 6 equ of Et₃N was reacted with 6 equ of freshly distilled methacryloyl chloride in dry CH₂Cl₂ under argon atmosphere. The reaction progress was monitored *via* NMR and TLC. After the work-up procedure (extraction), the crude product was purified *via* column chromatography to obtain CPM 3 as white crystals with a yield of around 60% and a melting point of 49.5-51.0 °C.

CPM 3 also showed limited solubility in the chosen reactive diluent (D3MA), and consequently no kinetic or mechanical behavior could be investigated.

3.1.3. Synthesis of N,N'-(2,2,4(2,4,4)-trimethylhexane-1,6-diyl) bis(N,N'-bismethylacrylamide) - CPM 4

Another strategy to obtain more flexibility and consequently liquid CPMs is the use of a sterically hindered spacer. Therefore, the commercially available mixture of (2,2,4) and (2,4,4) trimethylhexane-1,6-diamine was chosen for modification. The synthesis of CPM 4 was again carried out in a one-step reaction in accordance with a procedure published by Kopeinig *et al.*⁶⁰

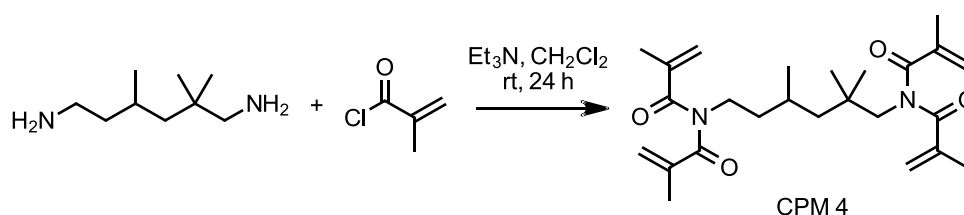


Figure 44: Schematic representation of the synthesis of the (2,2,4)-isomer of CPM 4.

For the synthesis of CPM 4, trimethylhexane-1,6-diamine and 6 equ of Et_3N was reacted with 6 equ of freshly distilled methacryloyl chloride in dry CH_2Cl_2 under argon atmosphere. The reaction progress was monitored *via* NMR and TLC. After the work-up procedure (extraction), the crude product was purified *via* column chromatography to obtain CPM 4 (2 isomers) as a colorless viscous liquid with a yield of around 50%.

CPM 4 (polymerized with 1 mol% PI Ivocerin[®]) was investigated regarding its kinetic and mechanical properties *via* attenuated total reflectance infrared spectroscopy (ATR-IR), photo differential scanning calorimetry (photo-DSC), real time near infrared (RT-NIR) photorheology, dynamic mechanic thermal analysis (DMTA) and tensile tests. The analysis will be discussed in chapter 4.3. Furthermore, this sterically hindered spacer was used for further symmetric and asymmetric modifications to obtain more reactive CPMs and two literature-related reference compounds (REF). These CPMs and REFs (described in chapter 4) were also investigated regarding their kinetic (4.3) and mechanical behavior (4.4), and their results were compared to each other.

4. CPMs and REFs based on

(2,2,4)/(2,4,4)-trimethylhexane-1,6-diamine

After the previously-mentioned investigation of the spacer unit (described in chapter 3), the mixture of (2,2,4) and (2,4,4) trimethylhexane-1,6-diamine was chosen as sterically hindered spacer unit for reactivity-enhancing modifications.

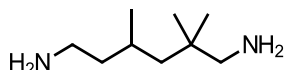


Figure 45: Structure of the (2,2,4)-isomer of the trimethylhexane-1,6-diamine spacer unit.

The aim was to synthesize several difunctional 1,6-diene-based CPMs and REFs modified with different functional groups in a symmetric and an asymmetric way and to analyze their kinetic and mechanical properties *via* ATR-IR spectroscopy, photo-DSC, RT-NIR photorheology, DMTA, and tensile tests.

As a starting point, two literature-related reference substances (REF 2⁶⁰ and REF 3⁶²), which presumably show low reactivity, were synthesized. REF 2 and REF 3 are the monofunctional counterparts of the methacrylamide compound, whereas REF 3 is additionally modified with a methyl-group for further steric hindrance. For the literature-related CPM 5,⁶² the spacer unit was symmetrically modified with allyl-groups, which is supposed to exhibit low reactivity.

As already mentioned in the previous chapter (3.1.3), the symmetric methacrylamide based modification CPM 4 could be obtained as liquid monomer. In general, the reactivity of CPMs can be improved by introducing α -substituents on the DB.⁴⁵ Therefore, the chosen bridging unit was modified symmetrically for CPM 6, which DBs are activated *via* electron-withdrawing ester-groups. Consequently, CPM 6 should show the highest reactivity in the whole library.

Asymmetric modifications are known to show an increased polymerization tendency.⁴⁵ Hence, the spacer unit was tried to be modified in an asymmetric way for CPM 7 and CPM 8, whereas REF 2 was used as starting material for these compounds.

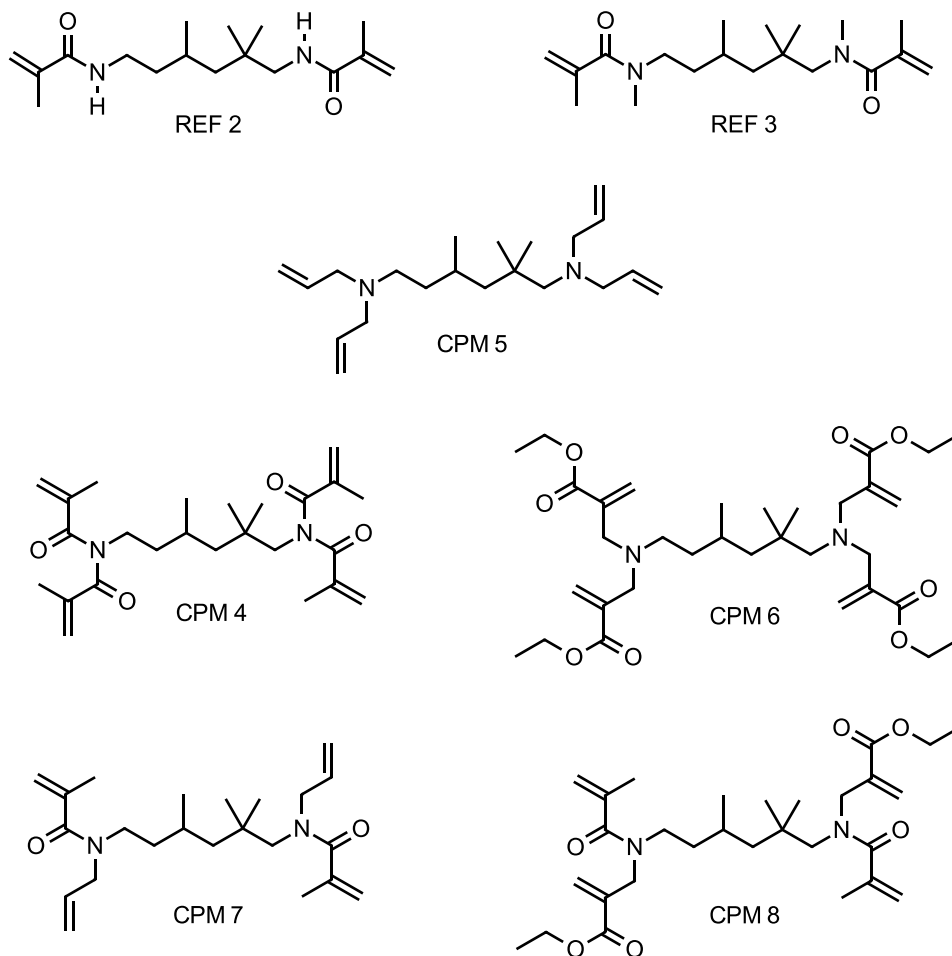


Figure 46: Schematically representation of REF 2, REF 3, CPM 4, CPM 5, CPM 6, CPM 7, and CPM 8.

All synthesized compounds based on the trimethylhexane-1,6-diamine spacer unit (CPM 4, CPM 5, CPM 6, CPM 7, REF 2, and REF 3) were then investigated regarding their kinetic and mechanical behavior, and the results were compared to each other.

4.1. Synthesis of the REF 2 and REF 3

4.1.1. Synthesis of N,N'-(2,2,4(2,4,4)-trimethylhexane-1,6-diyl)

bis(N-methylacrylamide) – REF 2

REF 2 is the intermediate product for the synthesis of the asymmetric modifications (REF 3, CPM 7, and CPM 8), and it was also chosen as reference substance for investigating the kinetic and mechanical properties. However, it is important to mention that REF 2 can form hydrogen-bonding, influencing its reactivity. The synthesis of REF 2 was carried out in a one-step reaction in accordance with a procedure published by Kopeinig *et al.*⁶⁰

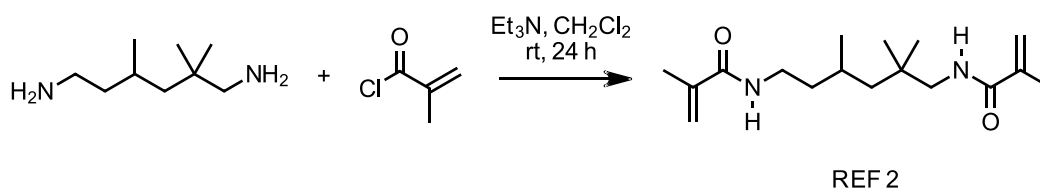


Figure 47: Schematic representation of the synthesis of the (2,2,4)-isomer of REF 2.

For the synthesis of REF 2, trimethylhexane-1,6-diamine and 2.4 equ of Et_3N was reacted with 2.4 equ of freshly distilled methacryloyl chloride in dry CH_2Cl_2 under argon atmosphere. The reaction progress was monitored *via* NMR and TLC. After the work-up procedure (extraction), the crude product was purified *via* column chromatography to obtain REF 2 (2 isomers) as a colorless viscous liquid with a yield of around 94%.

4.1.2. Synthesis of N,N'-(2,2,4(2,4,4)-trimethylhexane-1,6-diyl) bis(N-methyl-N'-methylacrylamide) - REF 3

1,6-Diene compounds are forecasted to show cyclopolymerization tendency if their monoene counterpart is just able to perform low homopolymerization, but has a general polymerization tendency.⁴⁵ Consequently, the monofunctional methacrylamide based counterpart (REF 3) was chosen as reference substance and investigated towards its reactivity. The reaction of REF 3 was performed in a two-step reaction according to a procedure published by Ho *et al.*,⁶² where REF 2 (described in chapter 4.1.1) was used as starting material.

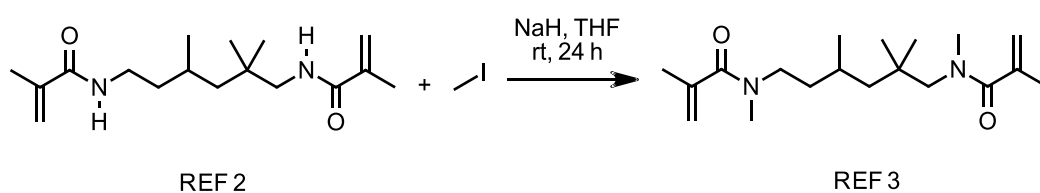


Figure 48: Schematic representation of the synthesis of the (2,2,4)-isomer of REF 3.

For the second step of the synthesis of REF 3, REF 2 was suspended in 5 equ of sodium hydride (NaH) in dry tetrahydrofuran (THF) under argon atmosphere. Afterwards, it was reacted with 5 equ of methyl iodide. The reaction progress was monitored *via* NMR and TLC. After work-up procedure (extraction), the crude product was purified *via* column chromatography to obtain REF 3 (2 isomers) as a clear, viscous liquid with a yield of around 66%.

4.2. Synthesis of CPM 5, CPM 6, CPM 7, and CPM 8

4.2.1. Synthesis of 1,6-bis(diallylamino)-2,2,4(2,4,4)-trimethylhexane – CPM 5

According to literature,^{57, 59} diallyl-compounds show a low degree of polymerization (DP), and they can perform cyclopolymerization with various spacer units. Hence, they seem to be an ideal compound for cyclopolymerizable modifications. The synthesis of CPM 5 was performed in a one-step reaction in accordance with a procedure published by Ho *et al.*⁶²

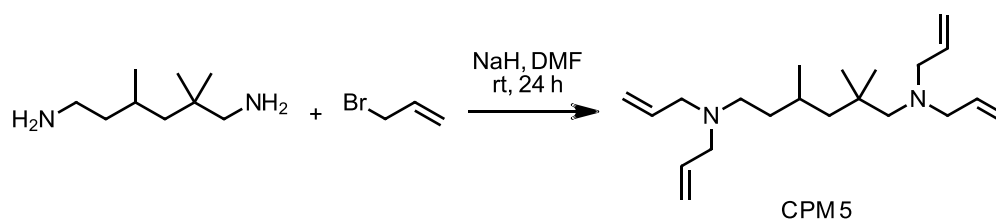


Figure 49: Schematic representation of the synthesis of the (2,2,4)-isomer of CPM 5.

For the synthesis of CPM 5, trimethylhexane-1,6-diamine was suspended in 10 equ of NaH in dry dimethylformamide (DMF) under argon atmosphere. Afterwards, it was reacted with 10 equ of freshly distilled methacryloyl chloride. The reaction progress was monitored *via* NMR and TLC. After work-up procedure (extraction), the crude product was purified *via* column chromatography on aluminum oxide to obtain CPM 5 (2 isomers) as a clear, viscous liquid with a yield of around 68%. Unfortunately, CPM 5 could not be obtained purely, but as a mixture with the trifunctionalized compound (2 isomers) (~ 25%). Nevertheless, CPM 5 was analyzed regarding its kinetic properties and compared to the other modifications.

4.2.2. Synthesis of tetraethyl-2,2',2'',2'''-(((2,2,4-trimethylhexane-1,6-diyl)bis(azanetriyl))tetrakis(methylene))tetraacrylate - CPM 6

Electron-withdrawing ester functionalities are influencing the reactivity of a DB to a great extent.⁵² Hence, ester-activated CPMs should show high reactivity as well as high cyclization tendency. These symmetrical ester-activated CPMs could already be successfully synthesized and polymerized in several research projects with thermal bulk and solution polymerization⁴⁶ as well as with photopolymerization.⁴⁷ It was shown that some of these CPMs, especially with bulky substituents, favor cyclization reactions with a high degree of cyclization (DC) near 100%.

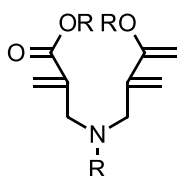


Figure 50: Schematic representation of a symmetric ester-activated compound.

Therefore, the aim was to synthesize the difunctional ester-activated compound CPM 6 and to investigate its kinetic and mechanical properties. We suppose that this compound should show the highest reactivity of all modifications. The synthesis of CPM 6 was performed in a one-step reaction in accordance with a procedure published by Peer and co-workers.⁴⁷

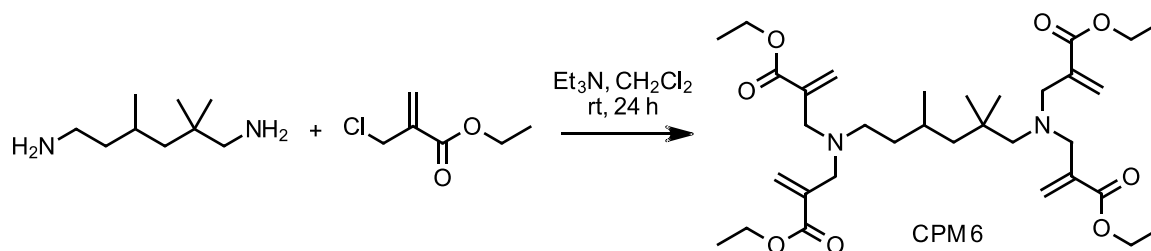


Figure 51: Schematic representation of the synthesis of CPM 6.

For the synthesis of CPM 6, trimethylhexane-1,6-diamine and 6 equ of Et_3N was reacted with 6 equ of ethyl-2-(chloromethyl)acrylate in dry CH_2Cl_2 under argon atmosphere. The reaction progress was monitored *via* NMR and TLC. After the work-up procedure (extraction), the crude product was purified *via* column chromatography to obtain CPM 6 as a colorless viscous liquid with a yield of around 75%.

4.2.3. Synthesis of N,N'-(2,2,4(2,4,4)-trimethylhexane-1,6-diyl)

bis(N-allyl-N'-methylacrylamide) - CPM 7

In order to see the behavior of mixed 1,6-diene-based CPMs, the mixed monomers CPM 7 and CPM 8 were synthesized for further kinetic and mechanical investigations. In general, asymmetric unconjugated dienes are known to show a lower cyclization tendency but a higher polymerization tendency, because there is a preference of one DB over the other, leading to pendant unsaturations.⁴⁵ The synthesis of the asymmetric CPM 7 was carried out in a two-step reaction in accordance with a procedure published by Ho *et al.*,⁶² while REF 2 was used as starting material.

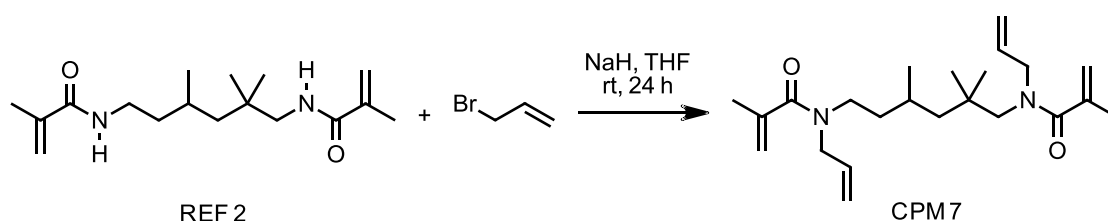


Figure 52: Schematic representation of the synthesis of the (2,2,4)-isomer of CPM 7.

For the second step of the synthesis of CPM 7, REF 2 was suspended in 10 equ of NaH in dry THF under argon atmosphere. Afterwards, it was reacted with 10 equ of allyl bromide. The reaction progress was monitored *via* NMR and TLC. After work-up procedure (extraction), the crude product was purified *via* column chromatography to obtain CPM 7 (2 isomers) as a clear, viscous liquid with a yield of around 53%.

4.2.4. Synthesis of N,N'-(2,2,4(2,4,4)-trimethylhexane-1,6-diyl) bis(N-(ethyl-2-(chloromethyl)acryloyl)-N'-methylacrylamide) - CPM 8

As already mentioned, electron-withdrawing groups with a high conjugative nature, like esters or aromatic moieties, can activate the allylic DBs leading to increased cyclopolymerization tendency.⁴⁵ Kodaira *et al.* already synthesized and investigated asymmetric CPMs (Figure 53), where just one allyl-group was activated *via* the ester-group. Their monomers could be polymerized *via* thermal bulk polymerization with a very high degree of cyclization of around 93%.⁶³

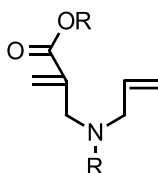


Figure 53: Schematic representation of a *N*-substituted-*N*-allyl-2-(ethoxycarbonyl)allylamine.⁶³

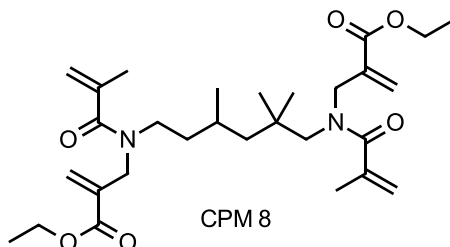


Figure 54: Schematic representation of the (2,2,4)-isomer of CPM 8.

Therefore, the aim was to synthesize an asymmetric ester-activated CPM (CPM 8) with trimethylhexane-1,6-diamine as spacer unit. Several synthetic approaches were tried to obtain the desired monomer unsuccessfully. The first approach series was carried out with REF 2 as starting material and the commercially available ethyl-2-(chloromethyl)acrylate compound as well as the more-reactive ethyl-2-(iodomethyl)acrylate compound, which was synthesized *via* a Finkelstein reaction with sodium iodide (NaI) in acetone. All the reaction conditions of the first series are summarized in Table 4. The reactions were monitored *via* NMR after reaction times of 2 h, 12 h, 24 h, and 48 h. Unfortunately, none of these conditions could give the desired product CPM 8.

Table 4: Reaction conditions for the synthesis of CPM 8 with ethyl-2-(chloromethyl)acrylate and ethyl-2-(iodomethyl)acrylate as starting material.

Trial	Base	Solvent	Temperature
1	NaH	THF	0 °C, RT
2	K ₂ CO ₃	CH ₃ CN	RT / 90 °C
3	Et ₃ N	CH ₂ Cl ₂	RT
4	K(t-BuO)	THF	RT / 60 °C
5	NaH	DMF	RT / 50 °C
6	K ₂ CO ₃	CH ₃ CN	RT / 90 °C
7	Cs ₂ CO ₃	CH ₃ CN	RT / 90 °C
8	DBU	DMF	80 °C

For the second approach series, trimethylhexane-1,6-diamine was modified first with ethyl-2-(chloromethyl)acrylate, and then with methacryloyl chloride.

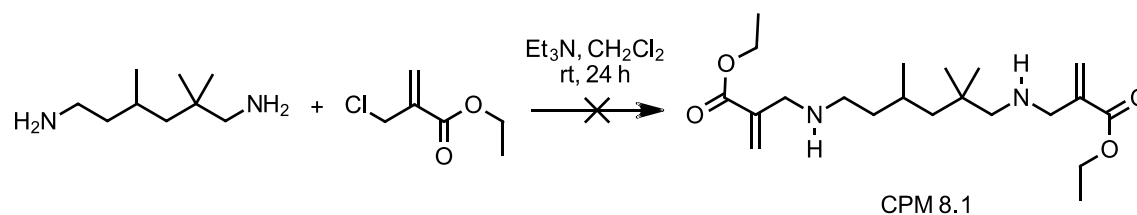


Figure 55: Schematic representation of the synthesis of the (2,2,4)-isomer of CPM 8.1.

For the synthesis of CPM 8.1, trimethylhexane-1,6-diamine and 2.2 equ of Et_3N was reacted with 2.2 equ of ethyl-2-(chloromethyl)acrylate in dry CH_2Cl_2 under argon atmosphere. The reaction progress was monitored *via* NMR and TLC. After the work-up procedure (extraction), the crude product was purified *via* column chromatography.

As already reported by Mangelinckx and co-workers,⁶⁴ the reaction mainly leads to the difunctional CPM 6 and the starting material trimethylhexane-1,6-diamine. The desired product CPM 8.1 could not be isolated, and no second step could be performed.

Unfortunately, none of these attempts led to the desired product CPM 8. The reason could be the higher steric hindrance due to the branched spacer as well as the bifunctionality of the spacer unit. Therefore, no investigations could be performed, and no further synthetic trials were planned with this monomer.

4.3. Reactivity studies of REF 2, REF 3, CPM 4, CPM 5, CPM 6, and CPM 7

After successful synthesis of all compounds, which are based on the (2,2,4)/(2,4,4) trimethylhexane-1,6-diamine spacer unit (CPM 4, CPM 5, CPM 6, CPM 7, REF 2, and REF 3), the reactivity of these compounds could be investigated *via* photo-DSC and RT-NIR-photorheology measurements. As a proof of concept, ATR-IR measurements were performed with a cured sample of CPM 4 and CPM 6 to demonstrate the formation of ring structures after polymerization and consequently the performance of cyclopolymerization.

The mechanical properties of REF 2, CPM 4, CPM 6, and CPM 7 could be analyzed *via* DMTA and tensile tests. It was not possible to obtain the mechanical data from REF 3 and CPM 5 due to their lack of reactivity.

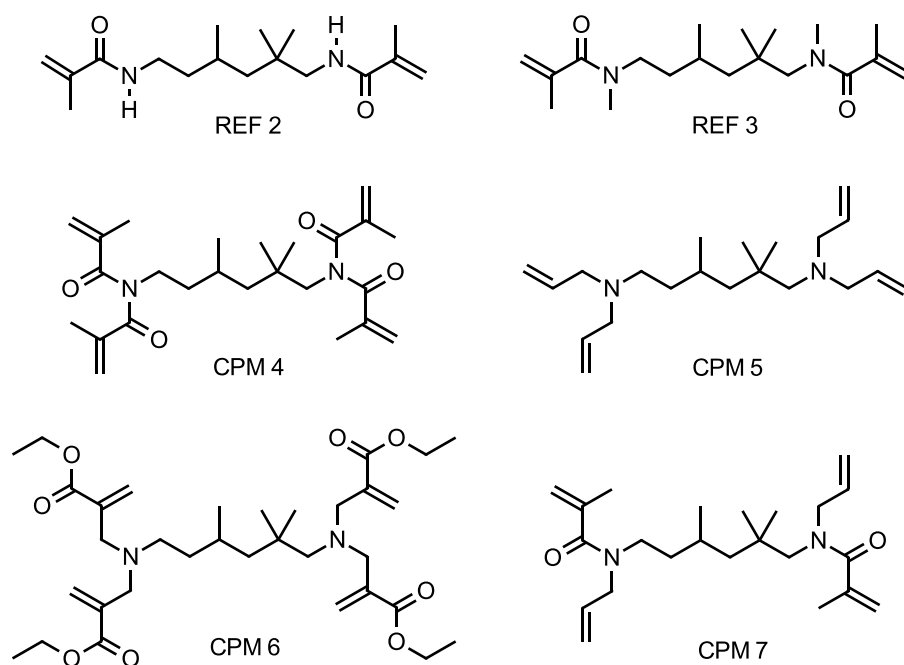


Figure 56: Schematic representation of the (2,2,4)-isomer of REF 2, REF 3, CPM 4, CPM 5, CPM 6, and CPM 7.

4.3.1. Photo-DSC measurement of REF 2, REF 3, CPM 4, CPM 5, CPM 6, and CPM 7

In order to obtain a first impression of the photoreactivity of all synthesized CPMs (CPM 4, CPM 5, CPM 6, and CPM 7) and reference compounds (REF 2 and REF 3), photo differential scanning calorimetry (photo-DSC) measurements were performed with 1 mol% of the germanium-based photoinitiator (PI) Ivocerin® at 25 °C, using a UV/VIS broadband light source (400-500 nm filter).

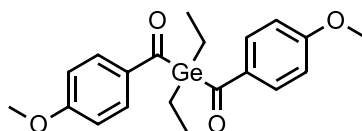


Figure 57: Structure of the PI Ivocerin®.

Each formulation was measured as triplicate under N₂-atmosphere with a light intensity of 1 W cm⁻¹ at the end of the light guide. 12 ± 2 mg were used as sample mass for each measurement. The most significant pieces of kinetic information gained out of this measurement are the times for the maximum evolution of the heat (t_{max}) and the evolution of 95% of the total heat (t_{95}), which indicates the speed of polymerization of a compound. However, t_{95} also depends on the ultimate conversion, which is another characteristic value determined by photo-DSC measurements.

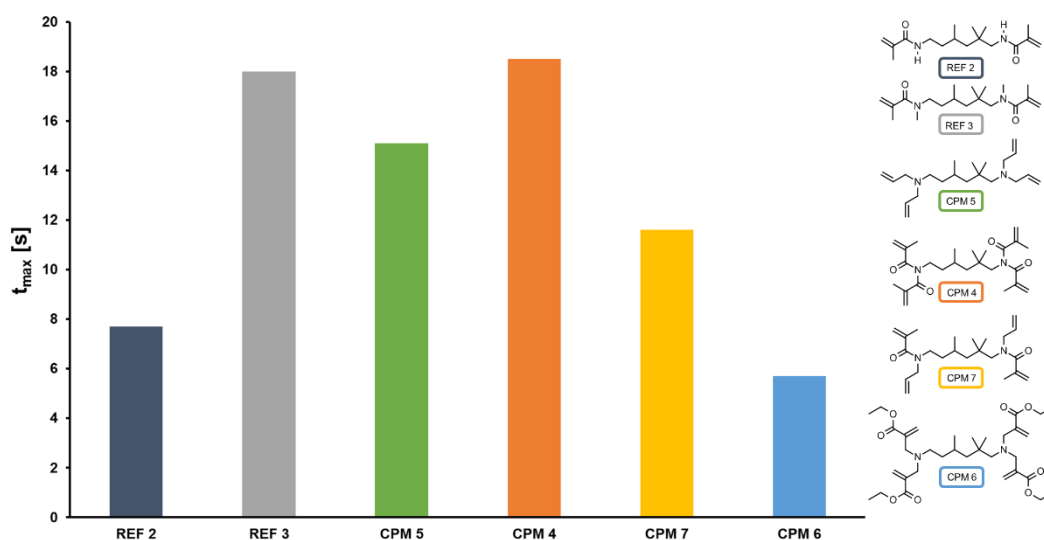


Figure 58: t_{max} of REF 2 (-), REF 3 (-), CPM 4 (-), CPM 5 (-), CPM 6 (-), and CPM 7 (-), (25 °C, 1.0 mol% PI).

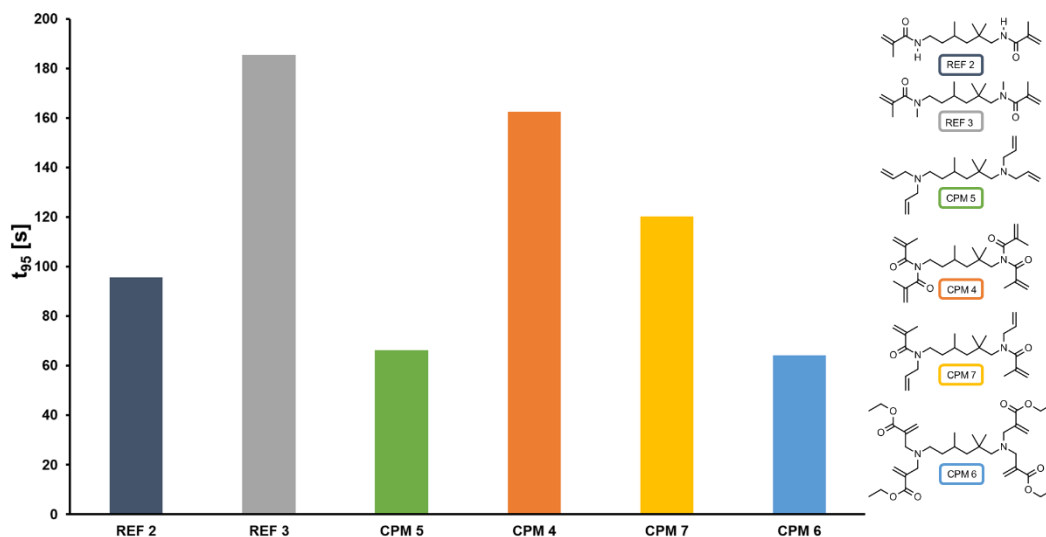


Figure 59: t_{95} of REF 2 (-), REF 3 (-), CPM 4 (-), CPM 5 (-), CPM 6 (-), and CPM 7 (-), (25 °C, 1.0 mol% PI).

In Figure 58 and Figure 59, t_{max} and t_{95} of REF 2, REF 3, CPM 4, CPM 5, CPM 6, and CPM 7 are pictured. Unexpectedly, the literature-related reference compounds (REF 2 and REF 3), which represents the monofunctional counterparts of the methacrylamide compounds, behave in a different way. While REF 2 shows an early t_{max} as well as t_{95} of 7.7 s and 95.6 s indicating a fast speed of its homopolymerization, the sterically hindered REF 3 exhibits a comparably late t_{max} and t_{95} (18.0 s and 185.6 s), illustrating its low reactivity. Surprisingly, also the literature-related CPM 5 reveals its really low reactivity, which was not expected according to literature.^{57, 59}

The symmetrically substituted CPM 4 also shows a comparably late t_{max} and t_{95} . As expected, t_{max} and t_{95} of the asymmetric modification (CPM 7) are shifted to earlier values compared to CPM 4, due to the asymmetric modification leading to a higher polymerization tendency. Furthermore, the ester-activation of the DBs (CPM 6) led to a comparably early t_{max} and t_{95} (5.7 s and 64.2 s), which signals the high reactivity of this compound.

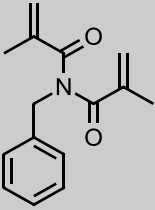
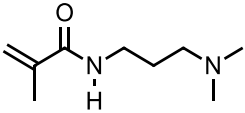
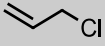
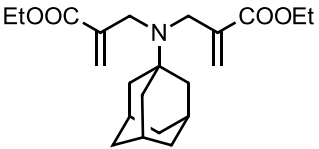
Another important characteristic, which can be determined *via* photo-DSC measurements, is the double bond conversion (DBC in %). The bifunctionality of all CPM and REF compounds leads to crosslinking during polymerization, and consequently the cured samples cannot be dissolved in any solvent. Therefore, the theoretical heat of polymerization (ΔH_0) per DB of a similar monomer (Table 5), as well as the heat of polymerization (ΔH) determined by photo-DSC measurement, was used to calculate the theoretical DBC (DBC_{theo}) (Equation 2). The obtained values of the photo-DSC measurement of all CPMs and REFs are summarized in Table 6.

Equation 2: Calculation of the theoretical DBC.

$$\text{DBC}_{\text{theo}} [\%] = \frac{\text{MW} * \Delta\text{H}}{\Delta\text{H}_0 * n_{\text{DB}}}$$

MW	Molecular weight of the monomer [g/mol]
ΔH	Heat of polymerization by photo-DSC (area) [J/g]
ΔH_0	Theoretical heat of polymerization of the reference monomer [J/mol DB]
n_{DB}	number of DBs []

Table 5: Theoretical Heats of polymerization.

Reference monomer	Structure	ΔH_0 [kJ/mol DB]
Bi-MAC ⁴⁷		76.5
Mono-MAC*		38.2
Allyl-chloride ⁶⁵		77.5
Allyl-ester ⁴⁷		59.8

*Value was determined via the experimental photo-DSC measurement of the monofunctional methacrylamide compound N-(3-dimethylaminopropyl)-methacrylamide.

In order to obtain precise DBC_{theo} -values, ΔH_0 (per DB) of different reference compounds was used for the calculation. The choice of the reference depended on its functional group, trying to use the most similar structure. Bi-MAC⁴⁷ (used for REF 3, CPM 4, and CPM 7) and allyl-ester⁴⁷ (used for CPM 6) were investigated on the same photo-DSC device in another project of this research group and therefore chosen as reference. The ΔH_0 -value of allyl-chloride⁶⁵ (used for CPM 5 and CPM 7) was taken from literature since it is a commercially available compound. The reason behind the approximation using allyl-chloride is that most other compounds, which are based on allyl-amines, lack in reactivity and consequently do not show representative heats of polymerization ΔH_0 . The monofunctional methacrylamide compound N-(3-dimethylaminopropyl)-methacrylamide was measured at the same photo-DSC device and used for the calculation of REF 2, due to the strong influence of the hydrogen on the reactivity of this compound.

Table 6: Results of the photo-DSC measurements: t_{max} , t_{95} , ΔH , and DBC_{theo} .

	t_{max} [s]	t_{95} [s]	ΔH [J/g]	Used ΔH_0 [kJ/mol DB]	DBC_{theo} [%]
REF 2	7.7 ± 0.7	95.6 ± 3.4	147.4 ± 0.7	38.2	56.8 ± 0.3
REF 3	18.0 ± 1.4	185.6 ± 8.2	11.7 ± 1.4	76.5	4.8 ± 0.3
CPM 4	18.5 ± 1.2	162.6 ± 4.2	222.4 ± 7.8	76.5	31.3 ± 1.1
CPM 5	15.1 ± 0.3	66.2 ± 13.5	34.0 ± 1.6	77.5	3.5 ± 0.2
CPM 6	5.7 ± 0.1	64.2 ± 2.1	314.1 ± 2.8	59.8	79.7 ± 0.7
CPM 7	11.6 ± 0.1	120.8 ± 1.6	363.4 ± 1.7	76.5 & 77.5	44.2 ± 0.2

The results in Table 6 demonstrate the fast reaction speed as well as the high DBC_{theo} of REF 2 (~ 57%), especially compared to REF 3, which shows a really low theoretical conversion of around 5%. The high reactivity of REF 2 expresses its high homopolymerization tendency. Also, the literature-known diallyl-compound CPM 5 shows almost no DBC_{theo} (~ 4%), which indicates its limited reactivity.

The symmetric CPM 4 has a comparably low DBC_{theo} of approximately 31%, followed by the asymmetric of CPM 7 of around 44%. As expected, the ester-activated compound CPM 6 shows not only the fastest reaction speed of the whole library but also a comparably high DBC_{theo} (~ 80%).

However, it is crucial to keep in mind that DBC_{theo} are calculated values and origin from the heat of polymerization. Therefore, RT-NIR photorheology measurements were performed to investigate the kinetic properties, especially the DBC determined via NIR-measurements, of these CPMs and REFs more in detail.

4.3.2. RT-NIR photorheology of REF 2, REF 3, CPM 4, CPM 5, CPM 6, and CPM 7

In order to obtain the kinetic and rheological properties of a monomer simultaneously, RT-NIR photorheology measurements were performed with all CPMs (CPM 4, CPM 5, CPM 6, and CPM 7) and reference compounds (REF 2 and REF 3). CPM 6 should show the highest reactivity due to the ester-activation of the DB, followed by the asymmetric CPM 7, which is expected to show a preference of one DB over the other. CPM 4 is supposed to show comparably low reactivity due to the steric hindrance of the methyl-group. It is further expected that the allyl-based compound CPM 5 should have the lowest polymerization tendency of all cyclopolymerizable compounds.

The measurements were performed in triplicates with 1 mol% PI Ivocerin® at 25 °C. Irradiation of the samples was performed with a broadband Hg-lamp using a 400-500 nm filter and a light intensity of 1 W cm⁻² at the end of the light guide. For each measurement, 150 µL of the sample was applied with an Eppendorf pipette on the glass disk, which was protected with a PE-tape. The gap between the glass disk and the measuring system (PP25) was kept at a constant size of 200 µm. The DBC (in %) could be calculated by integrating the DB-signal, which is around 6140 cm⁻¹, over time and comparing it to the integrated DB signal at t₀.

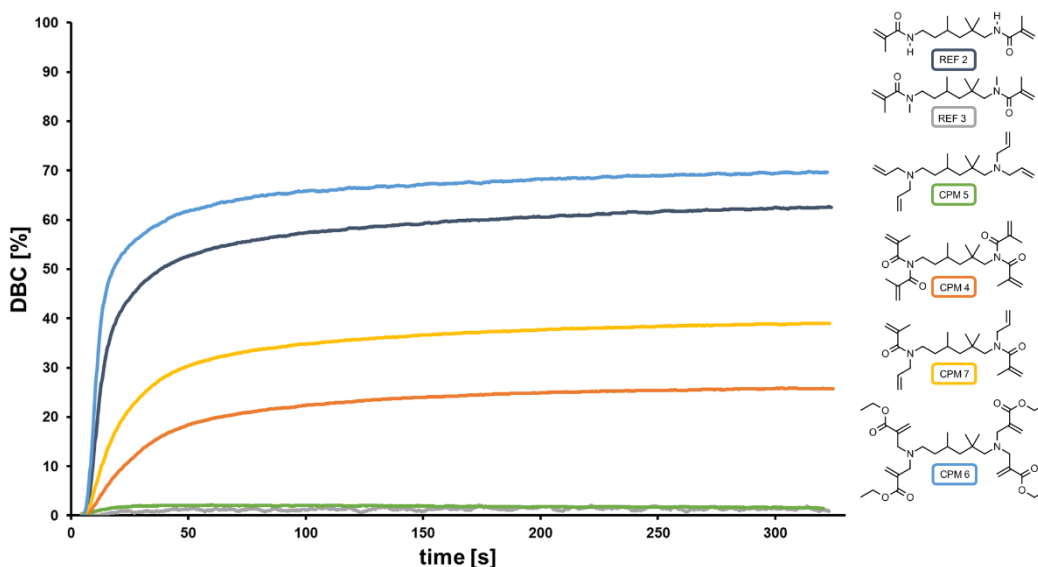


Figure 60: Conversion over time of REF 2 (-), REF 3 (-), CPM 4 (-), CPM 5 (-), CPM 6 (-), and CPM 7 (-), (25 °C, 1.0 mol% PI), light starts after 5 s.

Figure 60 shows the conversion of CPM 4, CPM 5, CPM 6, CPM 7, REF 2, and REF 3 over time at 25 °C with 1 mol% PI. Against the expectations, the comparison of the reference substances revealed that REF 2 has a comparably high conversion of around 62%, which is probably caused by the formation of hydrogen-bonding. The reference substance REF 3 shows no homopolymerization due to its higher steric hindrance caused by the methyl-group. Surprisingly, also the allyl-based compound CPM 5, which should have a low polymerization tendency according to literature,^{57, 59} shows no reactivity at all. The reason for this could be the bifunctionality, and consequently, the steric hindrance of this monomer. As a result of the lack of reactivity, no gel point (t_g) could be obtained from REF 2 and CPM 5, since they were still liquid after irradiation. The comparison of the difunctional CPMs revealed that CPM 4 shows a comparably low conversion of around 27%, followed by the asymmetric CPM 7 (DBC = 40%). The ester-activated compound CPM 6 reaches the highest conversion of around 69%. The values for the final DBC (DBC_{final}), as well as the time at 95% conversion (t_{95}), are summarized in Table 9.

The photo-DSC measurement (4.3.1) gives the DBC_{theo} , which is calculated from the heat of polymerization. DBC_{final} of the photorheological measurement is determined by the decrease of the NIR-signal of DBs during the polymerization reaction. Therefore, RT-NIR-measurements provide more accurate DBC-values and vary slightly from DBC_{theo} . Both DBC-values are summarized in Table 7, whereas the overall trend of both DBC-measurements shows the same result. REF 3 and CPM 5 have almost no reactivity and therefore minimal DBC. CPM 4 shows the lowest conversion of all reactive compounds, followed by CPM 6. The high DBC of REF 2 could be confirmed, which is caused by its high homopolymerization behavior. Furthermore, it could be verified that CPM 6 shows the highest conversion of all tested compounds.

Table 7: Comparison of DBC-values: DBC_{theo} (photo-DSC) and DBC_{final} (photorheology).

	DBC_{theo} [%] Photo-DSC	DBC_{final} [%] Photorheology
REF 2	56.8 ± 0.3	61.6 ± 1.0
REF 3	4.8 ± 0.3	1.4 ± 0.2
CPM 4	31.3 ± 1.1	26.6 ± 0.6
CPM 5	3.5 ± 0.2	1.6 ± 0.1
CPM 6	79.7 ± 0.7	68.5 ± 1.8
CPM 7	44.2 ± 0.2	40.4 ± 1.6

The asymmetric compound CPM 7, which is modified with allyl- and methacryl-groups, is supposed to show a preference of one DB over the other during polymerization. Since the NIR-signal of both DBs is in the same area, it was attempted to separate these peaks with the program PeakFit. A baseline correction with non-parametrical fitting and 2nd derivative zero algorithms of the NIR-spectrum at t_0 and t_{end} were performed, followed by peak deconvolution with loess smoothing. The peak signals of the methacryl-DB (6125 cm^{-1}) and ally-DB (6098 cm^{-1}) could be separated, integrated, and afterwards used for calculating the DBC. Both groups show precisely the same conversion of 42.2%, which coincides with the final conversion of 40.4%. Therefore, it can be stated that in the case of the asymmetric CPM 7, there is no preference for one DB over the other. Hereby, it is important to mention that there could be some misinterpretation due to the low intensity of the peaks.

The reaction speed, which can be determined from the slope of the curve at the beginning of the measurement (DBC per s; Table 8), reveals the same results as the conversion. The slope of REF 3 and CPM 5 is marginal, and hence it can be said that these compounds hardly react. However, REF 2 shows a comparably high reaction speed (5.0 $\% \text{ s}^{-1}$). The symmetric CPM 4 shows the lowest reaction speed (0.8 $\% \text{ s}^{-1}$) and the lowest conversion, followed by the asymmetric CPM 7 (1.5 $\% \text{ s}^{-1}$). As expected again, CPM 6 reacts fastest out of all compounds showing a reaction speed of around 7.3 $\% \text{ s}^{-1}$.

Table 8: DBC per s of REF 2, CPM 4, CPM 6, and CPM 7.

	DBC per s [% s ⁻¹]
REF 2	5.0
CPM 4	0.8
CPM 6	7.3
CPM 7	1.5

The gel point of a photocurable formulation is the transition point from the liquid to the gel-like state, and it can be determined with RT-NIR photorheology measurements. The polymerization time until gelation (t_g) corresponds with the intersection point of the storage modulus G' and the loss modulus G'' ($G'/G'' = 1$). The obtained t_g was then used to calculate the conversion at the gel point (DBC_g), which is also summarized in Table 9.

Table 9: Summarized results of the RT-NIR-photorheology measurements of REF 2, REF 3, CPM 4, CPM 5, CPM 6, and CPM 7.

	t_g [s]	DBC _g [%]	t_{95} [s]	DBC _{final} [%]	G' [MPa]
REF 2	3.2 ± 0.2	16.4 ± 0.2	145.5 ± 7.8	61.6 ± 1.0	485 ± 67
REF 3	-	-	-	1.4 ± 0.2	(5.0 ± 4.0) 10 ⁻⁴
CPM 4	58.2 ± 9.8	20.1 ± 0.5	153.0 ± 5.4	26.6 ± 0.6	136 ± 63
CPM 5	-	-	-	1.6 ± 0.1	(1.1 ± 0.1) 10 ⁻³
CPM 6	2.0 ± 0.1	15.3 ± 1.5	91.2 ± 2.6	68.5 ± 1.8	606 ± 36
CPM 7	12.7 ± 1.2	13.2 ± 1.3	148.2 ± 2.5	40.4 ± 1.6	453 ± 5

According to the results in Table 9, CPM 4 reaches t_g at the latest stage (58.2 s) of all reactive compounds, which is caused by the low reactivity of the methacryloyl-group. The asymmetric CPM 7 also has a relatively late t_g (12.7 s). As coinciding with the reactivity analysis, REF 2 shows its t_g at an early stage (3.2 s), exceeded by the most reactive CPM 6 ($t_g = 2.0$ s)

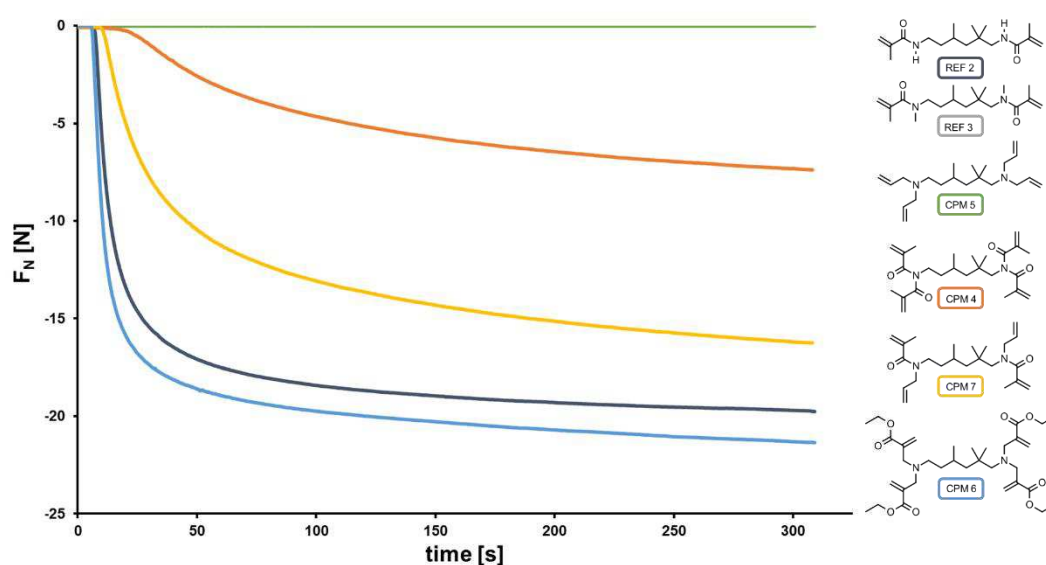


Figure 61: Shrinkage force over time of REF 2 (-), REF 3 (-), CPM 4 (-), CPM 5 (-), CPM 6 (-), and CPM 7 (-), (25 °C, 1.0 mol% PI), light starts after 5 s.

Figure 61 presents the shrinkage force (F_N) over time of REF 2, REF 3, CPM 4, CPM 5, CPM 6, and CPM 7 at 25 °C. Since F_N directly depends on the conversion, its comparison needs to be conducted at equal conversion values. Therefore, F_N was plotted as a function of the DBC (Figure 62) for REF 2, CPM 4, CPM 6, and CPM 7, and the comparison was taken at a DBC of around 25%, which had been reacted by all monomers, including the less reactive ones. REF 3 and CPM 5 were not included in this plot due to their marginal conversion leading to no shrinkage behavior.

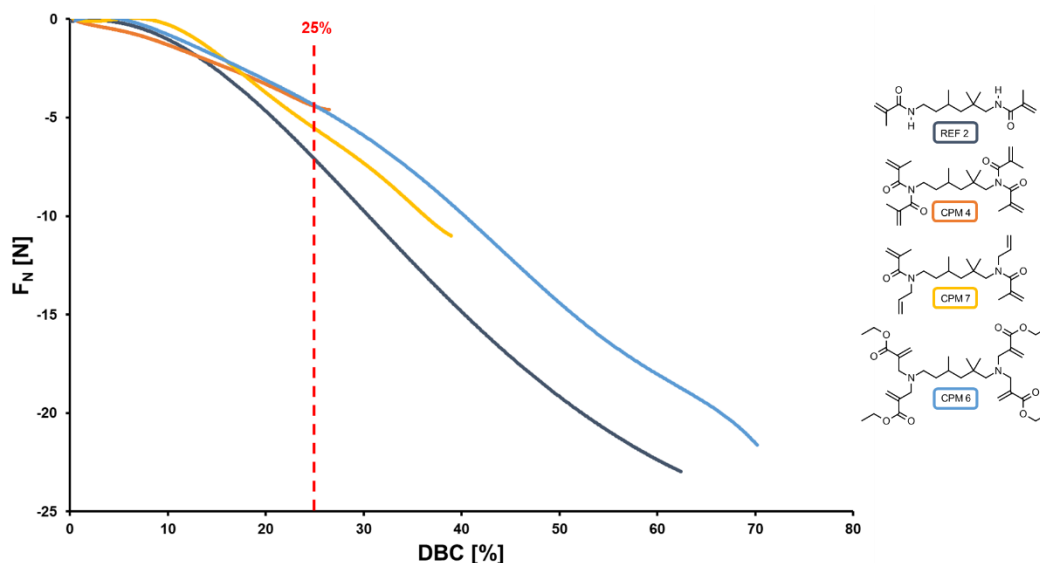


Figure 62: Shrinkage force over conversion of REF 2 (-), CPM 4 (-), CPM 6 (-), and CPM 7 (-), (25 °C, 1.0 mol% PI), light starts after 5 s.

In Figure 62, F_N is plotted as a function of the DBC of REF 2, CPM 4, CPM 6, and CPM 7 to compare the shrinkage forces at an equal conversion value of 25%. Hereby, it can be seen that REF 2 shows the highest F_N of -7.2 N. CPM 4 and CPM 6 exhibit the lowest shrinkage (-4.3 N) of all compounds at DBC = 25%. The shrinkage force of CPM 7 is marginally higher (-5.6 N). Overall, it is important to mention that the differences between the shrinkage behavior of all CPMs are relatively low and arguably neglectable. The exact values for the final F_N at 25% DBC are summarized in Table 10.

Table 10: Shrinkage force of REF 2, CPM 4, CPM 6, and CPM 7.

	F_N (25% _{DBC}) [N]	F_N (final) [N]
REF 2	-7.2	-22.9 ± 2.6
CPM 4	-4.3	-7.7 ± 1.9
CPM 6	-4.3	-21.2 ± 1.0
CPM 7	-5.6	-16.4 ± 1.3

In summary, the results of the RT-NIR photorheological measurements show that the ester-activated compound CPM 6 has not only the fastest reaction speed and the highest conversion, but also shows minimal reduced shrinkage compared to the other compounds at the same conversion level (DBC = 25%). Interestingly, the reference compound REF 2 also shows high reactivity and fast reaction speed, but also the most significant shrinkage force at 25% conversion. Overall, it is important to mention that the shrinkage force, which has to be compared at the same conversion level, varies minimally.

The sterically hindered reference compound REF 3 showed almost no reactivity, and consequently no reaction speed or shrinkage force could be determined. This lack of reactivity could also be observed for the allyl-based compound CPM 5, which was not expected, since there are some examples in literature,^{57, 59} where allyl-based compounds show cyclopolymerization tendency. The reason behind this could be the bifunctionality of CPM 5, which causes a higher steric hindrance and consequently limits the reactivity of this compound.

However, CPM 4 showed the lowest conversion as well as the lowest reaction speed of all reactive compounds due to the steric hindrance caused by the methyl group. Further predicted was the improved polymerization tendency of the asymmetric CPM 7. While it was unconventional that CPM 7 showed no preference of one DB over the other according to the calculations with the program PeakFit.

4.3.3. ATR-IR spectroscopy of polymerized CPM 4 and CPM 6

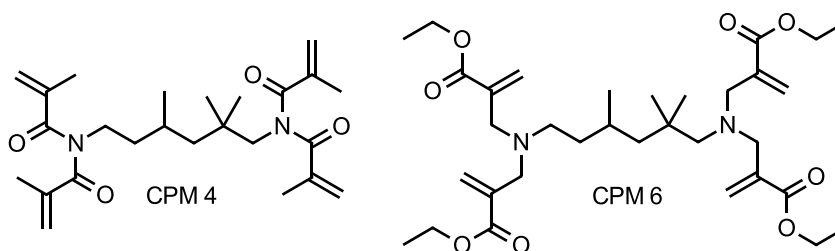


Figure 63: Schematic representation of the (2,2,4)-isomer of CPM 4 and CPM 6.

As proof of concept, ATR-IR measurements were performed to confirm the cyclopolymerization tendency of CPM 4 and CPM 6. Hereby, the formation of ring structures after polymerization could be proven *via* the absorption of light caused by the carbonyl group. Carbonyl-signals show a typical absorption at wavenumbers in the region around 1700-1790 cm^{-1} . Carbonyls located in 5-membered rings are supposed to show this absorption at a wavenumber of around 1770 cm^{-1} , while the higher ring-strain of the 6-membered ring leads to a shift of the absorption to 1730 cm^{-1} .⁶⁶ Consequently, ATR-IR measurements are not only a fitting tool to prove cyclopolymerization but also give an insight into the preference of ring formation of a specific CPM.

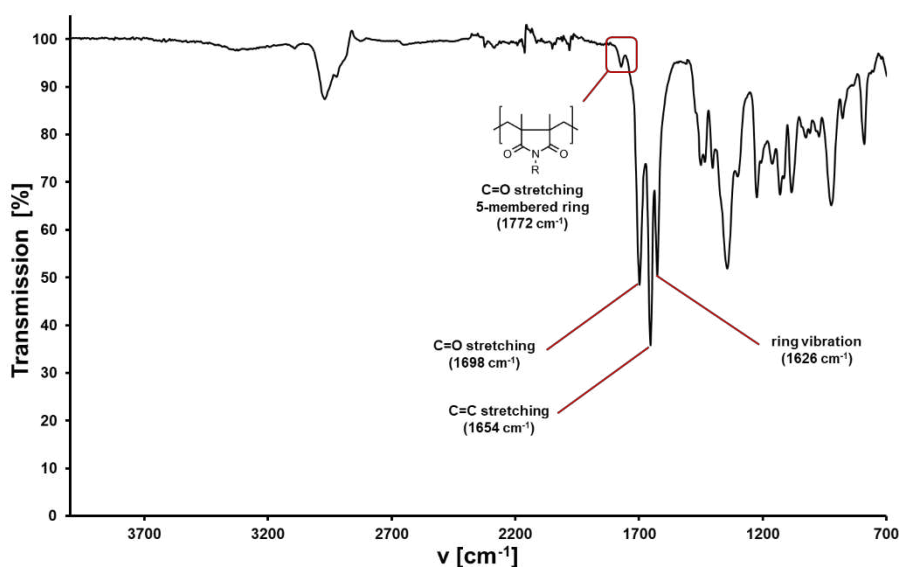


Figure 64: ATR-IR spectrum of *p*(CPM 4), (25 °C and with 1 mol% PI).

The ATR-IR spectrum of the polymerized sample of CPM 4 (p(CPM 4)), which was cured with 1 mol% PI Ivocerin® at 25 °C, is presented in Figure 64. A signal is visible at $\nu = 1698 \text{ cm}^{-1}$, which is characteristic for carbonyl stretchings located in a 5-membered ring. Consequently, it can be stated that CPM 4 can undergo cyclopolymerization forming mainly 5-membered rings in the polymeric backbone. 6-membered rings are rarely formed during the polymerization of CPM 4, since no absorption at $\nu = \sim 1730 \text{ cm}^{-1}$ could be observed in the IR-spectrum.

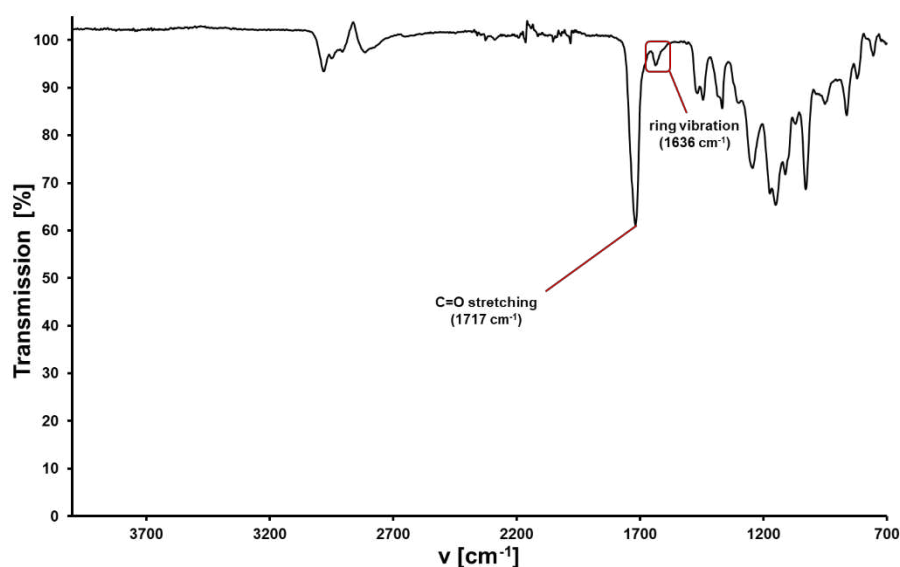


Figure 65: ATR-IR spectrum of p(CPM 6), (25 °C and with 1 mol% PI).

Figure 65 represents the ATR-IR spectrum of the polymerized sample of CPM 6 (p(CPM 6)), which was cured with 1 mol% PI Ivocerin® at 25 °C. The carbonyl-stretching causes a characteristic signal at $\nu = 1717 \text{ cm}^{-1}$. Unfortunately, the carbonyl-group of CPM 6 is not located inside the ring-structure after its polymerization. Consequently the information about the size of the formed ring-structure cannot be obtained. However, an absorption signal is clearly visible at $\nu = 1636 \text{ cm}^{-1}$, which is caused by ring vibration. Therefore, it can be concluded that CPM 6 is also performing cyclopolymerization.

4.4. Mechanical studies of REF 2, CPM 4, CPM 6, and CPM 7

4.4.1. DMTA of REF 2, CPM 4, CPM 6, and CPM 7

The viscoelastic properties of a material can be determined *via* dynamic mechanical thermal analysis (DMTA) measurements. Hereby, the material experiences a sinus-shaped force, which causes a measurable deformation as a function of time and temperature. The major information obtained from this measurement is the glass transition temperature (T_g), which indicates the beginning of long-range motions of the polymer chains and can be obtained from the maximum of the loss factor ($\tan \delta_{\max}$), as well as the point of inversion of the storage modulus (G'), which depends on the temperature. For applications, the storage modulus at RT (G'_{25}) and at the rubber plateau (G'_r), which reveals the degree of crosslinking and indicates the minimum of G' , are of interest (as pictured in Figure 66).

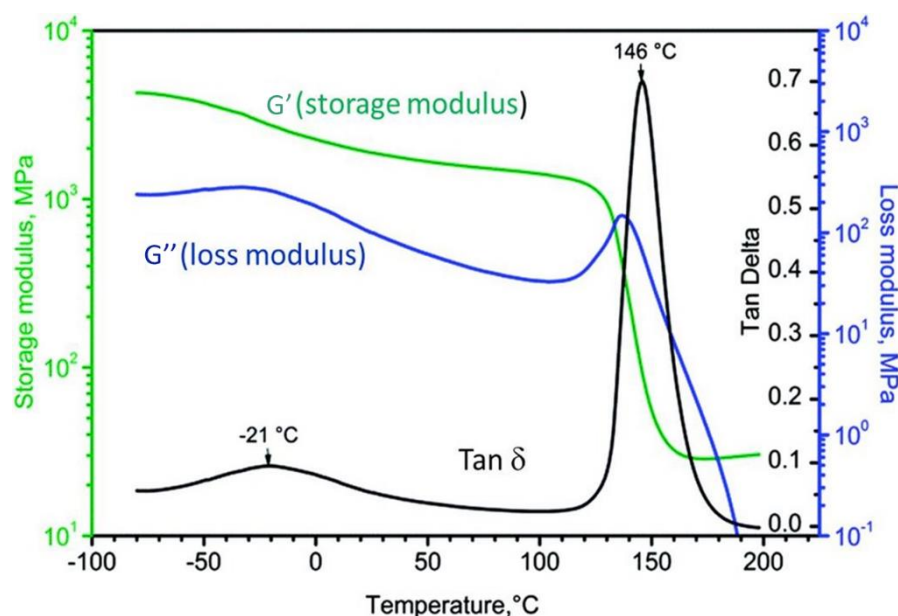


Figure 66: Schematic representation of a DMTA-curve (G' , G'' and $\tan \delta$).⁶⁷

The DMTA measurements were performed in a temperature range between -100 °C and 200 °C (heating rate: 2 °C min⁻¹) in oscillation mode with a torsional strain of 0.1% and 1 Hz. The monomer formulations contained 1 mol% PI Ivocerin[®] and they were cured in a silicone mold (sticks, 5 × 2 × 40 mm) with 400-500 nm UV-light for 10 min from both sides. The cured specimens were just tested once per monomer formulation due to the good reproducibility of the measurement.

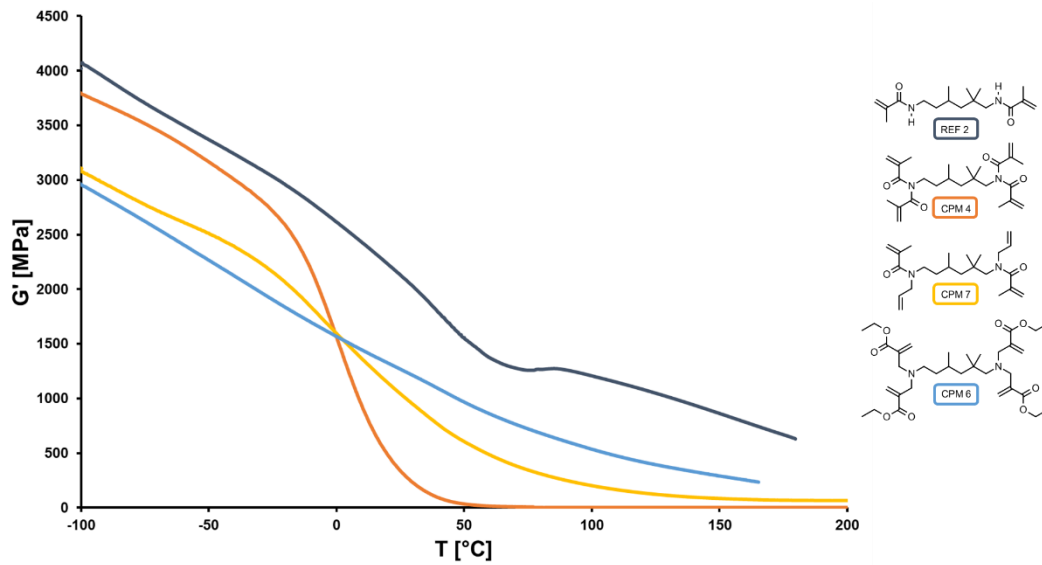


Figure 67: Storage modulus (G') over temperature (T) of REF 2 (-), CPM 4 (-), CPM 6 (-), and CPM 7 (-).

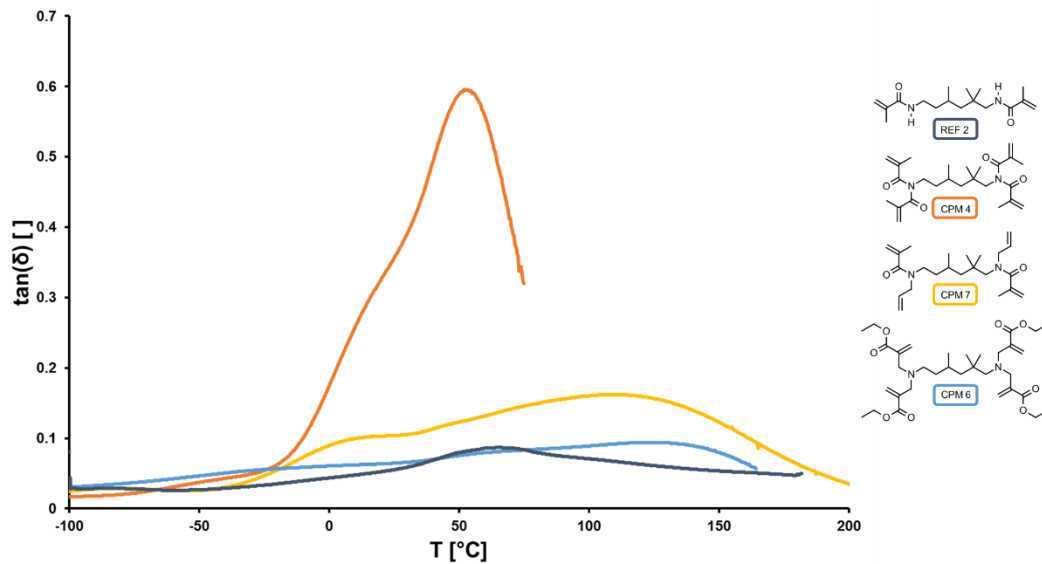


Figure 68: Loss factor ($\tan(\delta)$) over temperature (T) of REF 2 (-), CPM 4 (-), CPM 6 (-), and CPM 7 (-).

The storage modulus (G') and the loss factor ($\tan \delta$) of REF 2, CPM 4, CPM 6, and CPM 7 are presented in Figure 67 and Figure 68, and the exact values are summarized in Table 11. The maximum loss factor ($\tan \delta_{\max}$) correlates with the glass transition temperature (T_g) of a cured formulation. Overall, it is important to mention that increased conversion can lead to a broadening of the loss-curve. This phenomenon can be observed in Figure 68. The least-reactive CPM 4 shows clearly the sharpest T_g , followed by CPM 7. The most-reactive substances REF 2 and CPM 6 generate flat curves leading to a broad T_g -range.

The comparison of the difunctional 1,6-diene compounds (CPM 4, CPM 6, and CPM 7) reveals that the crosslinking density, which is indicated by the (G'_r)-values, increases with increasing reactivity of the CPMs.

The monofunctional specimen REF 2 shows a comparably low T_g (65.5 °C), but a high G'_r (574.4 MPa), which indicates high crosslinking of its methacrylamide-DBs during homopolymerization. As a result of the higher crosslinking density of CPM 6 and the resulting limited mobility of the polymer-chains, CPM 6 also shows the highest T_g (123.1 °C). The asymmetric CPM 7 showed a reduced T_g (109.0 °C), which is caused by the minor conversion of this compound. CPM 4 reaches the T_g at the lowest temperature of all CPMs (52.3 °C), whereas its specimen was ruptured at 75 °C.

Table 11: G'_{25} , G'_r , and T_g of REF 2, CPM 4, CPM 6, and CPM 7.

	G'_{25} [MPa]	T_g [°C]	G'_r [MPa]
REF 2	2133	65.5	574
CPM 4	331	52.3	5
CPM 6	1267	123.1	246
CPM 7	1040	109.0	66

4.4.2. Tensile Tests of REF 2, CPM 4, CPM 6, and CPM 7

Two of the most characteristic mechanical properties of a material are its toughness and deformation behavior. During tensile test measurements, the polymeric specimen is exposed to a uniaxial deformation until rupture. Crosslinked photopolymers are usually known as brittle plastics, showing high stress and low strain behavior, whereas the aim would be to create tough materials without creating elastomers. In general, the stress-strain performance of cured materials also depends on the temperature, particularly on the glass transition temperature (T_g). Since tensile tests are performed at RT, a high T_g contributes to the brittle nature of the polymer.

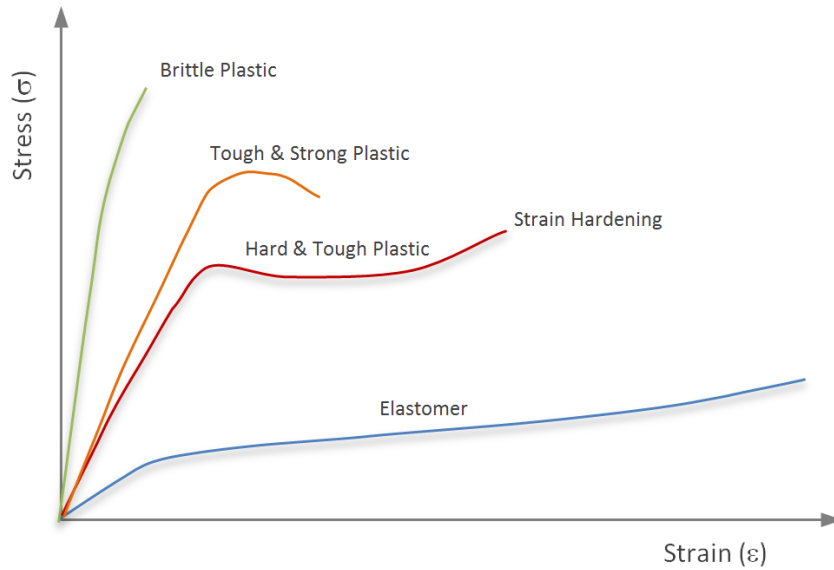


Figure 69: Stress-Strain behavior of polymers.⁶⁸

Tensile tests were performed in order to obtain the maximum stress (σ_M) and elongation at break (ϵ_B) from the chosen cured materials (REF 2, CPM 4, CPM 6, and CPM 7). The polymeric specimen, which were cured in a 5B-shaped silicone mold, were made out of the same formulation as the DMTA specimen, using the same procedure. The measurements were performed in accordance with ISO 527 using a traverse speed of 5 mm min^{-1} .

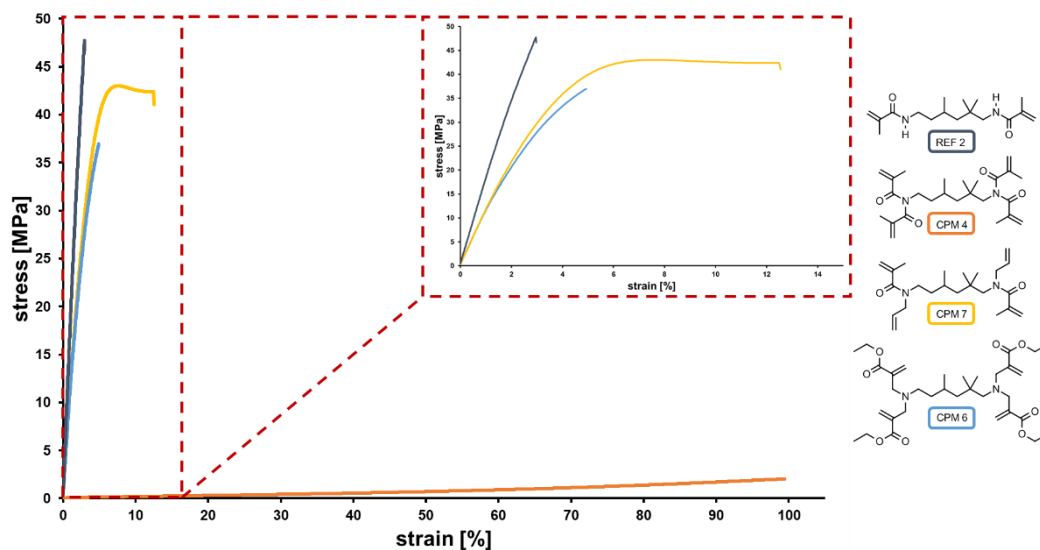


Figure 70: Stress-Strain curves of REF 2 (-), CPM 4 (-), CPM 6 (-), and CPM 7 (-).

Figure 70 presents the stress-strain curves of REF 2, CPM 4, CPM 6, and CPM 7. It can be seen that the highly crosslinked materials (REF 2 and CPM 6) show brittle behavior, whereas the homopolymerized REF 2 exhibits the highest maximum tensile strength ($\sigma_M = 50$ MPa) and low elongation at break ($\epsilon_B = 3\%$). CPM 6 shows reduced σ_M (36 MPa) and higher ϵ_B (5%). The brittle behavior of these compounds (REF 2 and CPM 6) is generated by the high DBC (REF 2 = 62%, CPM 6 = 69%) as well as by the early time of the gelation point (t_g) (REF 2 = 3.2 s, CPM 6 = 2.0 s) measured *via* RT-NIR photorheology (chapter 4.3.2). If the t_g is reached at an early conversion level, the whole network decreases in flexibility and consequently led to brittle materials. Therefore, shifting the t_g to a higher conversion level leads to a higher flexibility of the network.

The asymmetric CPM 7 can be classified as a tough and strong plastic with σ_M of around 44 MPa and ϵ_B of approximately 10%. This tough and strong behavior is caused by the lower conversion rate (CPM 7 = 40%) as well as the later t_g (CPM 7 = 12.7 s).

The symmetric CPM 4 shows clearly an elastomeric nature with σ_M of about 2 MPa and ϵ_B of around 101%, which is not desired. This elastomeric behavior originates from the steric hindrance created by methyl-group leading to lower conversion (CPM 4 = 27%) as well as a comparably late t_g (CPM 4 = 58 s). The exact values of the tensile test measurements are summarized in Table 12.

Table 12: Maximum tensile strength (σ_M) and elongation at break (ϵ_B) of CPM 4, CPM 5, CPM 6 and CPM 8.

	σ_M [MPa]	ϵ_B [%]
REF 2	50.03 ± 4.50	3.08 ± 0.24
CPM 4	2.05 ± 0.37	100.81 ± 3.21
CPM 6	35.85 ± 1.95	4.76 ± 0.32
CPM 7	43.85 ± 1.76	10.12 ± 2.92

Overall, it can be said that the asymmetric CPM 7 shows a tough and strong nature, while the more reactive compounds REF 2 and CPM 6, which also show a higher T_g according to the DMTA measurements (chapter 4.4.1), are brittle plastics. The symmetric CPM 4 has an elastomeric behavior, which is caused by the low conversion as well as the late t_g of this compound.

Summary

Free radical photopolymerization finds its use in several industrial fields (e.g. coatings, additive manufacturing, dental and medical industry) due to its vast advantages during the production process, such as high energy-, time- and cost-efficiency, as well as solvent-free usage. Consequently, industry is engaging an enormous effort to eradicate the major flaws of this technique, especially the appearance of volumetric shrinkage during polymerization (Figure 71). The mechanical properties of the final product can decline due to this volumetric shrinkage, which causes shrinkage stress in the cured material.

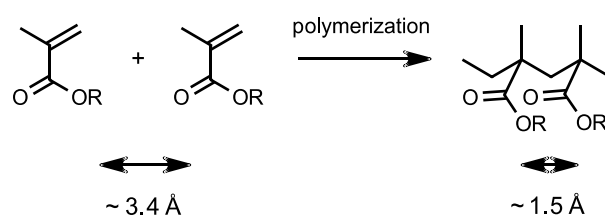


Figure 71: Schematic representation of the distance reduction between monomers during polymerization.³⁰

Nowadays, multiple strategies are under investigation to overcome this problem. One auspicious method is called cyclopolymerization (Figure 72), which was already discovered by Butler and co-workers in the 1950s. The specialty of this mechanism is the formation of cyclic units in the polymer backbone without any crosslinking or network formation, leading to linear and soluble polymers.

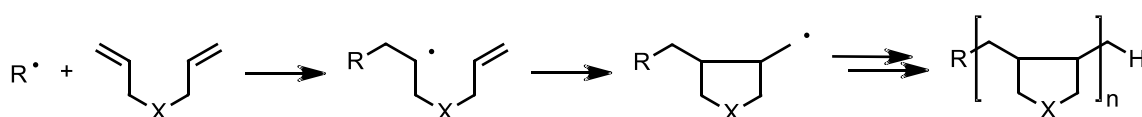


Figure 72: General mechanism of cyclopolymerization.

The analysis of different difunctional CPMs revealed their improved material properties, like high rigidity and low shrinkage. Consequently, they can be seen as ideal compounds for industrial applications.



Figure 73: Schematic representation of a difunctional diacrylamide with different spacer units.⁵⁰

The scope of this thesis was to generate new difunctional 1,6-diene cyclopolymerizable monomers (CPM) based on (meth)acrylamides and to investigate their reactivity *via* photo-DSC and RT-NIR photorheology as well as their thermomechanical behavior by DMTA and tensile tests.

In order to obtain a first insight into this topic, the literature-known difunctional compound CPM 1 was chosen as a starting point, which is supposed to show high reaction rates. Besides CPM 1, the difunctional monofunctional reference REF 1 was also synthesized and analyzed to prove the concept of cyclopolymerization.

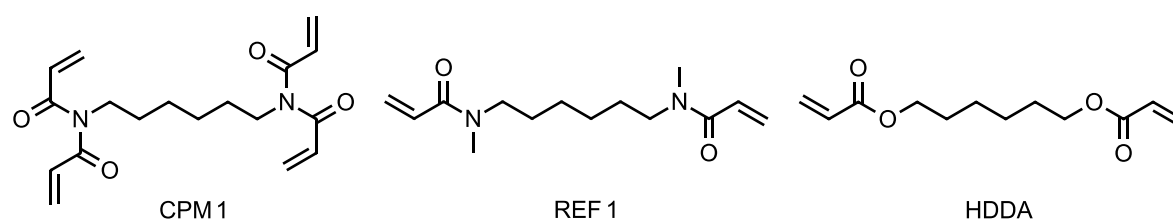


Figure 74: Schematic representation of CPM 1, REF 1 and HDDA.

The reactivity and the shrinkage behavior of CPM 1, REF 1, and the commercially available acrylate compound HDDA were investigated by means of RT-NIR photorheology. As expected, CPM 1 showed the highest conversion of all compounds (~ 78%), exceeding REF 1 (~ 61%) as well as the commercially used HDDA (~ 64%). Furthermore, CPM 1 also showed a reduced shrinkage at a conversion level of ~ 60%, which was used for comparison, since the shrinkage directly depends on the conversion and cannot be compared at different conversion levels.

Unfortunately, the high reactivity of CPM 1 also caused difficulties during the synthetic procedure yielding just 15% of CPM 1. Even after several different approaches, it was not possible to improve the synthesis. Consequently, the conclusion was drawn that difunctional diacrylamides are too reactive for reactivity-enhancing modifications. Therefore, the focus of this thesis was shifted to the less-reactive, but more stable difunctional dimethacrylamide-compounds.

In the second chapter, the influence of the spacer unit on the monomeric state of matter was investigated. Three different difunctional spacers (CPM 2, CPM 3, and CPM 4) were modified with methacryloyl-groups (Figure 75) with the aim of obtaining liquid monomers.

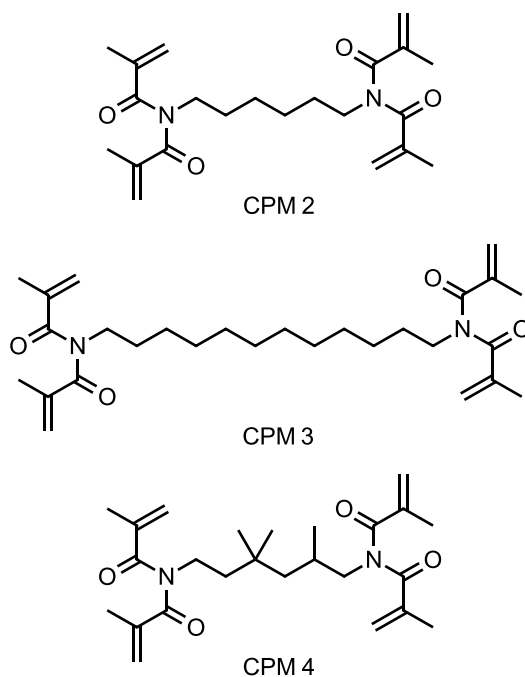


Figure 75: Schematically representation of CPM 2, CPM 3 and CPM 4.

Only CPM 4, which was created out of the sterically hindered spacer (2,2,4(2,4,4)-trimethylhexane-1,6-diamine), was a liquid monomer at room temperature. CPM 2 and CPM 3 were white crystals, exhibiting a melting point of ~ 95 °C and ~ 50 °C, respectively. Therefore, only CPM 4 could be investigated towards its kinetic and thermomechanical behavior. As a result of this, trimethylhexane-1,6-diamine was chosen as sterically hindered spacer for further symmetric and asymmetric modification, to observe the influence of several functional groups on the reactivity as well as the thermomechanical properties.

The third chapter of this thesis focuses on different modifications of this sterically hindered spacer unit. First, two literature-related monofunctional reference compounds (REF 2 and REF 3) were synthesized, where REF 3 is supposed to show further sterically hinderers due to the methyl-group.

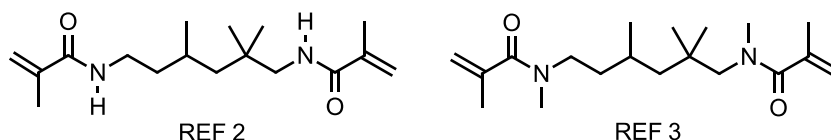


Figure 76: Schematic representation of the (2,2,4)-isomer of REF 2 and REF 3.

Afterwards, a literature-related allyl-based compound CPM 5, which is supposed to show low cyclopolymerization tendency, and an ester-activated allyl-based compound CPM 6, which is supposed to show the highest reactivity of all compounds due to the activation of the DBs *via* the electron-withdrawing ester groups, was chosen for synthesis and investigation.

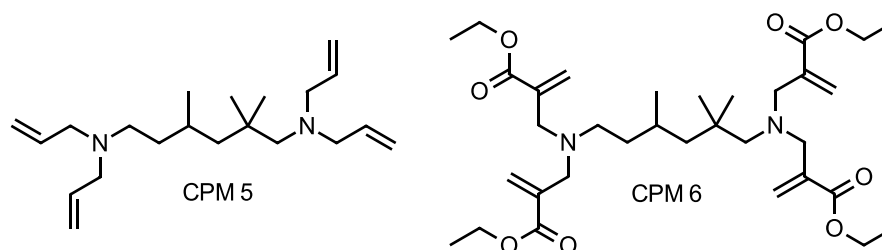


Figure 77: Schematic representation of the (2,2,4)-isomer of CPM 5 and CPM 6.

As last modification, two asymmetric CPMs (CPM 7 and CPM 8) were designed, of which only CPM 7 could be synthesized. CPM 7 had to be created in a two-step reaction, obtaining the monofunctional reference substance REF 2 as intermediate product. It was not possible to synthesize CPM 8 probably due to steric reasons.

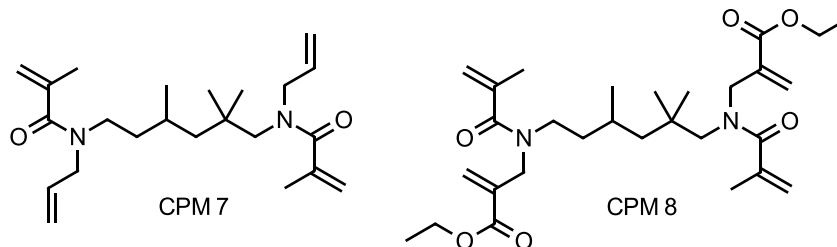


Figure 78: Schematic representation of the (2,2,4)-isomer of CPM 7, and CPM 8.

After the successful synthesis of these compounds, which are based on the sterically hindered trimethylhexane-1,6-diamine spacer, they were investigated towards their reactivity by means of photo-DSC and RT-NIR photorheology. Both methods provide the same trend of reactivity. As expected, CPM 6 showed the highest conversion (~ 69%) caused by the ester-activation of the DBs, followed by the asymmetric CPM 7 (~ 40%). CPM 4 showed a relatively low reactivity of ~ 27% caused by the steric hindrance of the methyl group. Surprisingly, the allyl-based CPM 5 was almost not reacting at all (~ 2%), which was not expected. The reason for this lack of reactivity could be the bifunctionality, and consequently, the steric hindrance of this monomer.

Another interesting result was the high reactivity of the monofunctional reference substance REF 2 (~ 62%) performing homopolymerization, probably caused by the formation of hydrogen-bonding. The monofunctional counterpart REF 3 showed a marginal reactivity (~ 1%), which was expected due to the requirements for cyclopolymerization.

The comparison of the shrinkage force of the reactive compounds (REF 2, CPM 4, CPM 6, and CPM 7) at a constant conversion value of 25% revealed no significant difference in their shrinkage behavior.

As a proof of concept, a polymerized sample of CPM 4 and CPM 6 were investigated towards its cyclization tendency by means of ATR-IR spectroscopy. Hereby, it could be seen that CPM 4 is clearly forming cyclic structures upon polymerization showing a preference for 5-membered ring formation. The formation of ring structures and consequently the performance of cyclopolymerization could also be proven for the most reactive CPM 6. Unfortunately, it was not possible to determine the preference of the formed ring-structures due to structural reasons.

The last part of this thesis focuses on the investigation of the thermomechanical properties of the cured materials. Since REF 3 and CPM 5 showed marginal polymerization tendency, only the reactive monomers (REF 2, CPM 4, CPM 6, and CPM 7) were analyzed *via* DMTA and tensile tests.

It could be shown that the most reactive CPM 6 also showed the highest T_g (~ 123 °C), followed by CPM 7 (~ 109 °C). The least reactive compound CPM 4 displayed the lowest T_g (~ 52 °C), followed by REF 2 (~ 66 °C). Furthermore, it was indicated that CPM 6, as well as REF 2, are more crosslinked, probably due to the higher reactivity of these compounds.

All materials could be classified by means of tensile tests. The more reactive REF 2 and CPM 6 were brittle, which is triggered by the high conversion, high T_g , as well as early t_g . The asymmetric modification CPM 7 showed a tough and strong nature, whereas the symmetric CPM 4 displayed already elastomeric behavior, which is not desired in industry.

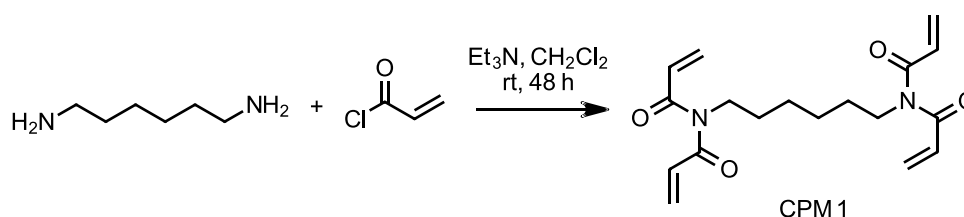
Overall, it can be stated that the activation process *via* the electron-withdrawing ester-group leads not only to an increased reactivity but also a higher T_g , which contributes to the brittle nature of this material. The asymmetric modification offers lower reactivity, but tough and strong mechanical behavior of the cured material. A significant difference in the shrinkage force between the investigated modifications could not be observed.

Experimental Part

2. Diacrylamides

2.1. Synthesis of CPM 1 and REF 1

2.1.1. Synthesis of N,N'-(hexane-1,6-diyl)bis(N,N'-bisacrylamide) - CPM 1



Compound	Equivalentents	MW [g/mol]	n [mmol]	m [g]	V [mL]
Hexamethylenediamine	1	116.21	18.59	2.16	
Acryloyl chloride	5	90.51	148.71	1.12	
Triethylamine (Et_3N)	5	101.19	148.71	0.73	
Dichloromethane (CH_2Cl_2)					85

The synthesis of CPM 1 was performed in accordance with Kopeinig *et al.*⁶⁰ Hexamethylenediamine (2.16 g, 18.59 mmol) and triethylamine (Et_3N) (0.73 g, 148.71 mmol) were combined with 60 mL dry CH_2Cl_2 in a 100 mL three-necked flask (purged with argon). The reaction mixture was cooled with ice/ NaCl to 0-5 °C. Afterwards, freshly distilled acryloyl chloride (1.12 g, 148.71 mmol) was diluted with 25 mL CH_2Cl_2 and added dropwise to the solution (30-60 min). The cooling bath was removed after the addition of acryloyl chloride, and the solution was stirred at RT for 48 h. For purification, the solvent was removed under reduced pressure, and the residues were taken up in distilled water (100 mL). The aqueous phase was extracted with ethyl acetate (3 x 40 mL) and the combined organic phases were dried over Na_2SO_4 . The solvent was removed under reduced pressure, and the crude product was purified *via* column chromatography (PE:EE 1:1). The pure product was obtained as a yellowish liquid (0.61 g, 15% of theory) and it was stabilized with 400 ppm MEHQ and 400 ppm phenothiazine as inhibitor.

CPM 1: 0.61 g (15% yield)

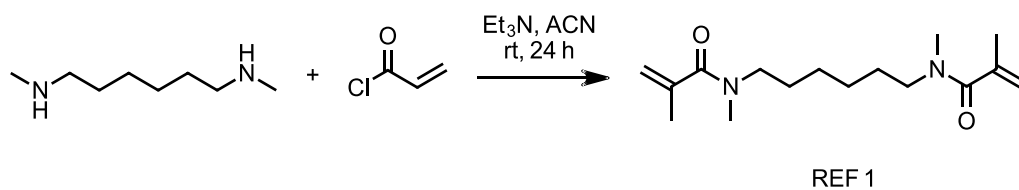
Purity (HPLC): t_R : 2.96 min (58% acetonitrile/42% water, v/v, detection at 220 nm)

R_f-value: 0.32 (PE:EE 2:1)

¹H NMR: (200 MHz, CDCl₃) δ (ppm): 6.62 (dd, 4H, N(COCH=CH₂)), 6.38 (dd, 4H, cis-N(COCH=CH₂)), 5.77 (dd, 4H, trans-N(COCH=CH₂)), 3.82 – 3.57 (t, 4H, N-CH₂-(CH₂)₄-CH₂-N), 1.70 – 1.10 (m, 8H, NCH₂-(CH₂)₄-CH₂N).

¹³C NMR: (50 MHz, CDCl₃) δ (ppm): 168.8 (C4), 130.6 (C3), 130.0 (C2), 44.5 (C2), 28.9 (C2), 26.3(C2).

2.1.2. Synthesis of N,N'-(hexane-1,6-diyl)bis(N-methyl-N'-acrylamide) – REF 1



Compound	Equivalents	MW [g/mol]	n [mmol]	m [g]	V [mL]
N,N'-Dimethyl-1,6-hexanediamine	1	144.26	16.71	2.41	
Acryloylchloride	4	90.51	66.95	6.06	
Triethylamine (Et₃N)	4	101.19	66.95	6.77	
Acetonitrile (ACN)					250

The synthesis of REF 1 was performed in accordance with Moszner *et al.*⁶¹ N,N'-Dimethyl-1,6-hexanediamine (2.41 g, 16.71 mmol) and Et₃N (6.77 g, 66.95 mmol) were combined with 150 mL dry ACN in a 500 mL three-necked flask (purged with argon). The reaction mixture was cooled with ice/ NaCl to 0-5 °C. Freshly distilled acryloyl chloride (6.06 g, 66.95 mmol) was diluted with 100 mL CH₂Cl₂ and added dropwise to the solution (30-60 min). The cooling bath was removed after the addition of acryloyl chloride, and the solution was stirred at RT for 24 h. Afterwards, the precipitate was filtered off and the solvent was removed under reduced pressure. The residues were dissolved in CH₂Cl₂ (250 mL) and extracted with 0.1 N HCl, 5w% NaHCO₃ solution and distilled water. The organic phase was dried over Na₂SO₄ and solvent was removed under reduced pressure. The crude product was purified *via* column chromatography (PE:acetone 1:10). The pure product was obtained as a yellowish liquid (1.82 g, 43% of theory) and it was stabilized with 400 ppm MEHQ and 400 ppm phenothiazine as inhibitor.

REF 1: 1.82 g (43.4 % yield)

R_f-value: 0.14 (PE:acetone 2:1)

¹H NMR: (200 MHz, CDCl₃) δ (ppm): 6.50 (m, 2H, N(COCH=CH₂)), 6.31 – 6.15 (dd, 2H, trans-N(COCH=CH₂)), 5.67 – 5.56 (dd, 2H, cis-N(COCH=CH₂)), 3.41 – 3.22 (m, 4H, N-CH₂-(CH₂)₄-CH₂-N), 2.96 (d, 6H, N-CH₃), 1.61 – 1.45, 1.34 – 1.22 (m, 8H, N-CH₂-(CH₂)₄-CH₂-N).

¹³C NMR: (50 MHz, CDCl₃) δ (ppm): 166.28 (C4), 166.07 (C4), 127.93 (C3), 127.83 (C3), 127.52 (C2), 127.38 (C2), 49.78 (C2), 47.65 (C2), 35.32 (C1), 33.83 (C1), 28.71 (C2), 26.93 (C2), 26.45 (C2), 26.33 (C2).

2.2. Reactivity studies of CPM 1 and REF 1

2.2.1. RT-NIR-photorheology of CPM 1 and REF 1

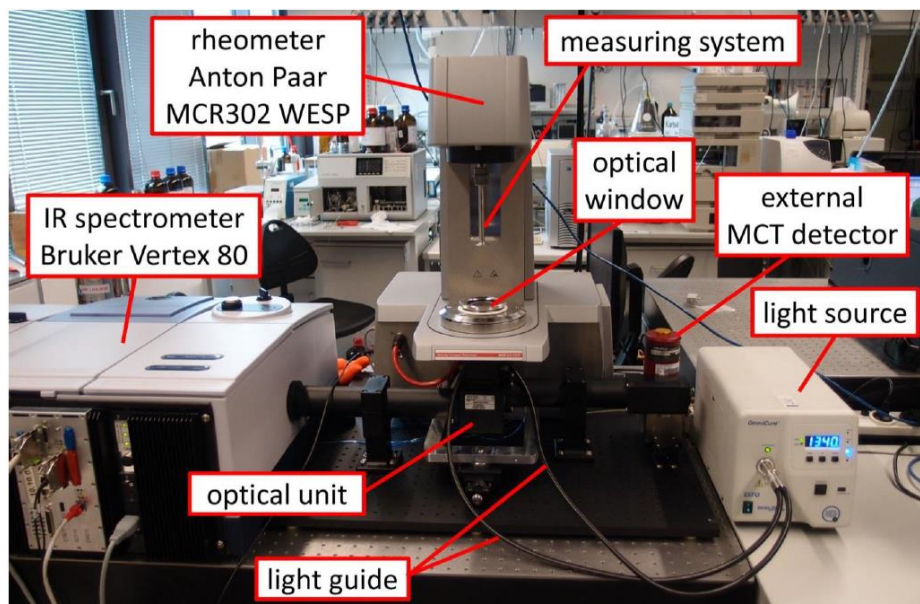


Figure 79: Setup of RT-NIR photorheometer.

The Real Time Near Infrared (RT-NIR) photorheometer is a device, which couples an Anton Paar MCR 302 WESP rheometer, which is equipped with a P-PTD 200/GL Peltier glass plate and a PP25 measuring system with a Bruker Vertex 80 Fourier-Transform Infrared (FTIR) spectrometer, which measures the conversion of the sample over time. In the Bruker Vertex 80 FTIR spectrometer, the IR-light is led from the NIR-spectrometer *via* external mirrors through the optical window and the sample onto the bottom of the rheology plate. Hereby, the IR-beam interacts with the sample and gets reflected to the external Mercury Cadmium Telluride (MCT) detector.

Each photorheological measurement was conducted with 200 μL of monomer formulation, which consists of the pure monomer and 0.5 mol% PI Ivocerin[®], at 25 °C with a constant gap size of 200 μm . The temperature was controlled *via* an Anton Paar H-PTD 200 heating hood. The formulations were sheared with a strain of 1% and a frequency of 1 Hz.

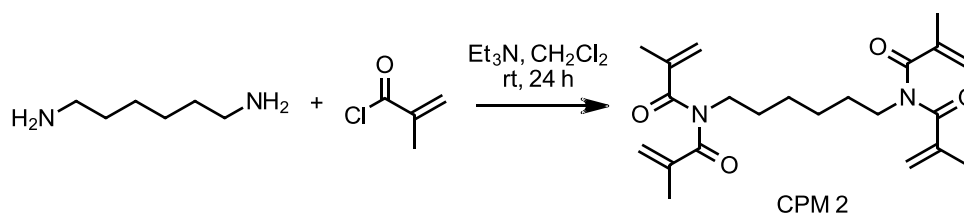
The photopolymerization was initiated *via* UV light from the bottom of the optical window. An Exfo OmniCureTM 2000 device with a broadband Hg-lamp (300 s, 400-500 nm, $\sim 10 \text{ mW cm}^{-2}$ on the surface of the sample, which was measured with an Ocean Optics USB 2000+ spectrometer) was used as external UV-source.

The rheometer device records the storage modulus (G') and the loss modulus (G'') according to the following time interval – one measurement point per s before initiation, one measurement point per 0.2 s during the first 60 s, one measurement point per s till irradiation period ends (4 min). The double bond conversion (DBC) of the (meth)acrylamide DB was obtained by recording a set of single spectra (time interval ~ 0.26 s) with an OPUS 7.0 software and integrating the DB-signals at a wavelength of ~ 6140 cm^{-1} . The DBC was then determined *via* the ratio of change of the peak area at the start and the end of the measurement.

3. Dimethacrylamides

3.1. Synthesis of CPM 2, CPM 3 and CPM 4

3.1.1. Synthesis of N,N'-(hexane-1,6-diy)bis(N,N'-bismethylacrylamide) – CPM 2



Compound	Equivalents	MW [g/mol]	n [mmol]	m [g]	V [mL]
Hexamethylenediamine	1	116.21	10.30	1.20	
Methacryloyl chloride	6	104.53	61.77	6.46	
Triethylamine (Et ₃ N)	6	101.19	61.77	6.25	
Dichloromethane (CH ₂ Cl ₂)					80

The synthesis of CPM 2 was performed in accordance with Kopeinig *et al.*⁶⁰ Hexamethylenediamine (1.20 g, 10.30 mmol) and Et₃N (6.25 g, 61.77 mmol) were dissolved in 60 mL dry CH₂Cl₂ in a 100 mL three-necked flask (purged with argon). The reaction mixture was cooled with ice/ NaCl to 0-5 °C. Afterwards, freshly distilled methacryloyl chloride (6.46 g, 61.77 mmol) was diluted with 20 mL CH₂Cl₂ and added dropwise to the solution (30-60 min). The cooling bath was removed after the addition of methacryloyl chloride, and the solution was continued to be stirred at RT for 24 h. The solution was extracted with 0.1 N HCl, sat. NaHCO₃ and brine, and the organic phase was dried over Na₂SO₄. The solvent was removed under reduced pressure, and the crude product was purified *via* column chromatography (PE:EE 2:1). The pure product was obtained as white crystals after recrystallization in methanol (1.53 g, 38% of theory) and it was stabilized with 200 ppm MEHQ and 200 ppm phenothiazine as inhibitor.

CPM 2: 1.53 g (38% yield)

Purity (HPLC): t_R : 12.66 min (58% acetonitrile/42% water, v/v, detection at 220 nm)

R_f-value: 0.49 (PE:EE 2:1)

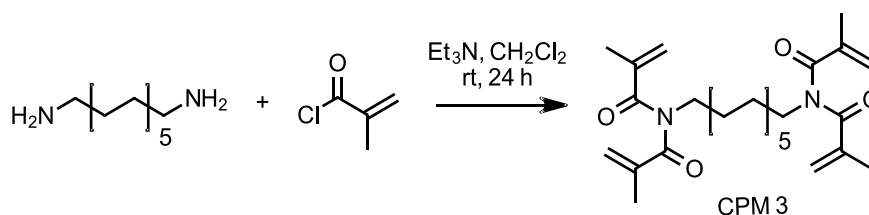
mp.: 95.4-96.6 °C

¹H NMR: (200 MHz, CDCl₃) δ (ppm): 5.30 (d, 4H, trans-N(COC(CH₃)=CH₂)), 5.12 (d, 4H, cis-N(COC(CH₃)=CH₂)), 3.72 (t, 4H, N-CH₂), 1.85 (s, 12H, N(COC(CH₃)=CH₂)), 1.58 (m, 4H, N-CH₂-CH₂-CH₂-CH₂-CH₂-CH₂-N), 1.34 (m, 4H, N-CH₂-CH₂-CH₂-CH₂-CH₂-CH₂-N).

¹³C NMR: (50 MHz, CDCl₃) δ (ppm): 174.90 (C4), 144.88 (C4), 119.68 (C2), 45.06 (C2), 28.34 (C2), 26.73 (C2), 19.11 (C2).

HR-MS: (ACN, ESI+, m/z): calcd.: 411.2254 [M+Na]⁺; found: 411.2265 [M+Na]⁺

3.1.2. Synthesis of N,N'-(dodecan-1,12-diyl)bis(N,N'-bismethacrylamide) – CPM 3



Compound	Equivalents	MW [g/mol]	n [mmol]	m [g]	V [mL]
1,12-Diaminododecan	1	200.37	4.23	0.85	
Methacryloyl chloride	6	104.53	25.39	2.65	
Triethylamine (Et ₃ N)	6	101.19	25.39	2.57	
Dichloromethane (CH ₂ Cl ₂)					40

The synthesis of CPM 3 was performed in accordance with Kopeinig *et al.*⁶⁰ 1,12-Diaminododecan (0.85 g, 4.23 mmol) and Et₃N (2.57 g, 25.39 mmol) were dissolved in 30 mL dry CH₂Cl₂ in a 100 mL three-necked flask (purged with argon). The reaction mixture was cooled with ice/ NaCl to 0-5 °C. Afterwards, freshly distilled methacryloyl chloride (2.65 g, 25.39 mmol) was diluted with 10 mL CH₂Cl₂ and added dropwise to the solution (30-60 min). The cooling bath was removed after the addition of methacryloyl chloride, and the solution was stirred at RT for another 24 h. The solution was extracted with 0.1 N HCl, sat. NaHCO₃, and brine, and the organic phase was dried over Na₂SO₄. The solvent was removed under reduced pressure, and the crude product was purified *via* column chromatography (PE:EE 4:1). The pure product was obtained as white crystals (1.20 g, 60% of theory) and it was stabilized with 200 ppm MEHQ and 200 ppm phenothiazine as inhibitor.

CPM 3: 1.20 g (60% yield)

R_f-value: 0.82 (PE:EE 2:1)

mp.: 49.5-51.0 °C

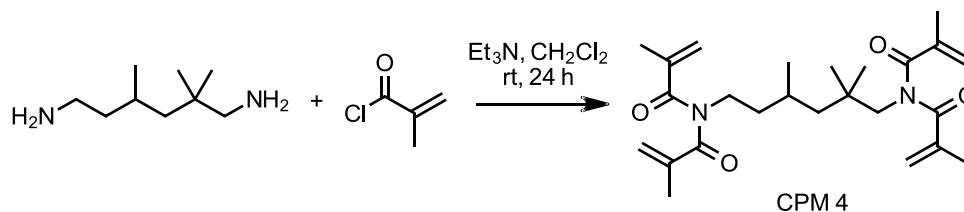
¹H NMR: (200 MHz, CDCl₃) δ (ppm): 5.24 (d, 4H, cis-N(COC(CH₃)=CH₂)), 5.12 (s, 4H, trans-N(COC(CH₃)=CH₂)), 3.74 – 3.57 (m, 4H, N-CH₂-CH₂-(CH₂)₈-CH₂-CH₂-N), 1.80 (s, 12H, N(COC(CH₃)=CH₂)), 1.61 – 1.42 (m, 4H, N-CH₂-CH₂-(CH₂)₈-CH₂-CH₂-N), 1.20 (m, 16H, N-CH₂-CH₂-(CH₂)₈-CH₂-CH₂-N).

¹³C NMR: (50 MHz, CDCl₃) δ (ppm): 175.06 (C4), 145.07 (C4), 119.74 (C2), 45.37 (C2), 29.63 (C2), 29.60 (C2), 29.38 (C2), 28.54 (C2), 27.12 (C2), 19.26 (C1).

HR-MS: (ACN, ESI+, m/z): calcd.: 495.3193 [M+Na]⁺; found: 495.3218 [M+Na]⁺

3.1.3. Synthesis of N,N'-(2,2,4(2,4,4)-trimethylhexane-1,6-diyl)

bis(N,N'-bismethylacrylamide) - CPM 4



Compound	Equivalents	MW [g/mol]	n [mmol]	m [g]	V [mL]
(2,2,4)/(2,4,4)- Trimethylhexane-1,6- diamine	1	158.28	9.29	1.47	
Methacryloylchloride	6	104.53	55.74	5.83	
Triethylamine (Et ₃ N)	6	101.19	55.74	5.64	
Dichloromethane (CH ₂ Cl ₂)					60

The synthesis of CPM 4 was performed in accordance with Kopeinig *et al.*⁶⁰ 2,2,4(2,4,4)-trimethylhexane-1,6-diamine (1.47 g, 9.29 mmol) and Et₃N (5.64 g, 55.74 mmol) were dissolved in 45 mL dry CH₂Cl₂ in a 100 mL three-necked flask (purged with argon). The reaction mixture was cooled with ice/ NaCl to 0-5 °C. Afterwards, freshly distilled methacryloyl chloride (5.83 g, 55.74 mmol) was diluted with 15 mL CH₂Cl₂ and added dropwise to the solution (30-60 min). The cooling bath was removed after the addition of methacryloyl chloride, and the solution was stirred at RT for 24 h. The solution was extracted with 0.1 N HCl, sat. NaHCO₃ and brine, and the organic phase was dried over Na₂SO₄. The solvent was removed under reduced pressure, and the crude product was purified *via* column chromatography (PE:EE 2:1). The pure product (2 isomers) was obtained as a slightly yellow, viscous liquid (2.01 g, 50% of theory) and it was stabilized with 200 ppm MEHQ and 200 ppm phenothiazine as inhibitor.

CPM 4: 2.01 g (50% yield)

Purity (HPLC): t_R : 6.23 min (58% acetonitrile/42% water, v/v, detection at 220 nm)

R_f-value: 0.80 (PE:EE 2:1)

¹H NMR: (400 MHz, CDCl₃) δ (ppm): 5.30 – 5.20 (m, 4H, cis-N(COC(CH₃)=CH₂)), 5.15 – 5.02 (m, 4H, trans-N(COC(CH₃)=CH₂)), 3.75 – 3.46 (m, 4H, N-CH₂-(CH₂)₄-CH₂-N), 2.02 – 1.90 (m, 1H, (2,4,4)-CH-CH₃), 1.80 (s, 12H, N(COC(CH₃)=CH₂)), 1.60 – 1.03 (m, 4H, N-CH₂-(CH₂)₄-CH₂-N and (2,2,4)-CH-CH₃), 0.97 – 0.82 (m, 9H, (2,2,4)/(2,4,4)-spacer C(CH₃)).

¹³C NMR: (101 MHz, CDCl₃) δ (ppm): 175.49 (C4), 175.13 (C4), 174.78 (C4), 144.91 (C4), 144.89 (C4), 144.87 (C4), 119.71 (C2), 119.66 (C2), 119.61 (C2), 55.12 (C2), 52.53 (C2), 48.00 (C2), 46.64 (C2), 43.49 (C4), 41.59 (C2), 40.37 (C2), 37.80 (C2), 37.54 (C2), 33.06 (C4), 28.70 (C3), 26.96 (C1), 26.89 (C1), 26.80 (C1), 26.00 (C1), 25.85 (C1), 22.48 (C1), 20.78 (C3), 19.33 (C1), 19.22 (C1), 19.10 (C1).

HR-MS: (ACN, ESI+, m/z): calcd.: 453.2723 [M+Na]⁺; found: 453.2723 [M+Na]⁺

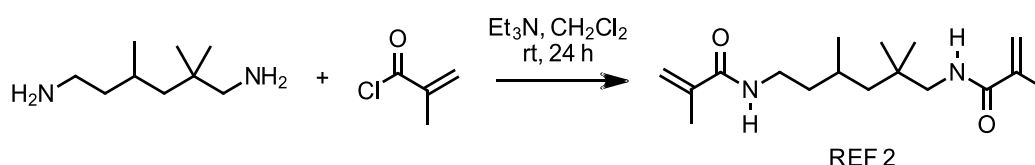
4. CPMs and REFs based on

(2,2,4)/(2,4,4)-trimethylhexane-1,6-diamine

4.1. Synthesis of the REF 2 and REF 3

4.1.1. Synthesis of N,N'-(2,2,4(2,4,4)-trimethylhexane-1,6-diyl)

bis(N-methylacrylamide) – REF 2



Compound	Equivalentents	MW [g/mol]	n [mmol]	m [g]	V [mL]
(2,2,4)/(2,4,4)- Trimethylhexane-1,6- diamine	1	158.28	34.0	5.38	
Methacryloylchloride	2.4	104.53	81.51	8.52	
Triethylamine (Et ₃ N)	2.4	101.19	81.51	8.25	
Dichloromethane (CH ₂ Cl ₂)					150

The synthesis of REF 2 was performed in accordance with Kopeinig *et al.*⁶⁰ 2,2,4(2,4,4)-trimethylhexane-1,6-diamine (5.28 g, 34.0 mmol) and Et₃N (8.25 g, 81.51 mmol) were combined with 100 mL dry CH₂Cl₂ in a 250 mL three-necked flask (purged with argon). The reaction mixture was cooled with ice/ NaCl to 0-5 °C. Afterwards, freshly distilled methacryloyl chloride (8.52 g, 81.51 mmol) was diluted with 50 mL CH₂Cl₂ and added dropwise to the solution (30-60 min). The cooling bath was removed after the addition of methacryloyl chloride, and the solution was stirred at RT for another 24 h. The solution was extracted with 0.1 N HCl, sat. NaHCO₃, and brine, and the organic phase was dried over Na₂SO₄. The solvent was removed under reduced pressure, and the crude product was purified *via* column chromatography (PE:EE 3:1). The pure product (2 isomers) was obtained as a slightly reddish, viscous liquid (9.32 g, 94% of theory) and it was stabilized with 300 ppm MEHQ and 300 ppm phenothiazine as inhibitor.

REF 2 9.32 g (94% yield)

R_f-value: 0.39 (PE:EE 3:1)

Purity (HPLC): t_R: 2.57 min (58% acetonitrile/42% water, v/v, detection at 220 nm)

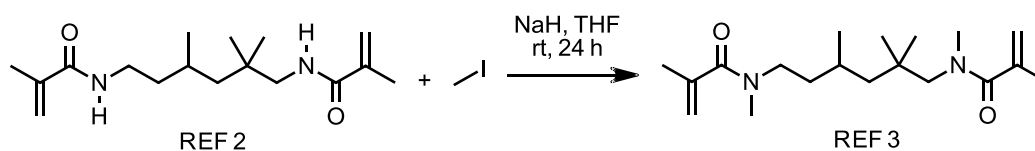
¹H NMR: (400 MHz, CDCl₃) δ (ppm): 6.56 (q, 1H, NH), 6.38 – 6.15 (m, 1H, NH), 5.66 – 5.56 (m, 2H, N(C(CH₃)=CH₂)), 5.24 – 5.17 (m, 2H, trans-N(C(CH₃)=CH₂)), 3.27 – 3.09 (m, 3H, N-CH₂), 2.93 – 2.82 (m, 1H, N-CH₂), 1.86 (ddd, 6H, N(C(CH₃)=CH₂)), 1.70 – 1.11 (m, 5H, NCH₂-(CH₂)₄-CH₂N), 1.01 – 0.76 (m, 9H, C(CH₃)).

¹³C NMR: (101 MHz, CDCl₃) δ (ppm): 168.73 (C4), 168.70 (C4), 168.58 (C4), 168.43 (C4), 140.33 (C4), 140.13 (C4), 140.08 (C4), 140.01 (C4), 119.17 (C2), 119.12 (C2), 119.08 (C2), 119.04 (C2), 48.79 (C2), 47.16 (C2), 46.37 (C2), 45.90 (C2), 41.04 (C2), 38.83 (C2), 37.51 (C2), 35.82 (C2), 35.16 (C4), 32.90 (C4), 29.06 (C3), 27.70 (C1), 27.56 (C1), 26.26 (C1), 26.09 (C1), 25.41 (C3), 22.36 (C1), 20.93 (C1), 20.80 (C1), 18.68 (C1), 18.59 (C1), 14.09 (C1)

HR-MS: (ACN, ESI+, m/z): calcd.: 317.2199 [M+Na]⁺; found: 317.2206 [M+Na]⁺

4.1.2. Synthesis of N,N'-(2,2,4(2,4,4)-trimethylhexane-1,6-diyl)

bis(N-methyl-N'-methylacrylamide) - REF 3



Compound	Equivalents	MW [g/mol]	n [mmol]	m [g]	V [mL]
REF 2	1	294.44	15.50	4.57	
Methyl iodide	5	141.84	77.52	11.00	
Sodium hydride (NaH) 60% in paraffin oil	5	23.99	77.52	3.72	
Tetrahydrofuran (THF)					90

The synthesis of REF 3 was performed in accordance with Ho *et al.*⁶² A suspension of NaH in paraffin oil (60%, 3.72 g, 77.52 mmol) was mixed with 50 mL dry THF in a 100 mL three-necked flask (purged with argon) and cooled with ice/ NaCl to 0-5 °C. REF 2 (4.57 g, 15.50 mmol) was diluted with 40 mL dry THF and was added dropwise to the stirring suspension. The reaction mixture was stirred for 1 h at this temperature. Afterwards, methyl iodide (11.00 g, 77.52 mmol) was added dropwise, and the suspension was stirred overnight, letting the ice/NaCl bath melt. The reaction mixture was quenched with distilled water (10 mL), and the solvent was removed under reduced pressure. The residues were dissolved in ether (30 mL), and the organic layer was washed with distilled water (3 x 30 mL). The organic phase was dried over Na₂SO₄, filtered, and the solvent was removed under reduced pressure. The crude product was purified *via* column chromatography (PE:EE 1:3) to give the pure product (2 isomers) as a clear, viscous liquid (3.32 g, 66% of theory) and it was not stabilized with MEHQ or phenothiazine as inhibitor.

REF 3: 3.32 g (66.4% yield)

Purity (HPLC): t_R : 3.10 min (58% acetonitrile/42% water, v/v, detection at 220 nm)

R_f-value: 0.38 (PE:EE 1:3)

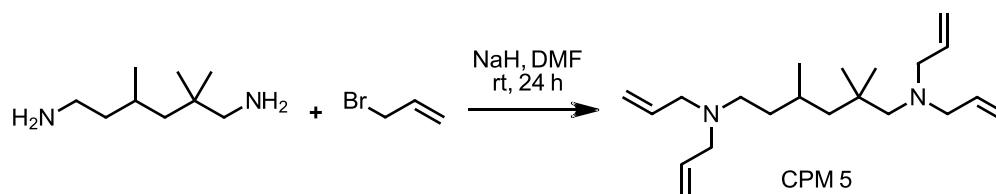
¹H NMR: (400 MHz, CDCl₃) δ (ppm): 4.95 (d, 2H, N-CO-C(CH₃)=CH₂), 4.81 (d, 1H, N-CO-C(CH₃)=CH₂), 3.28 – 2.93 (m, 4H, N-CH₂-CH₂-C(CH₃)₂-CH₂-CH(CH₃)-CH₂-N), 2.93 – 2.65 (m, 6H, N-CH₃), 1.78 – 0.82 (m, 5H, N-CH₂-CH₂-C(CH₃)₂-CH₂-CH(CH₃)-CH₂-N), 0.72 (dt, 9H, N-CH₂-CH₂-C(CH₃)₂-CH₂-CH(CH₃)-CH₂-N).

¹³C NMR was not possible to analyze, due to a lousy resolution!

HR-MS: (ACN, ESI+, m/z): calcd.: 323.2693 [M+H]⁺; found: 323.2692 [M+H]⁺

4.2. Synthesis of CPM 5, CPM 6, and CPM 7

4.2.1. Synthesis of 1,6-bis(diallylamino)-2,2,4(2,4,4)-trimethylhexane – CPM 5



Compound	Equivalents	MW [g/mol]	n [mmol]	m [g]	V [mL]
(2,2,4)/(2,4,4)- Trimethylhexane-1,6- diamine	1	158.29	25.12	4.00	
Allyl bromide	10	120.99	753.36	30.38	
Sodium hydride (NaH) 60% in paraffin oil	10	23.99	753.36	11.50	
Dimethylformamide (DMF)					160

The synthesis of CPM 5 was performed in accordance with Ho *et al.*⁶² A suspension of NaH in paraffin oil (60%, 11.51 g, 753.36 mmol) was mixed with 80 mL dry DMF in a 250 mL three-necked flask (purged with argon) and cooled with ice/water to 0 °C. 2,2,4(2,4,4)-trimethylhexane-1,6-diamine (4.00 g, 25.12 mmol) was added dropwise to the stirring suspension, and the reaction mixture was stirred for 1 h at this temperature. Afterwards, allyl bromide (30.38 g, 753.36 mmol) was diluted with 40 mL dry DMF and added dropwise to the stirring suspension (60 min). The cooling bath was removed after the addition of allyl bromide, and the suspension was stirred at RT for 24 h. The reaction mixture was then quenched with distilled water (10 mL) and extracted with ether (100 mL). The ether phase was washed with distilled water (5 x 30 mL), dried over Na₂SO₄, filtered, and the solvent was removed under reduced pressure. The crude product was purified *via* column chromatography (PE:EE 99:1) over aluminum oxide to give the product (2 isomers) with 25% impurities (trifunctional compound) as a clear liquid (5.41 g, 68% of theory). The monomer was stabilized with 200 ppm MEHQ and 200 ppm phenothiazine as inhibitor.

CPM 5: 5.41 g (67.6% yield)

Purity (NMR): ~ 75%

Rf-value: 0.81 (PE:EE 99:1)

¹H NMR: (400 MHz, CDCl₃) δ (ppm): 5.93 – 5.62 (m, 4H, N-CH₂-CH=CH₂), 5.21 – 4.88 (m, 8H, N-CH₂-CH=CH₂), 3.25 – 2.90 (m, 6H, N-CH₂-CH=CH₂), 2.59 – 2.46 (m, 1H, N-CH₂-CH₂-C(CH₃)₂-CH₂-CH(CH₃)-CH₂-N), 2.41 – 2.27 (m, 2H, N-CH₂-CH=CH₂), 2.25 – 1.99 (m, 3H, N-CH₂-CH₂-C(CH₃)₂-CH₂-CH(CH₃)-CH₂-N), 1.70 – 1.14 (m, 4H, N-CH₂-CH₂-C(CH₃)₂-CH₂-CH(CH₃)-CH₂-N), 1.02 – 0.81 (m, 9H, N-CH₂-CH₂-C(CH₃)₂-CH₂-CH(CH₃)-CH₂-N).

¹³C NMR: (101 MHz, CDCl₃) δ (ppm): 137.67 (C3), 137.63 (C3), 137.59 (C3), 137.51 (C3), 137.13 (C3), 136.72 (C3), 136.66 (C3), 136.52 (C3), 117.11 (C2), 117.06 (C2), 116.91 (C2), 116.87 (C2), 116.62 (C2), 116.37 (C2), 115.86 (C2), 115.81 (C2), 65.77 (C2), 62.28 (C2), 59.31 (C2), 57.43 (C2), 53.73 (C2), 53.64 (C2), 48.55 (C2), 48.33 (C2), 48.10 (C2), 47.79 (C2), 38.10 (C2), 38.00 (C2), 36.93 (C2), 36.80 (C2), 36.39 (C2), 33.29 (C2), 27.29 (C1), 27.17 (C1), 26.80 (C1), 25.97 (C1), 25.92 (C1), 25.73 (C1), 23.12 (C1), 22.89 (C1).

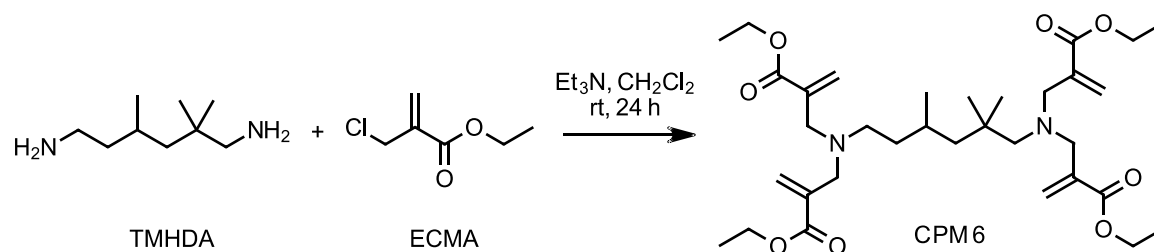
Tetrafunctional:

HR-MS: (ACN, ESI+, m/z): calcd.: 319.3108 [M+H]⁺; found: 319.3117 [M+H]⁺

Trifunctional:

HR-MS: (ACN, ESI+, m/z): calcd.: 279.2795 [M+H]⁺; found: 279.2801 [M+H]⁺

4.2.2. Synthesis of tetraethyl-2,2',2'',2'''-(((2,2,4-trimethylhexane-1,6-diy)bis(azanetriyl))tetrakis(methylene))tetraacrylate - CPM 6



Compound	Equivalents	MW [g/mol]	n [mmol]	m [g]	V [mL]
2,2,4 (2,4,4) – Trimethylhexane-1,6- diamine	1	158.28	8.24	1.30	
Ethyl-2- (chloromethyl)acrylate	6	148.59	49.44	7.35	
Triethylamine (Et₃N)	6	101.19	49.44	5.00	
Dichloromethane (CH₂Cl₂)					60

The synthesis of CPM 6 was performed in accordance with Peer *et al.*⁶⁰ 2,2,4(2,4,4)-trimethylhexane-1,6-diamine (1.30 g, 8.24 mmol) and Et₃N (5.00 g, 49.44 mmol) were dissolved in 45 mL dry CH₂Cl₂ in a 100 mL three-necked flask (purged with argon). The reaction mixture was cooled with ice/ NaCl to 0-5 °C. Afterwards, ethyl-2-(chloromethyl)acrylate (7.35 g, 49.44 mmol) was diluted with 15 mL CH₂Cl₂ and added dropwise to the solution (30-60 min). The cooling bath was removed after the addition of ethyl-2-chloromethylacrylate, and the solution was stirred at RT for 24 h. The solution was extracted with 0.1 N HCl, sat. NaHCO₃, and brine, and the organic phase was dried over Na₂SO₄. The solvent was removed under reduced pressure, and the crude product was purified *via* column chromatography (PE:EE 4:1). The pure product (2 isomers) was obtained as a slightly clear, viscous liquid (3.73 g, 75% of theory) and it was stabilized with 400 ppm MEHQ and 400 ppm phenothiazine as inhibitor.

CPM 6: 3.73 g (75% yield)

Purity (HPLC): t_R : 2.45 min (58% acetonitrile/42% water, v/v, detection at 220 nm)

R_f-value: 0.45 (PE:EE 4:1)

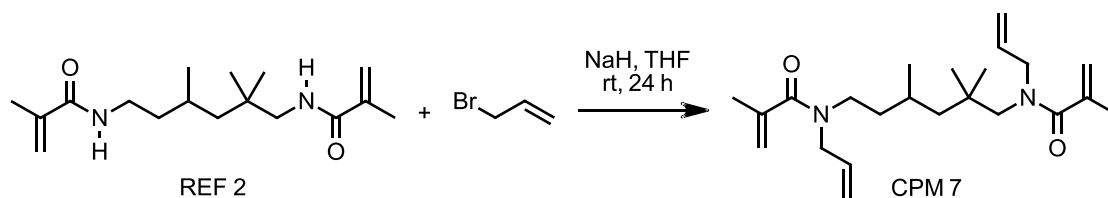
¹H NMR: (400 MHz, CDCl₃) δ (ppm): 6.23 – 6.09 (m, 4H, trans-N(CH₂-C-CH₂)), 5.83 – 5.70 (m, 4H, cis-N(CH₂-C-CH₂)), 4.12 (qt, 8H, COO-CH₂-CH₃), 3.34 – 2.99 (m, 8H, N(CH₂-C-CH₂)), 2.41 – 1.99 (m, 4H, N-CH₂-CH₂-C(CH₃)₂-CH₂-CH(CH₃)-CH₂-N), 1.44 – 0.67 (m, 15H, N-CH₂-CH₂-C(CH₃)₂-CH₂-CH(CH₃)-CH₂-N).

¹³C NMR (101 MHz, CDCl₃) δ (ppm): 166.87 (C4), 138.68 (C4), 138.53 (C4), 138.39 (C4), 126.54 (C2), 125.88 (C2), 125.48 (C2), 125.38 (C2), 66.37 (C2), 62.75 (C2), 60.48 (C2), 60.45 (C2), 57.28 (C2), 55.13 (C2), 54.61 (C2), 52.42 (C2), 49.78 (C2), 48.25 (C2), 47.21 (C2), 39.83 (C2), 36.90 (C2), 36.55 (C2), 32.89 (C2), 27.54 (C3), 27.23 (C3), 26.88 (C3), 25.37 (C3), 25.34 (C3), 22.82 (C3), 21.05 (C3), 14.18 (C3).

HR-MS: (ACN, ESI+, m/z): calcd.: 607.3954 [M+H]⁺; found: 607.3952 [M+H]⁺

4.2.3. Synthesis of N,N'-(2,2,4,4(2,4,4)-trimethylhexane-1,6-diyl)

bis(N-allyl-N'-methylacrylamide) - CPM 7



Compound	Equivalents	MW [g/mol]	n [mmol]	m [g]	V [mL]
REF 2	1	294.44	4.00	1.18	
Allyl bromide	10	120.99	40.05	4.85	
Sodium hydride (NaH) 60% in paraffin oil	10	23.99	40.05	1.92	
Tetrahydrofuran (THF)					40

The synthesis of CPM 7 was performed in accordance with Ho *et al.*⁶² A suspension of NaH in paraffin oil (60%, 1.92 g, 40.05 mmol) was mixed with 30 mL dry THF in a 100 mL three-necked flask (purged with argon) and cooled with ice/ NaCl to 0-5 °C. REF 2 (1.18 g, 4.00 mmol) was diluted with 10 mL dry THF and was added dropwise to the stirring suspension. The reaction mixture was stirred for 1 h at this temperature. Afterwards, allyl bromide (4.85 g, 40.05 mmol) was added dropwise, and the suspension was stirred overnight, letting the ice/NaCl bath melt. The reaction mixture was quenched with distilled water (10 mL), and the solvent was removed under reduced pressure. The residues were dissolved in ether (30 mL), and the organic layer was washed with distilled water (3 x 30 mL). The organic phase was dried over Na₂SO₄, filtered, and the solvent was removed under reduced pressure. The crude product was purified *via* column chromatography (PE:EE 1:3) to give the pure product (2 isomers) as a clear, viscous liquid (0.80 g, 53% of theory) and it was stabilized with 200 ppm MEHQ and 200 ppm phenothiazine as inhibitor.

CPM 7: 0.80 g (53.3% yield)

Purity (HPLC): t_R : 3.96 min (58% acetonitrile/42% water, v/v, detection at 220 nm)

R_f-value: 0.60 (PE:EE 3:1)

¹H NMR: (400 MHz, CDCl₃) δ (ppm): 5.62 (tdd, 2H, N-CH₂-CH=CH₂), 5.15 – 4.83 (m, 8H, N-CH₂-CH=CH₂ and N-CO-C(CH₃)=CH₂), 4.11 – 3.75 (m, 4H, N-CH₂-CH=CH₂), 3.17 (dt, 4H, N-CH₂-CH₂-C(CH₃)₂-CH₂-CH(CH₃)-CH₂-N), 1.86 (s, 6H, N-CO-C(CH₃)=CH₂), 1.52 – 0.91 (m, 5H, N-CH₂-CH₂-C(CH₃)₂-CH₂-CH(CH₃)-CH₂-N), 0.91 – 0.70 (m, 9H, N-CH₂-CH₂-C(CH₃)₂-CH₂-CH(CH₃)-CH₂-N).

¹³C NMR was not possible to analyze, due to a lousy resolution!

HR-MS: (ACN, ESI+, m/z): calcd.: 397.2825 [M+Na]⁺; found: 397.2823 [M+Na]⁺

4.3. Reactivity studies of REF 2, REF 3, CPM 4, CPM 5, CPM 6, and CPM 7

4.3.1. Photo-DSC measurement of REF 2, REF 3, CPM 4, CPM 5, CPM 6, and CPM 7

The Photo-DSC (Differential Scanning Calorimetry) measurements were performed in triplicates on a Netzsch DSC 204 F1 with autosampler at 25 °C under N₂ atmosphere. For the monomer formulations, 1 mol% Ivocerin[®] was used as PI, and these formulations (12 ± 2 mg) were irradiated twice with a filtered UV-light (400-500 nm) with an Exfo OmniCureTm series 2000 broadband Hg-lamp at 25 °C under constant N₂ flow rate (20 mL min⁻¹). The light intensity was set to ~20 mW cm⁻² on the surface of the sample, which corresponds to 1 W cm⁻² at the tip of the light guide. During the measurement, the heat flow of the polymerization reaction was recorded as a function of time. Consequently, two different time points could be determined: t_{max} (time point when the maximum heat evolution is reached) and t₉₅ (time point when 95% of the overall heat had evolved).

4.3.2. RT-NIR photorheology of REF 2, REF 3, CPM 4, CPM 5, CPM 6, and CPM 7

The analysis was carried out according to 2.2.1, using 1 mol% PI Ivocerin[®].

4.3.3. ATR-IR spectroscopy of polymerized CPM 4 and CPM 6

The ATR-IR experiments were performed on a Perkin Elmer Spectrum 65 FTIR Spectrometer, which is equipped with a Specac MKII Golfen Gate Single Reflection ATR System. The samples were polymerized during the RT-NIR photorheology experiments with 1 mol% Ivocerin[®] as PI at 25 °C, and afterwards homogenized with a mortar and pestle. The measurement of the IR-spectra was conducted at 25 °C and without any purification of the polymerized sample.

4.4. Mechanical studies of REF 2, CPM 4, CPM 6, and CPM 7

4.4.1. DMTA of REF 2, CPM 4, CPM 6, and CPM 7

All formulations were prepared with 1 mol% PI Ivocerin[®], homogenized using a vortex mixer and afterwards 30 min of sonification at 50 °C. The monomer formulations were polymerized in a silicone mold (sticks, 5 × 2 × 40 mm) cured in a Lumamat 100 light oven (provided by Ivoclar Vivadent AG) with 6 Osram Dulux L Blue 18 W lamps for 10 min on the top and the backside of the sample. The emitted wavelength spectrum was 400-580 nm at a measured total intensity of ~ 20 mW cm⁻² as determined with an Ocean Optics USB 2000+ spectrometer. The cured polymer specimens were ground to obtain a uniform dimension (< ± 0.1 mm).

The DMTA (dynamic mechanic thermal analysis) measurements were performed with an Anton Paar MCR 301 with a CTD 450 oven and an SRF 12 measuring system. The polymer specimen were tested in torsion mode with a frequency of 1 Hz and a strain of 0.1%. The temperature was increased from -100 °C to 200 °C with a heating rate of 2 °C min⁻¹. The storage modulus and the loss factor of the polymer samples were recorded with the software Rheoplus/32 V3.40 from Anton Paar.

4.4.2. Tensile Tests of REF 2, CPM 4, CPM 6, and CPM 7

The photocuring of the tensile test samples was performed in accordance with the procedure for DMTA samples. The dimension of the dog-chew-bone-shaped samples was in accordance with ISO 527 test specimen 5b (total length of 35 mm and a parallel region dimension of 2 × 2 × 12 mm). Five specimen were tested for each formulation. The tensile tests were performed on a Zwick Z050 with a maximum test force of 50 kN. The samples were fixed between two clamps and strained with a traverse speed of 5 mm min⁻¹. During the measurement, a stress-strain plot was recorded for analysis.

Materials & Methods

All chemicals, which were necessary for the synthesis of the final products and were commercially available, as well as their chemical suppliers, are listed below. Commercial grade dichloromethane (CH_2Cl_2 , Donau Chemie) and tetrahydrofuran (THF, Donau Chemie) were dried using a PureSolv system (Inert, Amesbury, MA).

Acetonitrile	VWR Chemicals
Acryloylchloride	abcr
Allylbromide	TCI Chemicals
1,12-Diaminododecan	TCI Chemicals
Dichloromethane	Donau Chemie
Diethylether	Donau Chemie
N,N'-Dimethyl-1,6-hexanediamine	TCI Chemicals
Dimethylformamide	Acros Organics
Ethyl acetate	Donau Chemie
Ethyl-2-(chloromethyl)acrylate	Ivoclar AG
Hexamethyldiamine	Sigma-Aldrich
Ivocerin	Ivoclar AG
Methacryloylchloride	abcs
Methyliodide	Merck KGaA
Petroleum ether	Donau Chemie
Phenothiazine	Sigma-Aldrich
p-Methoxyphenole	Sigma-Aldrich
Sodium hydride (60% in paraffin oil)	TCI Chemicals
Tetrahydrofuran	Donau Chemie
Triethylamine	Sigma-Aldrich
(2,2,4)/(2,4,4)-Trimethylhexane-1,6-diamine	TCI Chemicals

ATR-IR experiments of the cured sample were performed on a PerkinElmer Spectrum 65 FT-IR Spectrometer, using a Specac MKII Golden Gate Single Reflection ATR System.

Column chromatography was performed on a Büchi Sepacore Flash System (Büchi pump module C-605, Büchi control unit C-620, Büchi UV-Photometer C-635, Büchi fraction collector C-660), using glass columns, packed with silica gel 60 (Merck, 0.040-0.063 mm) or aluminum oxide 90 neutral (Carl Roth).

DMTA measurements were performed with an Anton Paar MCR 301 with a CTD 450 oven.

HPLC measurements were conducted on a reversed-phase HP1100 Chemstation HPLC system equipped with a diode array and a Waters Xterra MS C18 column, 5 μ m, 150 3.9 mm² inner diameter. Water/acetonitrile was used as solvent. Samples were prepared as 1 mg mL⁻¹ solutions in HPLC-grade acetonitrile.

HR-MS analysis was performed from the monomer samples, dissolved in HPLC-graded acetonitrile (concentration: 10 μ M), by using a HTC PAL system autosampler (CTC Analytics AG, Zwingen, Switzerland), an Agilent 1100/1200 HPLC with binary pumps, degasser, and column thermostat (Agilent Technologies, Waldbronn, Germany), and an Agilent 6230 AJS ESI-TOF mass spectrometer (Agilent Technologies, Palo Alto, CA).

NMR spectra were recorded on a Bruker DPX-200 FT-NMR spectrometer at 200 MHz for ¹H and 50 MHz for ¹³C, as well as on a Bruker Avance DRX-400 FT-NMR spectrometer at 400 MHz for ¹H and 100 MHz for ¹³C. The signals are recorded according to their chemical shifts, which were reported in ppm (s = singlet, d = doublet, t = triplet, q = quartet, qn = quintet, sep = septet, m = multiplet, bs = broad singlet) in comparison to tetramethylsilane (d = 0 ppm). The spectra were then referenced on the used NMR-solvent [¹H: CDCl₃ (7.26 ppm), ¹³C: CDCl₃ (77.16 ppm)]

Photo-DSC measurements were conducted on a Photo-DSC 204 F1 from Netzsch, using 15 μ aluminum pans. An Omnicure 2000 from Lumen Dynamics with glass fiber light wave guides was used as light source, which was calibrated *via* an Omnicure R2000 radiometer. All measurements were conducted under N₂-atmosphere (flow rate: 20 mL min⁻¹). The data analysis was performed with the program Netzsch Proteus Thermal Analysis in version 8.0.1.

Polymer specimens for DMTA and tensile tests were photocured in a Lumamat 100 light oven (provided by Ivoclar Vivadent), using 6 Osram Dulux L Blue 18 W lamps (400-580 nm).

RT-NIR photorheology was performed on an Anton Paar MCR 302 WESP with a P-PTD 200/GL Peltier glass plate, a H-PTD 200 heating hood, and a disposable PP25 measuring system. The rheometer was coupled with a Bruker Vertex 80 FTIR spectrometer.

Tensile tests were conducted employing a Zwick Z050 with a maximum test force of 50 kN. The recorded data was processed and evaluated *via* the software TestXpert II.

Thin layer chromatography (TLC) was performed on aluminum TLC-plates coated with silica gel 60 F245 (supplier: Merck).

Yellow light laboratory was used as location for all synthesis and preparation of the formulations. All windows of this laboratory were covered with adhesive foils (company: IFOHA), and the fluorescent lamps were type Osram lumilux with chip control light color 62 (filtration of wavelengths below 480 nm)

Abbreviations

ABr	Allyl bromide
AC	Acrylate
AM	Additive Manufacturing
ATR-IR	Attenuated Total Reflectance – Infrared
CI	Co-initiator
CPM	Cyclopolymerizable Monomer
CTA	Chain transfer agent
CTR	Chain transfer reaction
DADD	1,12-Diaminedodecan
DB	Double Bond
DBC	Double Bond Conversion
DMHMDA	N,N'-Dimethylhexamethylenediamine
DMTA	Dynamic Mechanical Thermal Analysis
DP	Degree of Polymerization
3DP	Three Dimensional Printing
ECMA	Ethyl-2-(chloromethyl)acrylate
FDM	Fusion Deposition Modeling
FG	Functional Group
F _N	Shrinkage Force
FRP	Free Radical Polymerization
FT-IR	Fourier-Transform – Infrared
G'	Storage Modulus
G''	Loss Modulus
HMDA	Hexamethylenediamine
HR-MS	High Resolution – Mass Spectroscopy
IC	Internal Conversion
IR	Infrared
ISC	Intersystem Crossing
M	Monomer
MAC	Methacrylates
MCT	Mercury Cadmium Telluride
MEHQ	p-Methoxyphenol

MI	Methyl iodide
MW	Molecular Weight
NMR	Nuclear Magnetic Resonance
PI	Photoinitiator
P _n	Polymer chain
REF	Reference Substance
R _i	Initiating Radical
R _f -value	Retarding-front value
ROP	Ring Opening Polymerization
RT	Room Temperature
RT-NIR	Real Time – Near Infrared
SLA	Stereolithography
tan(δ)	Loss Factor
T _c	Ceiling Temperature
T _g	Glass Transition Temperature
t _g	Time of the Gel Point
UV	Ultra Violet
σ _M	Maximum Tensile Strength
ε _B	Elongation at Break

References

1. Peiffer, R. W., Applications of Photopolymer Technology. In *Photopolymerization*, American Chemical Society: 1997; Vol. 673, pp 1-14.
2. Yagci, Y.; Jockusch, S.; Turro, N. J., Photoinitiated Polymerization: Advances, Challenges, and Opportunities. *Macromolecules* **2010**, *43* (15), 6245-6260.
3. Fouassier, J.-P., *Photoinitiation, Photopolymerization, and Photocuring: Fundamentals and Applications*. 1995.
4. Fouassier, J. P.; Allonas, X.; Burget, D., Photopolymerization reactions under visible lights: principle, mechanisms and examples of applications. *Progress in Organic Coatings* **2003**, *47* (1), 16-36.
5. Ligon-Auer, S. C.; Schwentenwein, M.; Gorsche, C.; Stampfl, J.; Liska, R., Toughening of photo-curable polymer networks: a review. *Polymer Chemistry* **2016**, *7* (2), 257-286.
6. Calignano, F.; Manfredi, D.; Ambrosio, E. P.; Biamino, S.; Lombardi, M.; Atzeni, E.; Salmi, A.; Minetola, P.; Iuliano, L.; Fino, P., Overview on Additive Manufacturing Technologies. *Proceedings of the IEEE* **2017**, *105* (4), 593-612.
7. Nannan GUO, M. C. L., Additive manufacturing: technology, applications and research needs. *Front. Mech. Eng.* **2013**, *8* (3), 215-243.
8. Lyons, B., Additive manufacturing in aerospace: Examples and research outlook. *The Bridge, linking engineering and society* **2012**, *42*, 13-19.
9. Melchels, F. P. W.; Feijen, J.; Grijpma, D. W., A review on stereolithography and its applications in biomedical engineering. *Biomaterials* **2010**, *31* (24), 6121-6130.
10. Ligon, S. C.; Liska, R.; Stampfl, J.; Gurr, M.; Mülhaupt, R., Polymers for 3D Printing and Customized Additive Manufacturing. *Chemical Reviews* **2017**, *117* (15), 10212-10290.
11. Hoyle, C. E., Photocurable Coatings. In *Radiation Curing of Polymeric Materials*, American Chemical Society: 1990; Vol. 417, pp 1-16.
12. Jirau-Colón, H. G.-P., L.; Martínez-Jiménez, J.; Adam, W.; Jiménez-Velez, B., Rethinking the Dental Amalgam Dilemma: An Integrated Toxicological Approach. *Int. J. Environ. Res. Public Health* **2019**, *16*, 1063.
13. Richard Bibb, C. E., Peter Evans, Alan Bocca, Adrian Sugar, Rapid manufacture of custom-fitting surgical guides. *Rapid Prototyping Journal* **2009**.
14. Moad, G.; Solomon, D. H., *The Chemistry of Radical Polymerization, Second Edition*. Elsevier Science: 2006.
15. Lee, T. Y.; Guymon, C. A.; Jönsson, E. S.; Hoyle, C. E., The effect of monomer structure on oxygen inhibition of (meth)acrylates photopolymerization. *Polymer* **2004**, *45* (18), 6155-6162.
16. Ligon, S. C.; Husár, B.; Wutzel, H.; Holman, R.; Liska, R., Strategies to Reduce Oxygen Inhibition in Photoinduced Polymerization. *Chemical Reviews* **2014**, *114* (1), 557-589.
17. Monroe, B. M.; Weed, G. C., Photoinitiators for free-radical-initiated photoimaging systems. *Chemical Reviews* **1993**, *93* (1), 435-448.
18. Quaranta, M.; Borisov, S. M.; Klimant, I., Indicators for optical oxygen sensors. *Bioanalytical Reviews* **2012**, *4* (2), 115-157.
19. Mitterbauer, M. Tin-based long wavelength photoinitiators for dental composites. Technical University of Vienna, Vienna, 2019.
20. Green, W. A., *Industrial Photoinitiators: A Technical Guide*. CRC Press LLC: 2017.
21. Husár, B.; Ligon, S. C.; Wutzel, H.; Hoffmann, H.; Liska, R., The formulator's guide to anti-oxygen inhibition additives. *Progress in Organic Coatings* **2014**, *77* (11), 1789-1798.

22. Moszner, N.; Fischer, U. K.; Ganster, B.; Liska, R.; Rheinberger, V., Benzoyl germanium derivatives as novel visible light photoinitiators for dental materials. *Dental Materials* **2008**, *24* (7), 901-907.
23. Fouassier, J.-P., Photochemistry and UV curing : a brief survey of the latest trends. In *Photochemistry & UV Curing: New Trends*, J.P, F., Ed. Research Signpost Trivandrum: 2006; p 1.
24. Lu, H.; Stansbury, J. W.; Nie, J.; Berchtold, K. A.; Bowman, C. N., Development of highly reactive mono-(meth)acrylates as reactive diluents for dimethacrylate-based dental resin systems. *Biomaterials* **2005**, *26* (12), 1329-1336.
25. Schwalm, R., UV Coating - Basics, Recent Developments Developments and New Applications. In *UV Coatings*, Schwalm, R., Ed. Elsevier: Amsterdam, 2007; p 322.
26. Cutié, S. S.; Henton, D. E.; Powell, C.; Reim, R. E.; Smith, P. B.; Staples, T. L., The effects of MEHQ on the polymerization of acrylic acid in the preparation of superabsorbent gels. *Journal of Applied Polymer Science* **1997**, *64* (3), 577-589.
27. Levy, L. B., Inhibition of acrylic acid polymerization by phenothiazine and p-methoxyphenol. *Journal of Polymer Science: Polymer Chemistry Edition* **1985**, *23* (5), 1505-1515.
28. Levy, L. B., Inhibition of acrylic acid polymerization by phenothiazine and p-methoxyphenol. II. Catalytic inhibition by phenothiazine. *Journal of Polymer Science Part A: Polymer Chemistry* **1992**, *30* (4), 569-576.
29. Sadhir, R. K.; Luck, R. M., *Expanding Monomers - Synthesis, Characterization, and Applications*. CRC Press: 1992.
30. Peer, G. Strategies for shrinkage stress reduction in photopolymers for dental restoratives. Technical University of Vienna, Vienna, 2020.
31. Gauss, P.; Ligon-Auer, S. C.; Griesser, M.; Gorsche, C.; Svajdenkova, H.; Koch, T.; Moszner, N.; Liska, R., The influence of vinyl activating groups on β -allyl sulfone-based chain transfer agents for tough methacrylate networks. *Journal of Polymer Science Part A: Polymer Chemistry* **2016**, *54* (10), 1417-1427.
32. Gorsche, C.; Koch, T.; Moszner, N.; Liska, R., Exploring the benefits of β -allyl sulfones for more homogeneous dimethacrylate photopolymer networks. *Polymer Chemistry* **2015**, *6* (11), 2038-2047.
33. Müller, A.; Matyjaszewski, K., *Controlled and Living Polymerizations*. Wiley-VCH: 2009.
34. Grubbs, R. B., Nitroxide-Mediated Radical Polymerization: Limitations and Versatility. *Polymer Reviews* **2011**, *51* (2), 104-137.
35. Xu, G.; Chung, T.-c., Borane chain transfer agent in metallocene-mediated olefin polymerization. Synthesis of borane-terminated polyethylene and diblock copolymers containing polyethylene and polar polymer [9]. *Journal of the American Chemical Society* **1999**, *121*, 6763-6764.
36. Karasu, F.; Arsu, N.; Yagci, Y., 2-Mercapto thioxanthone as a chain transfer agent in free-radical polymerization: A versatile route to incorporate thioxanthone moieties into polymer chain-ends. *Journal of Applied Polymer Science* **2007**, *103* (6), 3766-3770.
37. Gorsche, C.; Seidler, K.; Knaack, P.; Dorfinger, P.; Koch, T.; Stampfl, J.; Moszner, N.; Liska, R., Rapid formation of regulated methacrylate networks yielding tough materials for lithography-based 3D printing. *Polymer Chemistry* **2016**, *7* (11), 2009-2014.
38. Ge, J.; Trujillo, M.; Stansbury, J., Synthesis and photopolymerization of low shrinkage methacrylate monomers containing bulky substituent groups. *Dental Materials* **2005**, *21* (12), 1163-1169.
39. Butler, G. B., *Cyclopolymerization and Cyclocopolymerization*. Marcel Dekker: New York, 1992; p 1-536.
40. Stansbury, J. W., Cyclopolymerizable Monomers for Use in Dental Resin Composites. *Journal of Dental Research* **1990**, *69* (3), 844-848.
41. Peer, G.; Kury, M.; Gorsche, C.; Catel, Y.; Frühwirt, P.; Gescheidt, G.; Moszner, N.; Liska, R., Revival of Cyclopolymerizable Monomers as Low-Shrinkage Cross-Linkers. *Macromolecules* **2020**.

42. Butler, G., *Cyclopolymerization and Cyclocopolymerization*. 1st Edition ed.; CRC Press: 1992; p 560.
43. Hall, A. W.; Godber, M. J.; Blackwood, K. M.; Milne, P. E. Y.; Goodby, J. W., The photoinitiated cyclopolymerization of dienes in the creation of novel polymeric systems and three-dimensional networks. *Journal of Materials Chemistry* **2004**, *14* (17), 2593-2602.
44. Butler, G. B., Cyclopolymerization. *Journal of Polymer Science Part A: Polymer Chemistry* **2000**, *38* (19), 3451-3461.
45. Kodaira, T., Structural control during the cyclopolymerization of unconjugated dienes. *Progress in Polymer Science* **2000**, *25* (5), 627-676.
46. Avci, D.; Haynes, C.; Mathias, L. J., Cyclopolymerization of amine-linked diacrylate monomers. *Journal of Polymer Science Part A: Polymer Chemistry* **1997**, *35* (10), 2111-2121.
47. Peer, G. New Monomers for Radical Photopolymerization. Technical University of Vienna, Vienna, 2017.
48. Kodaira, T.; Satoyama, M.; Urushisaki, M.; Hashimoto, T., Cyclopolymerization XXIX. Radical Polymerizations of N-Methyl-N-(meth)allyl-2-(t-butoxycarbonyl)allylamines: Effect of a Bulky Ester Group on Cyclopolymerizability of 1,6-Dienes with Functional Groups of No Homopolymerization Tendencies. *Polymer Journal* **2000**, *32* (11), 954-960.
49. Dworak, C.; Kopeinig, S.; Hoffmann, H.; Liska, R., Photoinitiating monomers based on di- and triacryloylated hydroxylamine derivatives. *Journal of Polymer Science Part A: Polymer Chemistry* **2009**, *47* (2), 392-403.
50. Kopeinig, S. Synthese und Untersuchung photopolymerisierbarer Gruppen für Silikonbeschichtungen. Technical University of Vienna, Vienna, 2007.
51. Urushisaki, M.; Kodaira, T.; Furuta, T.; Yamada, Y.; Oshitani, S., Cyclopolymerization. 25. Five-Membered Ring Formation through Head-to-Head and Tail-to-Tail Additions in Radical and Anionic Polymerizations of α -(Allyloxymethyl)acrylates. *Macromolecules* **1999**, *32* (2), 322-327.
52. Tsuda, T.; Mathias, L. J., Cyclopolymerization of ether dimers of α -(hydroxymethyl)acrylic acid and its alkyl esters: substituent effect on cyclization efficiency and microstructures. *Polymer* **1994**, *35* (15), 3317-3328.
53. Lee, H.-J.; Kodaira, T.; Urushisaki, M.; Hashimoto, T., Cyclopolymerization. Part XXXII radical polymerization of α -(2-phenylallyloxy)methylstyrene: synthesis of highly cyclized polymers with high glass transition temperatures and thermal stability. *Polymer* **2004**, *45* (22), 7505-7512.
54. Yamada, B.; Kobatake, S., Radical polymerization, co-polymerization, and chain transfer of α -substituted acrylic esters. *Progress in Polymer Science* **1994**, *19* (6), 1089-1131.
55. Liu, Q.-Q.; Kodaira, T.; Urushisaki, M.; Hashimoto, T., Cyclopolymerization XXIII. Design of Unconjugated Dienes with High Polymerizability Using Functional Groups with No Homopolymerization Tendency and Synthesis of Completely Cyclized Polymers Therefrom: Radical Polymerizations of N-Substituted N-Allyl-2-(methoxycarbonyl)allylamines. *Polymer Journal* **1996**, *28* (11), 1000-1005.
56. Kodaira, T.; Urushisaki, M.; Iwasaki, T.; Kamata, Y.; Hashimoto, T., Cyclopolymerization, 30. Design of an Unconjugated Diene with High Polymerizability Using Functional Groups with No Homopolymerization Tendency, and Synthesis of Completely Cyclized Polymers therefrom: Radical Polymerizations of N-Phenyl-N-2-(methoxycarbonyl)allyl(meth)acrylamide. *Macromolecular Chemistry and Physics* **2001**, *202* (11), 2402-2411.
57. Zubov, V. P.; Kumar, M. V.; Masterova, M. N.; Kabanov, V. A., Reactivity of Allyl Monomers in Radical Polymerization. *Journal of Macromolecular Science: Part A - Chemistry* **1979**, *13* (1), 111-131.
58. Tuzun, N. S.; Aviyente, V.; Houk, K. N., A Theoretical Study on the Mechanism of the Cyclopolymerization of Diallyl Monomers. *The Journal of Organic Chemistry* **2003**, *68* (16), 6369-6374.

59. Hall, A. W.; Blackwood, K. M.; Milne, P. E. Y.; Goodby, J. W., Novel UV cured coatings and adhesives based on the photoinitiated cyclopolymerization of derivatives of diallylamine. *Chemical Communications* **2003**, (20), 2530-2531.
60. Liska Robert Dr, D.-I.; Kopeinig Stefan, D.-I.; Gruber Heinrich Dr, D.-I.; Knaus Simone Dr, D.-I.; Hummer Erwin Dr, D.-I. Acrylimides With Initiator Characteristics. EP 1956033 A1, 2008/02/05, 2008.
61. Moszner, N.; Zeuner, F.; Angermann, J.; Fischer, U. K.; Rheinberger, V., Monomers for Adhesive Polymers, 4. *Macromolecular Materials and Engineering* **2003**, 288 (8), 621-628.
62. Ho, T. C. T.; Jones, K., A synthesis of the tricyclic pyrroloquinoline core of martinelline. *Tetrahedron* **1997**, 53 (24), 8287-8294.
63. Urushisaki, M.; Kodaira, T.; Takahashi, H.; Hashimoto, T., Cyclopolymerization. Part XXXI. An attempt to control the reaction courses of the polymerizations of N-methyl-N-allyl-2-(ethoxycarbonyl)allylamine by using anionic and radical initiators. *Polymer* **2003**, 44 (23), 7113-7120.
64. Mangelinckx, S.; Žukauskaitė, A.; Buinauskaitė, V.; Šačkus, A.; De Kimpe, N., Synthesis of alkyl 2-(bromomethyl)aziridine-2-carboxylates and alkyl 3-bromoazetidine-3-carboxylates as amino acid building blocks. *Tetrahedron Letters* **2008**, 49 (48), 6896-6900.
65. J. Brandrup, E. H. I., and E.a. Grulke, *Polymer Handbook*. John Wiley & Sons: 1999.
66. Sokolova, T. A.; Rudkovskaya, G. D., Cyclic polymerization of N-dimethacrylamides. *Journal of Polymer Science Part C: Polymer Symposia* **1967**, 16 (2), 1157-1166.
67. Gotro, J. Thermoset Characterization Part 14: Introduction to Dynamic Mechanical Analysis (DMA). <https://polymerinnovationblog.com/thermoset-characterization-part-14-introduction-dynamic-mechanical-analysis-dma/> (19.08.20).
68. <https://polymerdatabase.com/polymer%20physics/Stress-Strain%20Behavior.html> (19.08.20).